

**Alpha-2 Adrenoceptors in the Paraventricular Thalamic  
Nucleus: Effects of Agonist Stimulation and Chronic  
Psychosocial Stress**

**Ph.D. Thesis**

in partial fulfilment of the requirements  
for the degree “Dr. rer. nat.”  
in the Graduate Program Neuroscience  
at the Georg-August University Göttingen,  
Faculty of Biology

**submitted by**

Urs Heilbronner

**born in**

Tübingen, Germany

## **Declaration**

This thesis has been written independently and with no other sources and aids than required.

Urs Heilbronner

## Table of contents

<b>List of abbreviations</b>	<b>6</b>
<b>Summary</b>	<b>8</b>
<b>Introduction</b>	<b>10</b>
<i>The adrenergic receptors</i>	<i>10</i>
<i>The alpha-2 adrenoceptor family</i>	<i>11</i>
<i>Alpha-2B adrenoceptors in the paraventricular thalamus</i>	<i>12</i>
<i>Cellular actions of alpha-2 adrenoceptor stimulation</i>	<i>14</i>
<i>The alpha-2 adrenoceptors and their relation to stress</i>	<i>15</i>
<i>Chronic psychosocial stress in male tree shrews</i>	<i>16</i>
<i>Summary of the aims of the thesis</i>	<i>17</i>
<b>Methods and materials</b>	<b>18</b>
<i>The whole-cell patch-clamp technique</i>	<i>18</i>
<i>Preparation of thalamic slices</i>	<i>18</i>
<i>Electrophysiological recording</i>	<i>19</i>
<i>Determination of membrane potential and input resistance</i>	<i>20</i>
<i>Solutions for electrophysiological recording</i>	<i>20</i>
<i>Chemicals and drugs for electrophysiological recording</i>	<i>21</i>
<i>Histochemical detection of neurobiotin</i>	<i>21</i>
<i>Morphometric analysis of neurons</i>	<i>22</i>
<i>Immunocytochemistry</i>	<i>24</i>
<i>In vitro receptor autoradiography with [<sup>3</sup>H]RX821002</i>	<i>24</i>
<i>In situ hybridization</i>	<i>26</i>
<i>Animal experiments</i>	<i>27</i>
<b>Results</b>	<b>29</b>
 Part I: Alpha-2 adrenoceptors in the paraventricular thalamus - effects of agonist stimulation and morphological characterization of cells	
 <i>Effect of alpha-methyl-norepinephrine on membrane potential and input resistance</i>	<i>29</i>

<i>Effects of alpha-methyl-norepinephrine on the membrane current</i> .....	29
<i>Pharmacological properties of the responses to alpha-methyl-norepinephrine</i> .....	32
<i>Influences of alpha-methyl-norepinephrine on neuronal firing</i> .....	35
<i>Involvement of putative K<sup>+</sup> conductances in the actions of alpha-methyl-norepinephrine</i> .....	43
<i>Morphology of neurons in the paraventricular thalamus</i> .....	47

Part II: Regulation of alpha-2B adrenoceptor expression by chronic psychosocial stress

<i>Immunocytochemistry against dopamine-beta-hydroxylase and phenylethanolamine-N-methyl-transferase</i> .....	55
<i>Characterization of [<sup>3</sup>H]RX821002 binding in the rat brain: Competition experiments</i> .....	55
<i>Quantification of [<sup>3</sup>H]RX821002 binding in the tree shrew thalamus</i> .....	56
<i>Expression studies: alpha-2B AR cDNA and cRNA probe</i> .....	58
<i>Quantification of alpha-2B AR expression by in situ hybridization</i> .....	59
<i>Peripheral reactions of the experimental animals during chronic psychosocial stress</i> .....	60

**Discussion**..... 62

<i>Cellular effects of alpha-2 adrenoceptor activation in the paraventricular thalamic nucleus</i> .....	62
<i>Activation of alpha-1 and alpha-2 adrenoceptors by alpha-methyl-norepinephrine</i> .....	63
<i>Influences of alpha-methyl-norepinephrine on neuronal firing</i> .....	65
<i>Alpha-methyl-norepinephrine affects putative K<sup>+</sup> currents</i> .....	66
<i>Resting properties of neurons in the paraventricular thalamus</i> .....	66
<i>Morphology of neurons in the paraventricular thalamus</i> .....	67
<i>Functional implications of the actions of alpha-methyl-norepinephrine</i> .....	69
<i>The alpha-2B adrenoceptor in the thalamus</i> .....	69
<i>Innervation of the paraventricular thalamus by noradrenergic and adrenergic fibers</i> .....	71
<i>Chronic psychosocial stress affects alpha-2 adrenoceptors: in situ hybridization and in vitro receptor autoradiography</i> .....	71
<i>Stress and alpha-2 adrenoceptors</i> .....	72
<i>Peripheral reactions of subordinate tree shrews during chronic psychosocial stress and recovery</i> .....	73
<i>Conclusions</i> .....	73

**References**..... 75

<b>List of figures</b>	<b>84</b>
<b>List of tables</b>	<b>85</b>
<b>Publications</b>	<b>86</b>
<i>Articles in peer-reviewed journals</i>	<i>86</i>
<i>Poster presentations</i>	<i>86</i>
<b>Courses taken during the M.Sc./Ph.D. Program</b>	<b>86</b>
<b>Acknowledgements</b>	<b>87</b>
<b>Curriculum vitae</b>	<b>88</b>

## List of abbreviations

ABC	–	avidin-biotin-complex
ACSF	–	artificial cerebrospinal fluid
AM	–	anteromedial thalamic nucleus
AMY	–	amygdala
ANOVA	–	analysis of variance
AP	–	action potential
aPVT	–	anterior paraventricular nucleus
AR	–	adrenoceptor
ATP	–	adenosine-triphosphate
AV	–	anteroventral thalamic nucleus
B <sub>max</sub>	–	maximal number of binding sites
BNST	–	bed nucleus of the stria terminalis
BSA	–	bovine serum albumin
cc	–	corpus callosum
CD	–	caudate nucleus
cDNA	–	complementary DNA
CNS	–	central nervous system
cRNA	–	complementary RNA
DAB	–	3,3'-diaminobenzidine
DBH	–	dopamine-beta-hydroxylase
DR	–	dorsal raphé nucleus
E	–	epinephrine
EGTA	–	ethylene glycol-(bis-beta-amino-ethylether)-N,N,N',N'-tetraaceticacid
E <sub>K</sub>	–	Nernst potential for potassium
GABA	–	gamma-amino butric acid
GFP	–	green fluorescent protein
GIRK	–	G-protein coupled inwardly rectifying K <sup>+</sup>
G-protein	–	guanine-nucleotide binding protein
H	–	hypothalamus
HEPES	–	(N-[2-hdroxyethyl]piperazine-N'-[2-ethane sulfonic acid])
Hip	–	hippocampus
HVA	–	high-voltage activated
I <sub>h</sub>	–	hyperpolarization-activated current
IR	–	immunoreactivity
K <sub>D</sub>	–	dissociation constant
LC	–	locus coeruleus
LJP	–	liquid junction potential
m-NE	–	alpha-methyl-norepinephrine
mOsm	–	milliosmo
mRNA	–	messenger ribonucleic acid
n	–	number
N.A.	–	numerical aperture
NAC	–	nucleus accumbens
NE	–	norepinephrine
ngs	–	normal goat serum
nss	–	normal sheep serum
PAP	–	peroxidase-anti-peroxidase
PB	–	parabrachial nucleus
PBS	–	phosphate-buffered saline
PC12	–	pheocromocytoma cell line PC12
PFA	–	paraformaldehyde
PFC	–	prefrontal cortex
PMNT	–	phenylethanolamine-N-methyl-transferase
pPVT	–	posterior paraventricular nucleus

PVT	–	paraventricular thalamic nucleus
$R_{in}$	–	input resistance
RMP	–	resting membrane potential
RT-PCR	–	reverse transcriptase polymerase chain reaction
SEM	–	standard error of the mean
Spont.	–	spontaneous
SSC	–	NaCl/Na <sup>+</sup> citrate
TASK	–	twin-pore acid sensitive
TAT	–	0.1 M lysine, 1% nss, 0.1% Triton-X-100 in TBS
TBS	–	tris-buffered saline
TM	–	transmembrane
Tris	–	tris(hydroxymethyl)aminomethane
TTX	–	tetrodotoxin
UTP	–	uracil triphosphate
$V_m$	–	membrane potential

## Summary

The catecholamines are important modulators of nerve cell activity. They exert their actions via G-protein coupled receptors among which are the alpha-2 adrenoceptors. The alpha-2 adrenoceptor family consists of three members, the alpha-2 adrenoceptor subtypes A, B and C that show differential expression in different areas of the mammalian brain. While subtypes A and C have been well studied before, little is known about subtype B that is strongly expressed in the thalamus. In the present thesis, the function of the alpha-2B adrenoceptor in the paraventricular thalamic nucleus (PVT) was studied using electrophysiological techniques (part I). The effects of chronic stress on expression of the thalamic alpha-2B adrenoceptor and on alpha-2 adrenoceptor ligand binding were investigated using *in situ* hybridization and *in vitro* receptor autoradiography, respectively (part II).

Part I: In order to elucidate the cellular actions of the alpha-2B adrenoceptor and the morphology of PVT cells that are modulated by this receptor, electrophysiological whole-cell recordings and cell tracing methods were applied to slices of the rat brain. Based on pharmacological and physiological characterization, three distinct classes of PVT neurons were identified. The first class of neurons exhibits membrane hyperpolarization and a reduction in input resistance mediated by postsynaptic alpha-2 adrenoceptors upon stimulation with the agonist alpha-methyl-norepinephrine. In a second class of neurons, alpha-methyl-norepinephrine induces a slow membrane depolarization and an increase in input resistance mediated by postsynaptic alpha-1 adrenoceptors. These two effects occur in distinct PVT neurons which differ in their resting properties and morphology. The actions of alpha-1/alpha-2 adrenoceptors are - at least partially - mediated through a modulation of putative K<sup>+</sup> currents. Also, the firing patterns of PVT cells are temporarily changed by the influence of alpha-methyl-norepinephrine. Finally, the third class of PVT neurons is insensitive to alpha-methyl-norepinephrine, has a lower input resistance and a larger dendritic tree compared to the two classes mentioned above.

Part II: Alpha-2 adrenoceptor expression is known to be regulated by endogenous norepinephrine and previous studies have shown that a stress-induced increase in noradrenergic activity leads to changes in expression of the alpha-2A autoreceptor. The present work describes the effect of chronic psychosocial stress on expression of the alpha-2B adrenoceptor in the thalamus using an established animal model, chronic social stress in tree shrews. In humans, chronic stress is known to play a role in psychiatric diseases such as depression and alpha-2 adrenoceptors have been reported to be changed in depressive subjects. *In situ* hybridization with a specific alpha-2B adrenoceptor probe was performed to quantify mRNA for the receptor, and *in vitro* receptor autoradiography with the non-selective alpha-2 adrenoceptor ligand [<sup>3</sup>H]RX821002 was used to determine receptor binding. The results show that the alpha-2B adrenoceptor is upregulated after a period of daily social



stress lasting 44 days and that this effect is also found after a 10 days *post stress* recovery period. These results show that the thalamus, a brain region known for its gating functions with respect to information transfer to cortical brain regions, is affected by stress and that the effect persists *post stress*.

Taken together, in the PVT, the neurophysiological function of the alpha-2B adrenoceptor is an induction of hyperpolarization and a reduction in membrane input resistance. Upregulation of alpha-2B adrenoceptor expression in the PVT after 44 days of daily social defeat reflects that the thalamus is a target brain region for stress. Thus, the present data support and extend previous findings indicating reduced noradrenergic activity after chronic stress exposure. Based on the results of the first part of the thesis, the changes induced by chronic psychosocial stress might profoundly influence both the input as well as the output characteristics of PVT cells sensitive to alpha-2 adrenoceptor agonists.

## Introduction

### The adrenergic receptors

In the central nervous system (CNS), slow neurotransmitter-mediated modulation is essential to alter both input and output characteristics of neurons. This is especially important to assure an appropriate reaction of the organism to behavioral challenges. The catecholamines norepinephrine (NE) and epinephrine (E) are neurotransmitters that modulate neuronal activity. The receptors for these compounds, the so-called adrenoceptors (ARs), belong to the superfamily of guanine-nucleotide binding protein (G-protein) coupled receptors (e.g. MacDonald et al., 1997; Saunders and Limbird, 1999). The secondary structure characteristics of these cell-surface proteins are seven transmembrane (TM) domains, each composed of 20-25 hydrophobic amino acids which span the plasma membrane in an alpha-helical fashion. The TM domains are connected by three intracellular and two extracellular loops that contain hydrophilic amino acid residues. The N-terminus of the receptor molecule is located on the extracellular side, the C-terminus faces the cytosol. The highest homology among members of the gene superfamily encoding G-protein coupled receptors is found in regions coding for TM domains (reviewed by Birnbaumer et al., 1990). Three-dimensionally, G-protein coupled receptors are believed to form a pore-like structure (see Nestler et al., 2001). Receptors of the 7TM class couple to their effectors via different heterotrimeric G-proteins which in turn activate different signal transduction pathways, thus modifying the activity of cells. Ligand binding induces a conformational change of the molecule and causes G-proteins to bind to the receptor (see Siegelbaum et al., 2000).

Historically, the ARs have been divided into alpha- and beta-ARs, according to different agonist potencies (Ahlquist, 1948). Langer (1974) further subdivided the alpha-adrenergic receptors into alpha-1 and alpha-2 ARs, based on anatomical localization. It was believed that alpha-2 ARs were situated pre-, whereas alpha-1 ARs were located postjunctionally. Later, however, the availability of numerous agonists and antagonists helped to establish a pharmacological rather than anatomical classification of alpha-1 versus alpha-2 ARs proposed by Berthelsen and Pettinger (1977). Bentley (1977) discovered that in blood vessels of the pithed rat, alpha-2 adrenergic receptors exist postsynaptically and this postsynaptic location has been shown for numerous other tissues since (see Hieble et al., 1997; Kable et al., 2000). With the availability of molecular biology techniques, nine ARs have been cloned and they were shown to have pharmacological profiles consistent with those of the previous classification of alpha-1, alpha-2 and beta-adrenoceptors (see Hieble and Ruffolo, 2002). Based on structural homology and pharmacology, the nine adrenoceptor clones were grouped into the alpha-1, alpha-2 and the beta adrenoceptor family, each family having three members. A fourth pharmacologically distinct alpha-2D subtype was found in

the rodent, but based on gene and protein homology, this subtype was grouped as ortholog of the human alpha-2A AR (Link et al., 1992).

Clinically, alpha-2 AR agonists have been shown to have numerous effects which are mediated by both central and peripheral ARs, such as the regulation of blood pressure, attenuation of the aversive symptoms accompanying morphine withdrawal and mediation of sedation and analgesia (Aantaa and Scheinin, 1993; see Ma et al., 2005). There are numerous clinically relevant drugs, including antidepressants, that affect alpha-2 ARs (see Cooper et al. 2003).

### **The alpha-2 adrenoceptor family**

The three alpha-2 adrenergic receptor subtypes have been cloned and named alpha-2A, B and C (Kobilka et al., 1987; Reagan et al., 1988; Lomasney et al., 1990). Each subtype is encoded by a distinct gene, all of which are located on different chromosomes. The receptor subtypes differ in their pharmacological profiles (MacDonald et al., 1997), intracellular trafficking (Saunders and Limbird, 1999) and desensitization properties (Eason and Liggett, 1992). Furthermore, each receptor has a unique expression pattern in the mammalian CNS, suggesting that the three receptors might have different physiological roles (Scheinin et al., 1994). Of the three subtypes, subtype A shows the most widespread expression in the CNS. It is strongly expressed in NE synthesizing neurons of the locus coeruleus (LC), the major source of NE in the mammalian brain, where the alpha-2A AR is located presynaptically and inhibits the release of NE from axon terminals. In addition, its expression is e.g. found throughout the brain stem, cortex, septum, hypothalamus, hippocampus and amygdala. Subtype C messenger ribonucleic acid (mRNA) is abundant in the striatum, where the receptors are located on medium-spiny GABAergic projection neurons (Holmberg et al., 1999). Subtype C is also expressed in the LC, cortex, olfactory tubercle and the hippocampus (see Scheinin et al., 1994).

The subtype B is of special interest, as its expression occurs strongly in the thalamus (Scheinin et al., 1994). Co-localization studies using *in situ* hybridization and immunocytochemistry (ICC) showed that in the dorsal thalamus, this receptor is expressed in cells immunoreactive for glutamate, but not in cells immunoreactive for gamma-aminobutyric-acid (GABA; Heilbronner, 2002). *In vitro* experiments (see Kable et al, 2000; Trendelenburg et al., 2001) indicate this alpha-2 adrenoceptor subtype has no autoreceptor function in the CNS. Olli-Lähdesmäki et al. (1999) showed that in nerve growth factor treated, transfected PC-12 cells that express different alpha-2 adrenoceptor subtypes, alpha-2B AR immunoreactivity (IR) was found evenly distributed on the plasma membrane. This indicates that *in vivo*, the alpha-2B AR might be located on cell bodies or dendrites of neurons, or on both. In contrast, alpha-2A adrenoceptor IR was found to be stronger on distal segments of

outgrown neurites than on the plasma membrane, congruent with a role of this subtype as a terminal autoreceptor. Also, in PC12 cells expressing the alpha-2B AR, epinephrine stimulated neurite outgrowth indicating that the receptor is involved in processes of differentiation (Taraviras et al., 2002). Studies in rats suggest that the antinociceptive actions of nitric oxide are mediated via alpha-2B ARs (Sawamura et al., 2000).

### **Alpha-2B adrenoceptors in the paraventricular thalamus**

A thalamic nucleus that almost exclusively expresses the alpha-2B AR subtype compared with the other alpha-2 subtypes (Scheinin et al., 1994) is the paraventricular thalamic nucleus (PVT). Strong alpha-2B AR expression has been detected both in rats and tree shrews (Scheinin et al., 1994; Heilbronner et al., 2004). In earlier anatomical studies, the name nucleus paramedianus was often used for this nucleus (e.g. van Buren and Borke, 1972). Numerous tracing studies have characterized the afferent and efferent connections of this nucleus in detail (e.g. Groenewegen and Berendse, 1994; Moga et al., 1995; Otake et al., 1995; Vertes, 2004; for review see van der Werf et al., 2002). The brain areas that provide input to the PVT are mainly the parabrachial nucleus, the bed nucleus of the stria terminalis, the dorsomedial hypothalamus, the supramammillary nuclei and the amygdala. The main output of the PVT occurs to the shell of the nucleus accumbens, the amygdaloid complex, the bed nucleus of the stria terminalis, the hippocampus and the prefrontal cortex (van der Werf et al., 2002; Vertes, 2004). Also, the PVT receives a strong input from cell groups in the brain stem containing the indolamines histamine and serotonin as well as from those containing the catecholamines dopamine and NE (for review see van der Werf et al., 2002). Important connections of the PVT are shown in Fig. 1.

On the basis of the strong monoaminergic input, it has been argued that the PVT is involved in state-setting properties in situations such as stress and fear (Chastrette et al., 1991; Beck and Fibiger, 1995). Several studies have shown that both stress (Beck and Fibiger, 1995; Bubser and Deutch, 1999) and psychostimulants (Deutch et al., 1998) induce expression of the immediate-early gene cFos in the PVT, indicating that intense neuronal activity in this nucleus occurs in response to external stimuli. Therefore, the PVT has been proposed as a relay nucleus that transfers stress-related information to the limbic forebrain (Bubser and Deutch, 1999). Fibers containing the "stress hormone" corticotropin-releasing factor (CRF) also terminate in this nucleus (Otake and Nakamura, 1995). A strong expression of cFos protein is found in the thalamus when rats are exposed to an environmental challenge previously paired with cocaine (Brown et al., 1992). Both Otake (1995) and van der Werf (2002) therefore classify the PVT as having "viscerolimbic function".

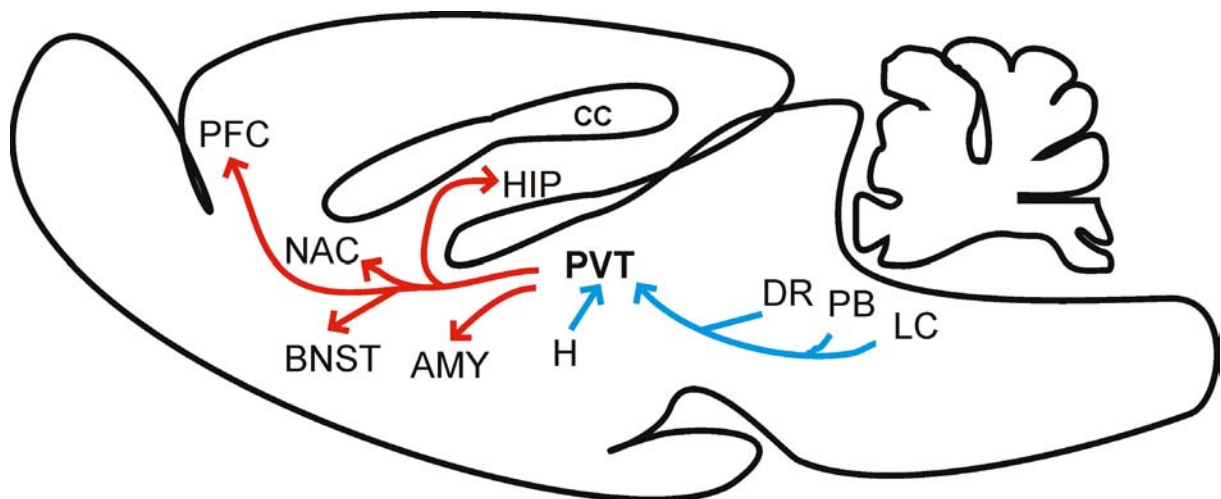


**Figure 1.** Important connections of the PVT. Schematic drawing of a sagittal section of the rat brain (redrawn from Otake et al., 2002). Important afferent (blue) and efferent (red) connections of the PVT are shown. *Abbreviations:* AMY – amygdala; BNST – bed nucleus of the stria terminalis; cc – corpus callosum; DR – dorsal raphe nucleus; H – hypothalamus; HIP – hippocampus; LC – locus coeruleus; NAC – nucleus accumbens; PB – parabrachial nucleus; PFC – prefrontal cortex; PVT – paraventricular thalamic nucleus.

The functional role of alpha-2 ARs in the PVT has not been studied before. In the present thesis, this issue was addressed by investigating the effects of postsynaptic alpha-2 AR activation in the PVT by single-cell electrophysiology in slices of the rat brain. Also, very few studies have so far examined the morphology of cells in the PVT and data on the dendritic tree of PVT cells are not available. Knowledge of the morphological characteristics and the relation of resting properties and membrane receptors to these characteristics are essential to gain a better understanding of the cellular constituents of the PVT. Consequently, one part of this thesis is concerned with the morphology of cells in the PVT.

A major drawback in the investigation of alpha-2 adrenergic subtype function and distribution is the lack of truly subtype-specific agonists (e.g. Scheinin et al., 1994). Hence, the analysis of alpha-2 AR proteins has relied on immunological techniques or on pharmacological experiments with various subtype-preferring ligands. Antibodies have been produced against the alpha-2A (Talley et al., 1996) and the alpha-2C AR (Rosin et al., 1996) subtypes. The results of these studies indicate that moderate IR in the PVT is found with the antibody directed against the alpha-2A subtype, revealing IR in neuropil but not in perikarya. Alpha-2C-like IR is not found in this region.

In order to confirm the presence of alpha-2B ARs in the PVT we performed competition binding experiments using the subtype non-selective alpha-2 agonist [<sup>3</sup>H]RX821002 and with imiloxan, an allegedly specific antagonist for the alpha-2B AR subtype as competitor (Michel et al., 1990). In rat kidney, where the alpha-2B AR is present (Meister et al., 1994; Huang et al., 1996), imiloxan showed a higher affinity than in rabbit spleen, where the alpha-2A but not the alpha-2B AR is present (Michel et al., 1989). Furthermore, the subtype non-selective alpha-2 agonist UK14,304 and the D<sub>2</sub>-like dopamine receptor antagonist chlorpromazine were used in these experiments. To compare the results, we also included sections of the LC, where alpha-2B ARs are not expressed, in the present experiments.

### **Cellular actions of alpha-2 adrenoceptor stimulation**

The cellular effects of alpha-2 AR activation have been thoroughly studied in cells of the LC. In neurons of the LC, agonist stimulation of alpha-2 ARs hyperpolarizes the membrane (Aghajanian and Wang, 1987) and reduces the spontaneous firing rate (Williams and Marshall, 1987). Alpha-2 ARs activate G-protein coupled K<sup>+</sup> currents both in slice preparations (North et al., 1987) and in dissociated neurons (Arima et al., 1998). Actions on K<sup>+</sup> currents have since been shown for a number of G-protein coupled receptors such as alpha-1 ARs in the thalamus (reviewed by McCormick et al., 1991), dopamine receptors (e.g. Kröner et al., 2005), opioid receptors (Brunton and Charpak, 1998) and GABA<sub>B</sub> receptors (e.g. Takigawa and Alzheimer, 2002). Also, alpha-2 AR agonists inhibit high-voltage activated (HVA) Ca<sup>2+</sup> channels (e.g. Czesnik et al., 2001). This is a prominent feature by which presynaptic transmitter release is inhibited via alpha-2 ARs situated on axon terminals. Membrane hyperpolarization, activation of a G-protein coupled K<sup>+</sup> current, inhibition of a HVA Ca<sup>2+</sup> current and inhibition of spontaneous firing have also been shown in slices of hypothalamic hypocretin/orexin neurons in response to alpha-2 agonists (Li and van den Pol, 2005).

As mentioned above, the cellular actions of alpha-2 ARs in the thalamus remain poorly understood and the studies in which the actions of alpha-2 agonists were investigated have used *in vivo* recordings (Rogawski and Aghajanian, 1980; Buszaki et al., 1990; Funke et al., 1993). Based on their findings, Buszaki et al. (1990) hypothesize alpha-2 ARs in the thalamus to be located postsynaptically on thalamic cells where they induce thalamic oscillations via an increase of a putative K<sup>+</sup> conductance. The present study therefore also addresses the question whether activation of alpha-2 ARs in the PVT also affects K<sup>+</sup> currents, as reported before in other brain regions (e.g. Bünemann et al., 2001).

The firing of thalamic neurons is of particular interest as they exhibit two characteristic modes of firing: bursting or tonic firing (for review see Sherman and Guillery, 2001). At hyperpolarized potentials (around -70 mV), the cells fire in burst mode. This kind of firing is

due to a low-threshold  $\text{Ca}^{2+}$  conductance that is de-inactivated at this potential and thus becomes activated when current is injected into the cell, giving rise to a so-called “calcium shoulder”, crowned by one or more action potentials. This calcium conductance is mediated by T-type  $\text{Ca}^{2+}$  channels. At depolarized membrane potentials (e.g. -55 mV), thalamic cells fire in tonic mode (conventional  $\text{Na}^+/\text{K}^+$  mediated action potentials) as the calcium conductance is inactivated in this voltage range. Historically, these two modes of firing have been proposed to be associated with the animal's behavioral state. It was thought that during phases of sleep or drowsiness, cells fire in burst mode, whereas in awake or alert states, thalamic cells fire in the tonic mode. However, recent evidence (e.g. Fanselow et al., 2001; Swadlow and Gusev, 2001) suggests that bursting also occurs during wakefulness, serving as preparatory signal to prime a given sensory system for signal detection. Nevertheless, burst and tonic firing are fundamentally different output modes of thalamic cells. These different firing modes are also reflected in the electro-encephalogram, with single-cell burst firing leading to the above mentioned thalamic oscillations (reviewed by McCormick et al., 1991). It is accepted that the tonic firing mode is important for the faithful transmission of information, whereas the burst firing mode allows for better signal detection (see Sherman and Guillery, 2001). The firing mode of a cell can be temporarily changed during the actions of modulators such as opioids (Brunton and Charpak, 1998) or NE mediated via alpha-1 ARs (McCormick and Pape, 1990). One aim of the present investigations was therefore to delineate the actions of alpha-2 ARs on the membrane potential and on the firing of PVT cells to find out whether the inhibitory actions and a change in firing mode can also be observed in the PVT through the activation of alpha-2 ARs.

### **The alpha-2 adrenoceptors and their relation to stress**

On the behavioral level, NE has been noted to be involved in processes such as arousal and stress (Anisman and Zacharko, 1992; Leonard, 2001; Duman et al., 1997; for review see Stanford, 1993). Social stress is a causal factor in the precipitation of mental disorders such as depression or post-traumatic stress disorder and is considered to be a risk factor for several other diseases (for review see Kessler, 1997). Among other factors, the alpha-2 ARs have been thought to play an important role in the context of depressive states and have been shown to exhibit changes in expression, number and affinity induced by chronic psychosocial stress (e.g. Flügge, 2000). Through these mechanisms, alpha-2 ARs are thought to be important determinants of the neurochemistry of the brain.

The effects of chronic stress on alpha-2 ARs include desensitization of presynaptic alpha-2 autoreceptors (Birch et al., 1986) and it was suggested that reduced alpha-2 AR functioning occurs in the LC during both stress and depression (Weiss and Simson, 1986). Chronic social stress in male tree shrews had time-dependent effects on alpha-2 ARs in different

brain regions (see Flügge, 2000). For example, an approximately 25% decrease in transcript levels of the alpha-2A adrenoceptor was observed in LC neurons after four weeks of chronic psychosocial stress (Meyer et al., 2000), and six weeks of the same kind of stress induced upregulation of alpha-2A ARs in brain stem glutamatergic neurons (Flügge et al., 2003). Research concerning alpha-2 receptors and their role during episodes of stress has so far mainly focused on the alpha-2A and alpha-2C subtypes (e.g. Sallinen et al., 1999; Flügge et al., 2003). The question if the alpha-2B adrenergic receptor, its main center of expression being the thalamus, is also influenced by stress has so far not been investigated. Few studies have addressed the influence of stress on the thalamus (e.g. Hsu et al., 2001; Otake et al., 2002), although this brain region plays a prominent role in the control of arousal and relays sensory information to cortical and limbic brain regions (e.g. Steriade et al., 1993; McCormick and Bal, 1997; Jones, 1998; Sherman and Guillery, 2001). Therefore, in the second part of this thesis, it was investigated whether chronic psychosocial stress has an impact on thalamic alpha-2 ARs, in particular on the expression of the subtype B. We have focused our attention on the PVT, the nucleus that strongly expresses alpha-2B ARs and that has been shown to be relevant in the context of stress (see above).

### **Chronic psychosocial stress in male tree shrews**

When modeling a psychiatric disorder in laboratory animals, a number of criteria have to be fulfilled to ensure that the model adequately reflects the disorder. One criterion is “face validity” and assesses how well the symptoms observed in the animals resemble those observed in human patients. A second criterion, “predictive validity”, looks at the question of how well animals respond favorably to the same therapeutic interventions as humans do under the same treatment conditions. The third criterion, “construct validity” assesses to what extent the model is consistent with the theoretical rationale (Willner, 1991). Here, the chronic psychosocial stress model in male tree shrews (e.g. Fuchs et al., 1996; van Kampen et al., 2002; Fuchs and Flügge, 2002) was used, a non-rodent animal model for depression that satisfactorily meets the above mentioned criteria. Both in their natural habitat and in the laboratory, male tree shrews show pronounced territoriality, meaning that they vigorously attack other male tree shrews that intrude their territory. Under laboratory conditions, when two males are housed together in one cage, there are short social encounters whereupon a clear dominant-subordinate hierarchy is established. During a period of chronic social stress lasting several weeks, the subordinate male tree shrew is confronted with the dominant counterpart daily for 1 h only. During the rest of the day, a wire mesh divides the cages so that the animals are housed separately next to each other. During this period, the subordinate has both visual and olfactory contact to the dominant animal at all times. In subordinate animals, this leads to a number of symptoms which can also be observed in



depressive patients. These include persistent activation of both the hypothalamic-pituitary-adrenal axis and the sympathetic nervous system, which is reflected by elevated urinary cortisol and NE levels, respectively. Chronic psychosocial stress also leads to decreases in body weight, reduced function of the gonads, deficits in grooming behavior, reduced motor activity and disturbances in sleeping behavior (see Fuchs et al., 1993; Fuchs and Flügge, 2002).

### **Summary of the aims of the thesis**

The primary aim of the present thesis was to clarify the functional role of the alpha-2B adrenoceptor in the PVT (part I of this thesis). Therefore, the influence of adrenergic agonists and antagonists on the membrane potential, the influence of K<sup>+</sup> channel blockers on induced currents and the firing of PVT neurons were investigated using the whole-cell patch-clamp technique in slices of the rat thalamus. The compounds used in these experiments were the alpha-2 agonists alpha-methyl-norepinephrine (m-NE) and clonidine, the alpha-2 antagonist yohimbine, as well as the alpha-1 agonist phenylephrine and the alpha-1 antagonist prazosin. The morphology of the cells that were recorded was studied to assign both the resting as well as the pharmacological properties to individual neurons. To visualize the morphological aspects, the cells were filled with the tracer neurobiotin during recording. Afterwards, the tracer was detected using histochemical techniques and analyzed with morphometric techniques. Immunocytochemical experiments with antibodies against dopamine-beta-hydroxylase and phenylethanolamine-N-methyl-transferase were performed to visualize the fibers containing norepinephrine and epinephrine in the PVT.

The second aim of the present thesis (part II) was to investigate if chronic psychosocial stress affects expression of alpha-2B ARs in the thalamus and if putative changes in alpha-2B AR gene expression are reflected by alterations in alpha-2 AR binding in this region. These studies were performed in male tree shrews using an established chronic social stress model. Quantification of gene expression was performed by *in situ* hybridization using a radioactively labeled probe for the alpha-2B adrenoceptor gene, and receptor binding was quantified by *in vitro* receptor autoradiography with the alpha-2 AR ligand [<sup>3</sup>H]RX821002. In an attempt to visualize subtype specific radioligand binding, competition experiments were performed in the rat brain. In humans, psychosocial stress can precipitate mental disorders that often manifest themselves only some time after a stressful time period. It was therefore also investigated to which extend presumptive changes in alpha-2B AR expression and alpha-2 binding persist if the animals are allowed to recover after the stressful period. In order to evaluate the stress level of the animals, urinary cortisol and body weight were determined daily during the entire experimental period. Results from the stress experiments have been already published (Heilbronner et al., 2004).

## **Methods and materials**

### **The whole-cell patch-clamp technique**

The patch-clamp technique is an electrophysiological method that allows recording of currents that flow across biological membranes through ion channels (Sakmann and Stuart, 1995). The technique has been originally described in a publication by Hamill and colleagues (Hamill et al., 1981). Briefly, a cell is approached with a small fire-polished glass pipette with a tip diameter of approximately 1  $\mu\text{m}$  filled with solution (intracellular solution) and with a recording electrode. Positive air pressure is often put on the pipette to prevent that cellular debris, which might be present in tissue slices, clogs the pipette. The pipette tip is held in contact with the cell membrane and the pressure is released, causing the cell membrane to be sucked in direction of the pipette, forming a tight seal between cell membrane and pipette tip. This is aided by applying a very gentle pulse of suction to the pipette. The resistance of the aforementioned seal is critical for the experiment and should be in the range of gigaohms (GOhm) ("gigaseal"). By again applying gentle pulses of suction to the pipette, the membrane under the pipette tip is broken, creating a hole in the cell membrane and gaining low-resistance access to the cell interior. The formation of this so-called "whole-cell" configuration does not compromise the formation of the gigaseal. This is of primary importance as it prevents both leak currents between the pipette and the reference electrode and flooding of the cell with bath solution. Within minutes, the intracellular solution is exchanged with the pipette solution. In the whole-cell configuration, it is possible to clamp the cell at a potential defined by the experimenter and to observe the resulting current flowing through the ion channels of the entire cell. Another possibility is to apply a constant current to the cell and measure changes in membrane potential (current clamp). The parameter that has to be held constant (voltage or current) is controlled by an amplifier via a feedback system. The current clamp technique makes it possible to monitor effects on the membrane potential such as subthreshold depolarizations, hyperpolarizations or action potentials whereas the voltage clamp allows to observe and to investigate the corresponding currents.

### **Preparation of thalamic slices**

Male Wistar rats 4-8 weeks of age at the time of recording were obtained from Harlan-Winkelmann (Borchen, Germany). The animals were sacrificed by decapitation. The brain was quickly dissected out and submerged in ice-cold oxygenated artificial cerebro-spinal fluid (ACSF) of the following composition (in mM): NaCl 125; KCl 2.5; L-ascorbic acid 1; MgSO<sub>4</sub> 2; Na<sub>2</sub>HPO<sub>4</sub> 1.25; NaHCO<sub>3</sub> 26; d-glucose 14; CaCl<sub>2</sub> 1.5 for about 30 s. A block of tissue containing the PVT was then glued onto a stage using cyanoacrylate glue (UHU, Bühl/Baden, Germany). Subsequently, 400  $\mu\text{m}$  coronal slices were made in ice-cold ACSF

from the anterior PVT to the beginning of the posterior PVT (-1.30 to -3.80 mm bregma according to Paxinos (1986); see Fig. 2) using a vibratome (FBT Feinwerk Technik, Villingen, Germany). Slices were then allowed to recover for 1 h in ACSF bubbled with 95% O<sub>2</sub>/5% CO<sub>2</sub> (carbogen) to a pH of 7.3 at 33°C, and subsequently stored for up to 10 h at room temperature in carbogen-bubbled ACSF. A single slice was transferred to the recording chamber and submerged in oxygenated ACSF flowing in from gravity-fed syringes at a flow rate of 1-2 ml per min. The tissue was fixed by a horseshoe-shaped platinum wire with nylon threads glued onto the wire.

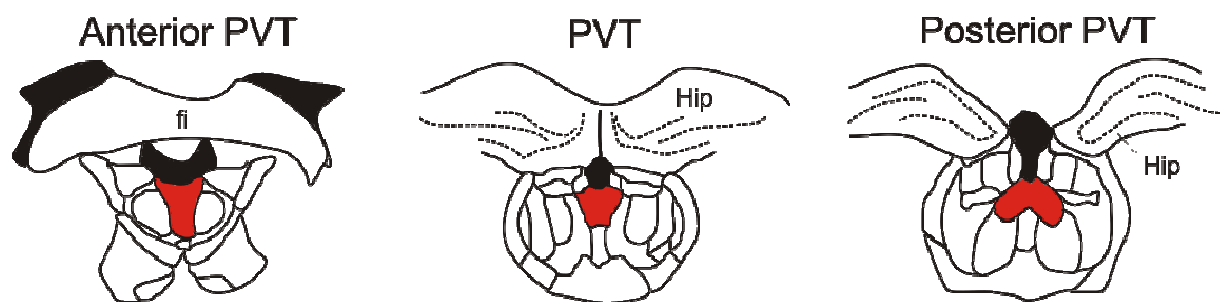


**Figure 2.** Schematic description of the recording sites. Shown are three drawings of the rat thalamus at different anterior-posterior levels (redrawn from Paxinos and Watson, 1986). The positions according to bregma (in mm) are: anterior PVT, -1.4; PVT, -2.56; posterior PVT, -3.6. The PVT is shown in red color, the ventricles are shown in black color. *Abbreviations:* Hip, hippocampus; fi, fimbria hippocampus; PVT, paraventricular thalamic nucleus.

### Electrophysiological recording

Neurons located at a depth of up to 50 µm in the slice were approached under visual control (Axioskop 2 FS with a 40x objective, numerical aperture (N.A.) 0.8; Zeiss, Jena, Germany) using infrared videomicroscopy (C/F 601 camera; Kappa opto-electronics, Gleichen, Germany). Electrophysiological recordings were performed using the patch-clamp technique in whole-cell mode (Hamill et al., 1981) with a patch-clamp amplifier (Axopatch 200B, Axon Instruments, Foster City, CA, USA). The extracellular solution was flowing through a heating tube (HPT-1, npi electronics, Tamm, Germany) connected to a temperature controller (TC-10, npi electronics) that monitored the bath temperature through a sensor. Recordings were performed at 31-33°C. Pipettes were made from borosilicate glass (Hilgenberg, Malsfeld, Germany) using a Narishige pipette puller (Model PP-830, Narishige, Tokyo, Japan) and had a resistance of 3-6 megaohms (MΩ). After the whole-cell configuration was obtained, cells

were held at -80 mV. In each slice, only one neuron was recorded. Series resistance was always < 20 MOhm. In voltage-clamp experiments, series resistance was checked just before drug application and - if increased - improved by applying gentle pulses of suction to the pipette. Seal resistance was at least 1 GOhm. The data were digitized and stored on a Personal Computer with Pulse software (HEKA, Lambrecht/Pfalz, Germany). Data analysis was performed using PulseFit (HEKA) and GraphPad Prism software (GraphPad, San Diego, CA, USA). All data are presented as mean  $\pm$  SEM.

### **Determination of membrane potential and input resistance**

The input resistance was determined by the magnitude of voltage deflections to current pulses of -25 pA or by the slope of a straight line fitted through the linear parts of the I-V relationship just before the drugs were washed in and during the peak of the response. In the dose-response experiments and in the experiments investigating the firing of PVT cells, a significant change in membrane potential in response to an agonist was defined as a change  $\pm$  3 mV from resting potential. In the dose response experiments, the membrane potential changes induced by low agonist concentrations (< 1  $\mu$ M) was only taken into account when the cell subsequently showed a response to a higher agonist concentration. When the agonist was administered repetitively, the response was only included in the analysis when the membrane potential and input resistance returned to pre-drug values.

### **Solutions for electrophysiological recording**

The pipette solution used in all experiments contained (in mM): K-MeSO<sub>4</sub> 120, KCl 20, HEPES 10, EGTA 0.2, ATP (magnesium salt) 2, phosphocreatine (disodium salt) 10, GTP (tris-salt) 0.3. In most recordings, 2-4 % neurobiotin (Vector Labs, Burlingame, CA, USA) was added for morphological analysis (see below). The osmolarity of the solution before addition of neurobiotin (50  $\mu$ l volume; dissolved in *A. bidest.*) was approximately 295 milliosmo (mOsm).

In current clamp experiments, ACSF (see *Preparation of thalamic slices*) was used as extracellular solution (solution I). In experiments investigating the effect on K<sup>+</sup> currents, Na<sub>2</sub>HPO<sub>4</sub> was omitted (solution II). In experiments in which the extracellular K<sup>+</sup> concentration was elevated to 5 mM, this was compensated by an equimolar amount of NaCl. Where indicated, the I<sub>h</sub> blocker ZD7288 (20  $\mu$ M) was routinely added to the perfusing saline as it is also activated in negative voltage range (e.g. Takigawa and Alzheimer, 2002) and this current has been shown to be influenced by alpha-2 ARs in the CNS (e.g. Yagi and Sumino, 1998). The voltage-gated sodium channel blocker tetrodotoxin (TTX; 0.5-1  $\mu$ M) was added to the bath solution where indicated to functionally isolate neurons from presynaptic influences. Liquid junction potentials between the intracellular solution and solution I (10.9 mV) and the

intracellular solution and solution II (11.2 mV) were calculated with pClamp software (Barry, 1994) and taken into account according to Neher (1992).

### **Chemicals and drugs for electrophysiological recording**

All chemicals and drugs were obtained from Sigma (Taufkirchen, Germany) except TTX and ZD7288, which were from Tocris (Langford, UK), and tertiapin, which was obtained from Alomone Labs (Jerusalem, Israel). The drugs were added to the external ACSF from stock solutions, except for alpha-methyl-norepinephrine, which was weighted out freshly before each experiment. All drugs were applied directly to the recording chamber. The volume of the ACSF in the recording chamber was approximately 3 ml. The final concentrations which are indicated in the graphs were calculated assuming an ACSF volume of 3 ml.

### **Histochemical detection of neurobiotin**

In most experiments, the tracer neurobiotin (2-4%, see *Solutions for electrophysiological recording*) was added to the pipette solution to fill the neuron throughout the recording time. After recording for at least 20 min, the pipette was carefully withdrawn from the membrane and slices containing neurobiotin-filled cells were immersion-fixed for 24-48 h in 4% paraformaldehyde (PFA). They were then processed after a slightly modified protocol from Hammam and Kennedy (2003). Each slice was processed in a single well of a standard 24 well plate (Corning Inc., NY, USA) per step. The tissue was gently agitated on an orbital shaker (model Titramax 1000; Heidolph, Schwabach, Germany).

. All procedures were carried out at room temperature, except where indicated. First, the slices were washed 3 times in phosphate-buffered saline (PBS) for 10 min and incubated in a solution of 1% H<sub>2</sub>O<sub>2</sub> in 70% methanol for 30 min to suppress endogenous peroxidase activity. The tissue was then incubated in a solution containing 1% normal goat serum (Vector Labs) and 0.3% Triton X-100 in PBS to block non-specific protein binding and to permeabilize the cells. Subsequently, the slices were incubated in avidin-biotin-complex (ABC) reaction solution (Vector Labs), prepared according to the manufacturers instructions, at 4°C overnight. The following day, the slices were washed in PBS 3 times for 5 min, one time for 30 min, one time for 60 min and finally overnight. On the fourth day, the tissue was equilibrated by washing for 3 times in tris-buffered saline (TBS, pH 7.6) and the histochemical reaction was completed by incubating the slices for 3-10 min in a solution containing 0.04% NiCl<sub>2</sub>, 0.5 mg per ml 3,3'-diaminobenzidine (DAB) and 0.01% H<sub>2</sub>O<sub>2</sub> (Vector Labs) in TBS. The reaction was monitored under a light microscope (Axioskop, Zeiss) and stopped after 3-15 min by rinsing the slices 3 times for 10 min in TBS. The tissue was then dehydrated in an ascending series of ethanol (30-100%) for 10 min at each concentration,

cleared by two times incubation in xylene for 10 min. The slices were coverslipped using a xylene-based medium (Eukitt; Kindler, Freiburg, Germany).

### **Morphometric analysis of neurons**

The labeled cells were visualized with a light microscope (Axioskop, Zeiss) and evaluated for staining-quality criteria. Only cells that were entirely stained in dark black color and possessed at least two dendrites each with secondary branches were used for analysis. If a neurite appeared thinner compared to other processes of the cell and was uniform in diameter from its origin at the soma, it was identified as axon and therefore not included in the dendritic analysis. If one or more primary dendrite(s) were cut close to the cell body, as indicated by sudden termination of a branch going towards the surface of the slice, the dendritic tree of this cell was not included in the dendritic analysis. In these cells, only data concerning the cell body was taken into account (see below; Table 1). Optimally labeled cells were quantified for dendritic morphometry using NeuroLucida software (MicroBrightField Inc., Colchester, VT, USA) in combination with an automated stage and focus control connected to a microscope (Zeiss II RS) equipped with a 40x oil immersion objective (N.A. 1.0, Zeiss). The final magnification on the screen was 40 000x. The data were collected as line drawings. A correction factor to account for the shrinkage of tissue during ethanol dehydration and xylene clearance was not applied. Such a correction factor would not influence the statistical significance of the results, but is used to compare the results to previous studies which – as mentioned above – are not available in this case. To give an approximate estimation of the error, Kole (2003) used a similar protocol to visualize neurobiotin-filled CA3 pyramidal neurons and determined a correction factor of 1.35. Numerical analysis and graphical processing of the neurons was performed with Neuroexplorer software (MicroBrightField). In order to evaluate the distribution of dendritic arborizations in detail, the dendrites were subject to Sholl analysis (Sholl, 1953). In this analysis, a series of virtual circles (“Sholl circles”; see Fig. 3) is drawn around the soma (center of the soma set at zero) with a fixed starting radius that is incremented by the same amount as the starting radius. These radii can be defined by the experimenter. The first Sholl circle radius and the increments used in this analysis were 10  $\mu\text{m}$ . The numbers of intersections of the cell processes with these circles, as well as the summed dendritic length within two circles can be determined by the Neuroexplorer software (MicroBrightField). So-called Sholl plots were then constructed by plotting the intersections with the circles or the summed dendritic length within two circles as a function of distance from the soma. In the latter case, the outer Sholl circle radius is indicated in the graphs. When dendrites ended between two circles, the dendritic length within these two circles was added to the previous pair of circles (Neuroexplorer manual).

The use of 400  $\mu\text{m}$  slices greatly facilitates the reconstruction of the complete dendritic structure of a neuron, as opposed to the procedure of sectioning the slice into thinner sections, but does not allow to resolve the anatomical fine structures such as dendritic spines due to the thickness of the slice (see also Ishizuka et al, 1995; Henze et al., 1996), so the present measurements of dendritic length and surface should be accepted tentatively as estimates. Statistics on morphological parameters were performed using the software Prism (GraphPad).

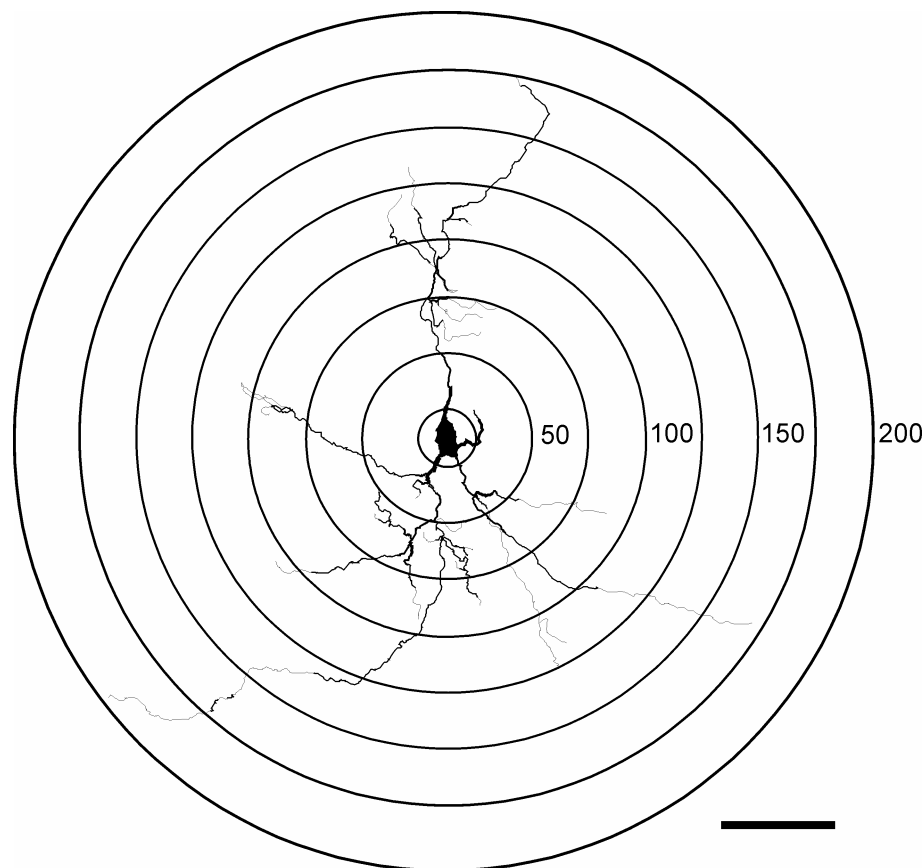


**Figure 3.** Schematic description of the Sholl analysis. Drawing of a PVT neuron stained with neurobiotin. In the Sholl analysis, a series of virtual circles is drawn around the soma (the center of the soma is set as zero; circles are superimposed on the drawing). Then, the numbers of intersections with the circles and the summed dendritic length within two circles can be determined. For clarity, this example shows a Sholl circle radius is 25  $\mu\text{m}$  (the distances from the center of the soma, in  $\mu\text{m}$ , are shown on the right hand side of the respective circles), although in the present study dendritic morphology was analyzed with a Sholl circle radius of 10  $\mu\text{m}$ . See text. Scale bar: 50  $\mu\text{m}$ .

## **Immunocytochemistry**

Immunocytochemistry was performed as described (Hökfelt et al., 1984). All incubations were carried out on an orbital shaker (model Titramax 1000; Heidolph). For staining with anti-dopamine-beta-hydroxylase (DBH; Biotrend Chemikalien, Cologne, Germany) antibody, coronal vibratome sections of rat brain (40 µm) were incubated for 1.5 h in 0.4% Triton-X in 3% normal sheep serum (nss) in TBS. Subsequently, sections were treated with 1% H<sub>2</sub>O<sub>2</sub> for 15 min, followed immediately by a 1 h incubation in 0.1 M lysine, 1% nss, 0.1% Triton-X-100 in TBS (TAT). Sections were then incubated with the antibody directed against DBH (diluted 1:1000 in TAT) for 3 days at 4°C. Subsequently, sections were washed 2 times for 10 min in 2% milk powder in TBS, and then incubated with goat-anti-rabbit antibody (DAKO, Glostrup, Denmark) diluted 1:70 in bovine serum albumin (BSA) for 2.5 h, followed by a 10 min wash in 2% milk powder in TBS. Sections were incubated for 2.5 h with rabbit peroxidase-anti-peroxidase (PAP) complex (DAKO) diluted 1:100 in BSA. This was followed by two washes in TBS. Anti-DBH immunoreactivity was detected through a DAB Kit (Vector Labs) according to the manufacturer's instructions. After a final wash in TBS, sections were dehydrated in an ascending series of alcohol and mounted in a xylene-based medium (Eukitt; Kindler).

For staining with the antibody against phenylethanolamine-N-methyl-transferase (PNMT; Biotrend Chemikalien; diluted 1:2000 in TAT), vibratome rat brain sections (40 µm) were washed in 0.1 M PBS. They were then incubated for 30 min in 0.5% H<sub>2</sub>O<sub>2</sub> and subsequently washed in PBS containing 0.5% Triton-X, followed by 1 h incubation in 5% normal goat serum (ngs; Vector Labs) in 0.5% Triton-X-PBS. To block nonspecific binding of the antibody, sections were incubated for 1 h in 5% ngs, 0.5% Triton-X-PBS. Sections were subsequently incubated with the antibody (diluted 1:1000 in TAT) for 3 days at 4°C. Then, sections were incubated with a biotinylated goat-anti-rabbit antibody (DAKO) diluted 1:400 in 1% ngs in 0.5% Triton-X-PBS and afterwards washed overnight at 4°C in 0.5 Triton-X-PBS. Sections were incubated for 2 h in streptavidin-horseradish peroxidase (Vector Labs) diluted 1:200 in 1% ngs in 0.5% Triton-X-PBS. This was followed by two times washing for 5 min in PBS and a wash in 0.05 M Tris (pH 7.2 with HCl) for 5 min. Anti-PNMT immunoreactivity was detected with a DAB-Kit (Vector Labs) according to the manufacturer's instructions. After final washing steps in 0.05 M Tris (pH 7.2 with HCl) and in 0.1 M PBS, sections were dehydrated in an ascending series of ethanol (30-100%) for 10 min at each concentration and mounted in a xylene-based medium (Eukitt; Kindler).

## ***In vitro* receptor autoradiography with [<sup>3</sup>H]RX821002**

In order to investigate alpha-2 AR binding, cryostat sections of the tree shrew brain from the anatomical level P 5.0 (Tigges and Shanta, 1969) of one *Stress*, one *Recovery* and one *Control* animal were mounted side by side on the same slide. Three sections per radioligand



concentration and animal were used to determine total binding (24 sections per animal for the eight concentrations of radioligand corresponding to 120 sections per each group of animals). Sections were labeled with [<sup>3</sup>H]RX821002 (specific activity 67  $\mu$ Ci per mmol; Amersham Pharmacia Biotech UK Limited, Buckinghamshire, UK) as described previously (Flügge, 1996). Briefly, incubations were performed in 50 mM Na<sup>+</sup>/K<sup>+</sup> phosphate buffer, pH 7.4, containing 10  $\mu$ M pargyline, for 60 min at 37°C. To detect nonspecific binding, a 1000-fold excess of the alpha-2 agonist UK 14,304 (Research Biochemicals International, Natick, MA, USA) was added to the incubation medium. Sections were then washed twice in cold phosphate buffer, dipped into cold water and dried under a stream of cold air. For determination of  $B_{max}$  values, saturation experiments with 0.05 to 8.0 nM [<sup>3</sup>H]RX821002 were performed. Quantification of binding was performed by autoradiography with tritium-sensitive Hyperfilm-<sup>3</sup>H (Amersham, Braunschweig, Germany). Sections were exposed together with <sup>3</sup>H-microscale standards for five weeks. Autoradiograms were quantified by computerized image analysis using the Microcomputer Image Device (software AIS; Imaging Systems, St. Catherines, Ontario, Canada). Gray values of the microscale standards were used to determine the amount of radioactivity bound to the tissue and expressed as fmol per mg tissue equivalent. Nonspecific binding was subtracted from total binding to yield specific binding.  $B_{max}$  and  $K_d$  values were calculated by non-linear regression using GraphPad Prism software (GraphPad). Data were evaluated with ANOVA and Scheffé *post hoc* test using the same software.

Competition experiments were performed to characterize binding of [<sup>3</sup>H]RX821002 to the thalamic alpha-2 ARs in the rat brain. The ability of imiloxan, an allegedly selective alpha-2B receptor antagonist (Michel et al., 1990), UK14,304, a specific alpha-2 agonist and chlorpromazine, an antagonist at D<sub>2</sub>-like dopamine receptors, to displace [<sup>3</sup>H]RX821002 binding (specific activity 60  $\mu$ Ci per mmol; Amersham Pharmacia Biotech UK Limited) in the PVT and the LC was investigated on coronal cryostat brain sections (10  $\mu$ m) of an adult Wistar rat (Harlan-Winkelmann). The concentrations of the competitors were 10<sup>-11</sup> to 10<sup>-4</sup> M. In the presence of the different competitors, sections of the PVT as well as sections of the LC, where the alpha-2B adrenoceptor is not expressed, were incubated with [<sup>3</sup>H]RX821002, four sections per each concentration of radioligand for the PVT and two sections for the LC, as described previously (Flügge, 1996). Incubations were performed in 50 mM sodium potassium phosphate buffer, pH 7.4, containing 10  $\mu$ M pargyline and 5 mM MgCl<sub>2</sub>, for 60 min at 37°C. The sections were then washed two times for 2 min each in cold phosphate buffer, 30 s in cold water and dried under a stream of cold air. Quantification of binding was performed by autoradiography with tritium-sensitive Hyperfilm-<sup>3</sup>H (Amersham, Braunschweig, Germany). Sections were exposed together with <sup>3</sup>H-microscale standards (Amersham) for ten weeks. The resulting autoradiograms were quantified by computerized image analysis

using the AIS software. Gray values of the microscale standards were used to determine the amount of radioactivity bound to the tissue and expressed as fmol per mg tissue equivalent. Nonspecific binding was subtracted from total binding to yield specific binding.  $B_{max}$  and  $K_d$  values were calculated by non-linear regression using GraphPad Prism software (GraphPad).

### ***In situ* hybridization**

In order to obtain a specific probe for *in situ* hybridization experiments, a cDNA for the tree shrew alpha-2B AR gene was cloned using RT-PCR techniques by Dr. H. Meyer (Meyer, 2000). The clone contains the complete coding region of the receptor gene (GeneBank accession No. AY150333). Alignment of sequences showed 91% DNA sequence identity with the human (Lomasney et al., 1990) and 84% identity with the rat gene (Zeng et al., 1990) (Meyer, 2000). The cDNA was ligated into plasmids (pGEM; Promega, Madison, WI, USA) possessing promoters for both SP6 and T7 bacterial RNA polymerases oriented in opposite directions near the cloning site. For *in situ* hybridization, the plasmid was cut with XhoI (Fermentas, St. Leon-Rot, Germany) to generate a 1356-nucleotide fragment complementary to the cloned cDNA fragment (antisense), or with BamHI (Fermentas) to generate the sense probe. The linearized cDNA was *in vitro* transcribed with the Riboprobe In Vitro Transcription System (Promega), using SP6-polymerase to produce the antisense and T7-polymerase for the sense probe in the presence of [<sup>33</sup>P]UTP (500 µCi; ICN Radiochemicals, Asse-Reglem, Belgium). The probes were purified with S400 HR MicroSpin columns (Pharmacia, Freiburg, Germany). To quantify alpha-2B AR mRNA in thalamic nuclei and single neurons, respectively, frozen brains from *Control*, *Stress* and *Recovery* animals were cut on a cryostat, and sections (10 µm) were thaw-mounted on gelatin-coated slides. Brain sections from the same anatomical level (P 5.0 according to Tigges and Shanta, 1969) of one *Stress*, one *Recovery* and one *Control* animal were mounted side by side on the same slide. Three sections per animal (corresponding to three slides) were subjected to the *in situ* hybridization procedure (15 sections per group of animals). The cryostat sections were then dried at room temperature for 20 min, fixed in 4% PFA, rinsed in PBS, dehydrated through graded alcohols, air-dried and stored at -80° C. The *in situ* hybridization was performed as previously described (Meyer et al., 2000) with two modifications: (1) hybridization was carried out at 60°C for 18 h and (2) when washing the sections, RNase treatment was followed by a high stringency wash (0.2 x SSC; NaCl/Na<sup>+</sup> citrate), 60 min, 65°C). The labeled sections were exposed on BioMax film (Kodak, Rochester, NY, USA) for 7 days at 4° C. The specificity of the antisense hybridization signal was checked by comparing it with sections hybridized with the sense probe. Alpha-2B AR mRNA expression was visualized on films using the Microcomputer Image Device and the software AIS (Imaging Systems). Anatomical

localization of thalamic nuclei was performed with the aid of an atlas of the tree shrew brain (Tigges and Shanta, 1969). To visualize hybridization on the cellular level, slides were coated with NTB2 nuclear emulsion (Kodak) and exposed for 25 days at 4°C. Silver grains were developed in D 19 (Kodak). Slides were rinsed in water and fixed with Unifix (Kodak). Sections were faintly counterstained with 0.05% toluidine blue in 0.1% di-sodium tetraborate. Silver grains over single neurons were inspected with a light microscope (Carl Zeiss, Jena, Germany) using a 40x oil immersion objective (Axioplan-APOCHROMAT; N.A. 1.0) connected to a digital camera (DAGE-MTI, Michigan City, IN, USA) and the AIS software. Silver grains were quantified in neurons of the PVT inspecting observation areas of approximately 15 750  $\mu\text{m}^2$  (magnification of objects on the screen was 15 000x) on the three sections from each animal. Within the observation areas, labeled cells were defined as those displaying at least five times more silver grains per sample area than the surrounding area. In all sections these were in total 3 103 cells in the *Control*, 3 050 cells in the *Stress*, and 2 843 cells in the *Recovery* animals in the PVT. Cell bodies and nuclei of neurons were delineated manually and the relative number of silver grains over the cytoplasm was determined as number of pixels (mean size of a silver grain: 5.2 pixels). Nonspecific labeling (mean number of silver grains on sections hybridized with the sense probe) was subtracted to obtain specific labeling. For statistical analysis, data were subjected to analysis of variance (ANOVA) and Tukey's *post hoc* test using GraphPad Prism software (GraphPad).

### **Animal experiments**

Male tree shrews (*Tupaia belangeri*) from the breeding colony at the German Primate Center were used for the chronic social stress experiments. The animal experiments were performed by Dr. M. van Kampen. All animal experiments were in accordance with the European Communities Council Directive of November 24, 1986, (86/EEC) and with the National Institutes of Health Guide for the Care and Use of Laboratory Animals, and were approved by the Government of Lower Saxony, Germany. Animals were singly housed on a regular day/night cycle (lights on from 08:00 to 20:00 h) at 26°C, 55% relative humidity with tree shrew diet (Altromin, Lage, Germany). They were accustomed to frequent handling since their birth. The experimental groups (*Control*, *Stress*, *Recovery*, n = 5 per group) and the experimental design are displayed in Fig. 4. The first experimental phase (*No Stress*) lasted 10 days, during which all animals remained undisturbed. The second phase of the experiment was a 44-day period, during which the animals of the *Stress* and the *Recovery* group were submitted to daily psychosocial conflict. For the induction of the psychosocial conflict, each naïve male was introduced into the cage of a socially experienced male. After establishment of a clear dominant/subordinate relationship, the two animals were separated by a wire mesh barrier. As in earlier studies (Fuchs et al., 1996; van Kampen et al., 2002) all

of the naïve animals became subordinate. The barrier was removed every day for approximately 1 h allowing physical contact between the two males only during this time. By this procedure, the subordinate animal was protected from repeated attacks, but it was constantly exposed to olfactory, visual and acoustic cues from the dominant. Under these conditions, subordinate animals displayed characteristic subordination behavior such as reduced locomotor activity and marking behavior (see Fuchs and Flügge, 2002). The third experimental phase consisted of the recovery period lasting 10 days (Fig. 4). During this time the animals were transferred to their home cages and remained undisturbed. Animals of the *Control* group were individually housed and undisturbed in separate quarters elsewhere in the animal facility. During all experimental phases body weight from all animals was recorded and morning urine was collected daily before lights on. The stress level of the subordinates was determined by measuring daily body weight and cortisol in morning urine. Free cortisol was determined using a scintillation proximity radioimmunoassay with anti-rabbit antibodies (Paesel and Lorei, Frankfurt, Germany) bound to fluomicrospheres, according to the manufacturers' instructions with [<sup>3</sup>H]cortisol as the tracer (Amersham, Braunschweig, Germany; see Fuchs et al., 1996). Resulting data were related to creatinine concentrations, which were determined with a Beckman Creatinine Analyzer 2 (Beckman Diagnostics, Fullerton, CA, USA) to correct for physiological dilutions. Physiological data were grouped in blocks representing the different phases of the experiment: *No Stress* (days 1–10), *Stress 1* (days 11–21), *Stress 2* (days 22–32), *Stress 3* (days 33–44), *Stress 4* (days 44–54), and *Recovery* (days 55–64). The data were analyzed by repeated measures analysis of variance (ANOVA) followed by Dunnet's *post hoc* test using the software Prism (Graph Pad) to detect significant differences compared with the *No Stress* phase. At the end of the experimental period, animals were decapitated between 08:00 and 09:00 h. The brains were immediately removed and frozen over liquid nitrogen.

<b>Group</b>	<b>Experimental Phases</b>		
<b><i>Stress</i></b>	<i>no stress</i>	<i>psychosocial stress</i>	
<b><i>Recovery</i></b>	<i>no stress</i>	<i>psychosocial stress</i>	<i>no stress</i>
<b><i>Control</i></b>	<i>no stress</i>	<i>no stress</i>	<i>no stress</i>
<b>Days</b>	<b>1-10</b>	<b>11-54</b>	<b>55-64</b>

**Figure 4.** Time course of the stress experiment in male tree shrews. *Control* animals remained unstressed during the entire experimental period of 64 days. After the initial 10 days *no stress* phase, *Stress* and *Recovery* animals passed the 44 days *psychosocial stress* period. Animals of the *Recovery* group subsequently passed a *no stress* period of 10 days without stress.

## Results

### Part I: Alpha-2 adrenoceptors in the PVT - effects of agonist stimulation and morphology of PVT neurons.

Electrophysiological recordings were derived from a total of 164 neurons in the paraventricular thalamus (PVT). In 90 recordings, neurobiotin was added to the intracellular solution (see *Solutions for electrophysiological recording*).

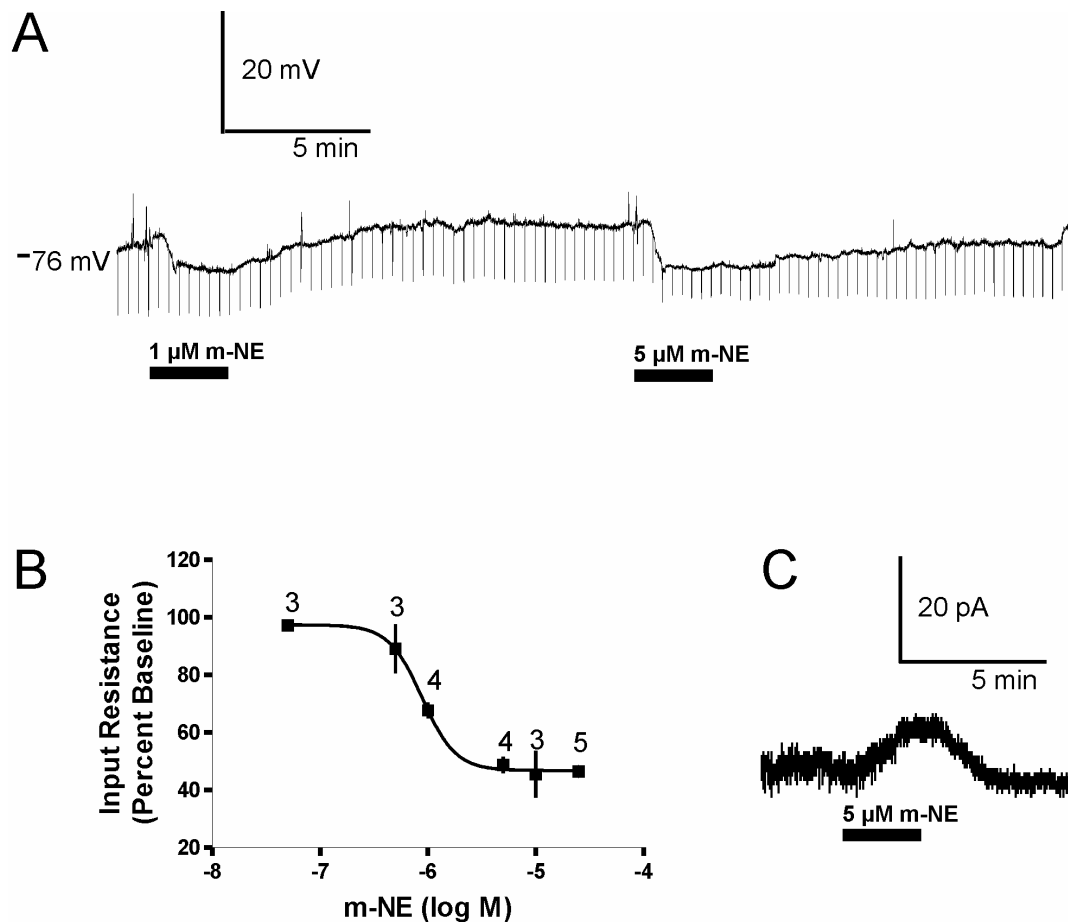
#### Effects of alpha-methyl-norepinephrine on membrane potential and input resistance

Bath application of the alpha-2 agonist alpha-methyl-norepinephrine (m-NE; 0.1 - 25  $\mu$ M) induced different responses in PVT cells. In 17 out of 52 cells, m-NE induced a hyperpolarization of the resting membrane potential (RMP;  $-7.6 \pm 1.1$  mV at 5  $\mu$ M m-NE, determined in  $n = 4$  cells) that was paralleled by a dose-dependent reduction in input resistance ( $48.8 \pm 2.8\%$  at 5  $\mu$ M m-NE, determined in  $n = 4$  cells; Fig. 5A,B; 0.1 - 25  $\mu$ M m-NE). The  $IC_{50}$  value for the reduction in input resistance was 0.88  $\mu$ M.

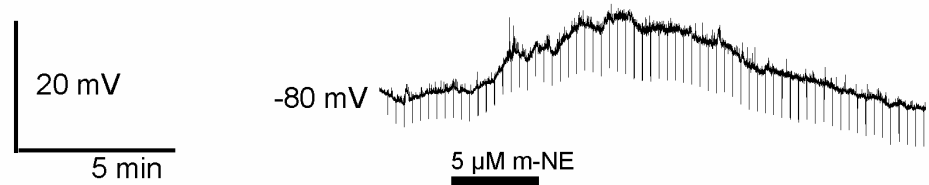
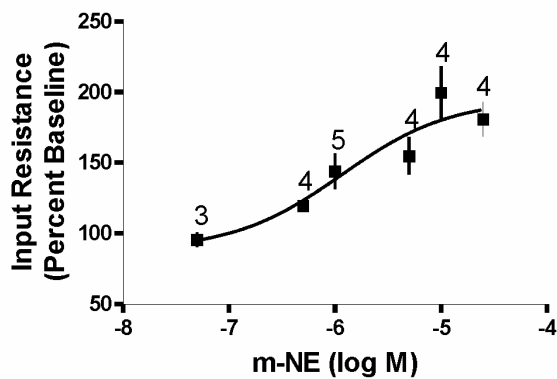
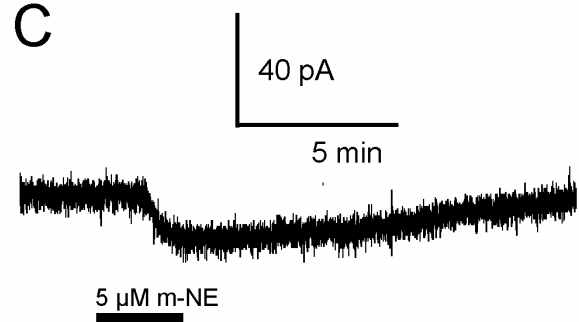
In out of 52 cells, m-NE elicited a slow depolarization of the RMP ( $13.7 \pm 3.8$  mV at 5  $\mu$ M, determined in  $n = 4$  cells; Fig. 6A) accompanied by a dose-dependent increase in input resistance ( $154.8 \pm 13.3\%$  at 5  $\mu$ M, determined in  $n = 4$  cells; Fig. 6B; 0.1 - 25  $\mu$ M m-NE). The  $EC_{50}$  value for the increase in input resistance was 1.16  $\mu$ M. In a third group of cells (14 out of 52), no reliable effect of m-NE (5 - 25  $\mu$ M) on the membrane potential was observed (data not shown). In these experiments, TTX (0.5 - 1  $\mu$ M) was added to the bath solution, thus indicating direct postsynaptic responses of the recorded cells. The three groups of cells (hyperpolarizing, depolarizing, no effect) differed both in baseline membrane potential and input resistance (Fig. 7A,B; ANOVA followed by Tukey's *post hoc* test). In the subsequent long-term current experiments and in the long-term voltage recordings in which the effects of yohimbine, clonidine, phenylephrine and prazosin were assessed, all cells with an input resistance < 200 MOhm were discarded not to record cells that did not react to agonists.

#### Effects of alpha-methyl-norepinephrine on the membrane current

In order to observe the currents induced by m-NE (5  $\mu$ M), voltage clamp recordings were performed (constant holding potential of -76 mV) in the presence of TTX (0.5  $\mu$ M). The hyperpolarizing response was mirrored by an outward current of  $20.5 \pm 5.3$  pA ( $n = 4$ , Fig. 5C). In depolarizing cells, m-NE induced a larger inward current of  $-30.9 \pm 5.2$  pA ( $n = 4$ ; Fig. 6C).



**Figure 5.** Inhibitory actions of m-NE in the PVT (hyperpolarizing cells). Substance applications are indicated below the traces. **A** Long-term voltage recording of a PVT neuron ( $I = 0$  pA). In a subset of cells (17 of 52), m-NE caused a hyperpolarization of the membrane and a concomitant decrease in input resistance. Current pulses of  $-25$  pA were periodically injected (downward deflections). **B** Dose dependent effects of m-NE on the input resistance of PVT cells. A total of  $n = 17$  cells were measured. The number of cells per concentration is indicated in the graph. Note that on 5 cells, two different concentrations of m-NE were tested (see *Determination of membrane potential and input resistance*). **C** Long-term current recording of a PVT cell. In voltage clamp mode, the hyperpolarization was mirrored by an outward current (constant holding potential of  $-76$  mV; see text). The traces in **A** and **C** are from two different cells.

**A****B****C**

**Figure 6.** Excitatory actions of m-NE in the PVT (depolarizing cells). Substance applications are indicated below the traces. **A** Long-term voltage recording of a PVT neuron ( $I = 0$  pA). In a subset of PVT neurons (21 of 52), m-NE caused a depolarization of the membrane and a concomitant increase in input resistance. Current pulses of  $-25$  pA were periodically injected (downward deflections) **B** Dose dependent effects of m-NE on the input resistance of PVT cells. The number of cells per concentration is indicated in the graph. Note that on 3 cells, two different concentrations of m-NE were tested (see *Determination of membrane potential and input resistance*). **C** In voltage clamp mode, the depolarization was mirrored by an inward current (constant holding potential of  $-76$  mV; see text). The data in **A** and **C** are from two different cells.

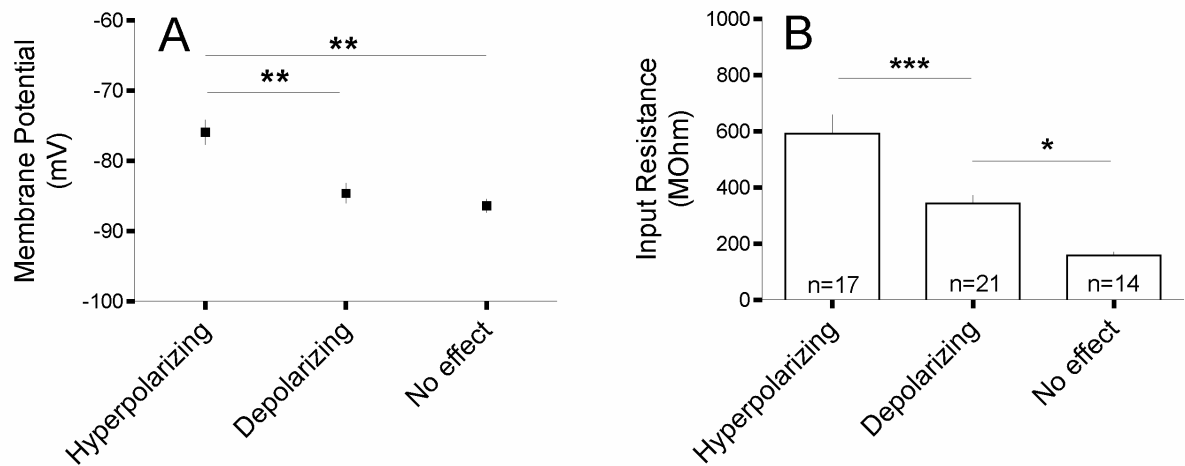


**Figure 7.** The three types of recorded cells differ in their resting properties. When grouped according to their reaction to m-NE, PVT cells differ in membrane potential (**A**) and baseline input resistance (**B**). ANOVA followed by Tukey's *post hoc* test.

### Pharmacological properties of the responses to alpha-methyl-norepinephrine

Current clamp experiments on PVT cells using several adrenergic agonist and antagonist were performed in order to identify the receptors activated by m-NE. In all cases, TTX (0.5  $\mu$ M) was added to the extracellular solution to confirm postsynaptic actions on the recorded cells. The drugs employed were yohimbine (alpha-2 antagonist), clonidine (alpha-2 agonist), low doses of prazosin (alpha-1 antagonist) and phenylephrine (alpha-1 agonist). The baseline input resistance and membrane potential of each group is indicated in brackets. Results (Figs. 8, 9,10) show that the hyperpolarizing effect of m-NE on PVT cells was reversibly blocked by the alpha-2 antagonist yohimbine (1  $\mu$ M; Fig. 8A; n = 4;  $V_m = -79.6 \pm 6.7$  mV;  $R_{in} = 861.6 \pm 69$  MOhm), was not affected by the alpha-1 antagonist prazosin (0.75  $\mu$ M; Fig. 8B; n = 12;  $V_m = -80.3 \pm 2.5$  mV;  $R_{in} = 601.1 \pm 58.6$  MOhm), and mimicked by the alpha-2 agonist clonidine (10  $\mu$ M; Fig. 8C; n = 5;  $V_m = -75.8 \pm 5.6$  mV;  $R_{in} = 779.9 \pm 69.1$  MOhm). In contrast, the membrane depolarization was unaffected by yohimbine (Fig. 9A; n = 7;  $V_m = -85.2 \pm 2.3$  mV;  $R_{in} = 429.5 \pm 39.9$  MOhm). The alpha-1 agonist phenylephrine mimicked the depolarization whereas subsequent application of alpha-2 agonist clonidine had little effect on this group of PVT cells (Fig. 9B; n = 9;  $V_m = -81.7 \pm 3.1$  mV;  $R_{in} = 397 \pm 10.9$  MOhm). The alpha-1 antagonist prazosin irreversibly blocked the depolarization (Fig. 9C; n = 7;  $V_m = -83.6 \pm 1.5$  mV;  $R_{in} = 363.2 \pm 58.6$  MOhm), and clonidine (10  $\mu$ M;  $V_m = -83.4 \pm 2.6$  mV;  $R_{in} = 378.4 \pm 60.3$  MOhm Fig. 10A) had little effect on this type of cell. According to their reaction to the above mentioned drugs, cells were assigned to either the group of hyperpolarizing cells or



depolarizing cells (Fig. 10). Cells in which the depolarizing effects of m-NE were irreversibly blocked by prazosin, or which showed little effect to the application of clonidine alone, were grouped as depolarizing cells, as their input resistance indicated them to belong to this group of cells.

Taken together, these results show that the inhibitory effect of m-NE in the PVT is mediated by alpha-2 adrenoceptors, whereas the depolarizing effect appears to be due to a stimulation of alpha-1 adrenoceptors.

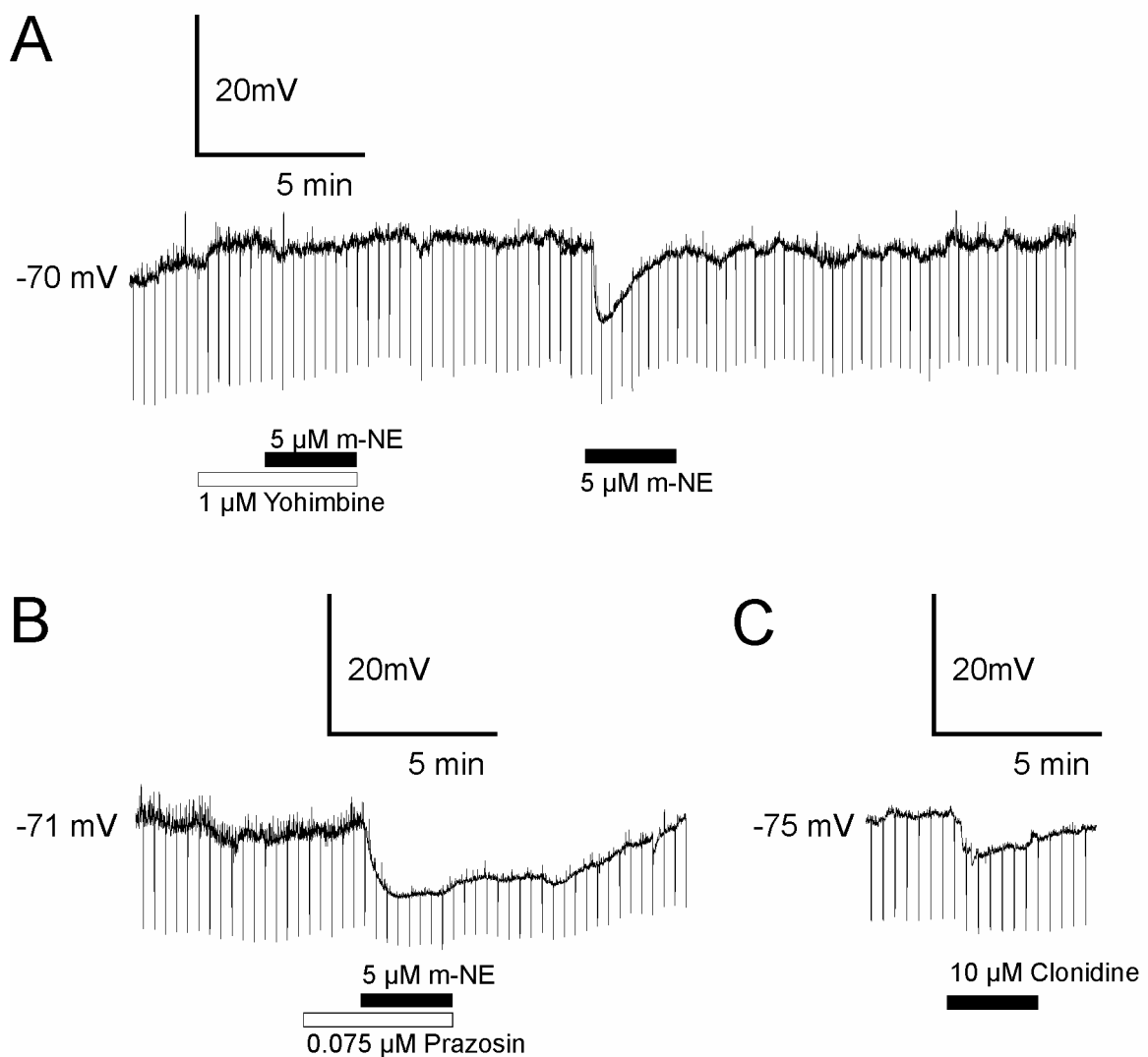


**Figure 8.** The inhibitory response to m-NE is mediated by alpha-2 adrenoceptors. Representative traces of long-term voltage recordings of three PVT cells (A - C; hyperpolarizing cells). Substance applications are indicated below the traces. **A** The hyperpolarizing response was reversibly blocked by yohimbine. **B** The alpha-1 antagonist prazosin did not block the hyperpolarizing effect. **C** The hyperpolarizing effect was mimicked by the alpha-2 agonist clonidine.

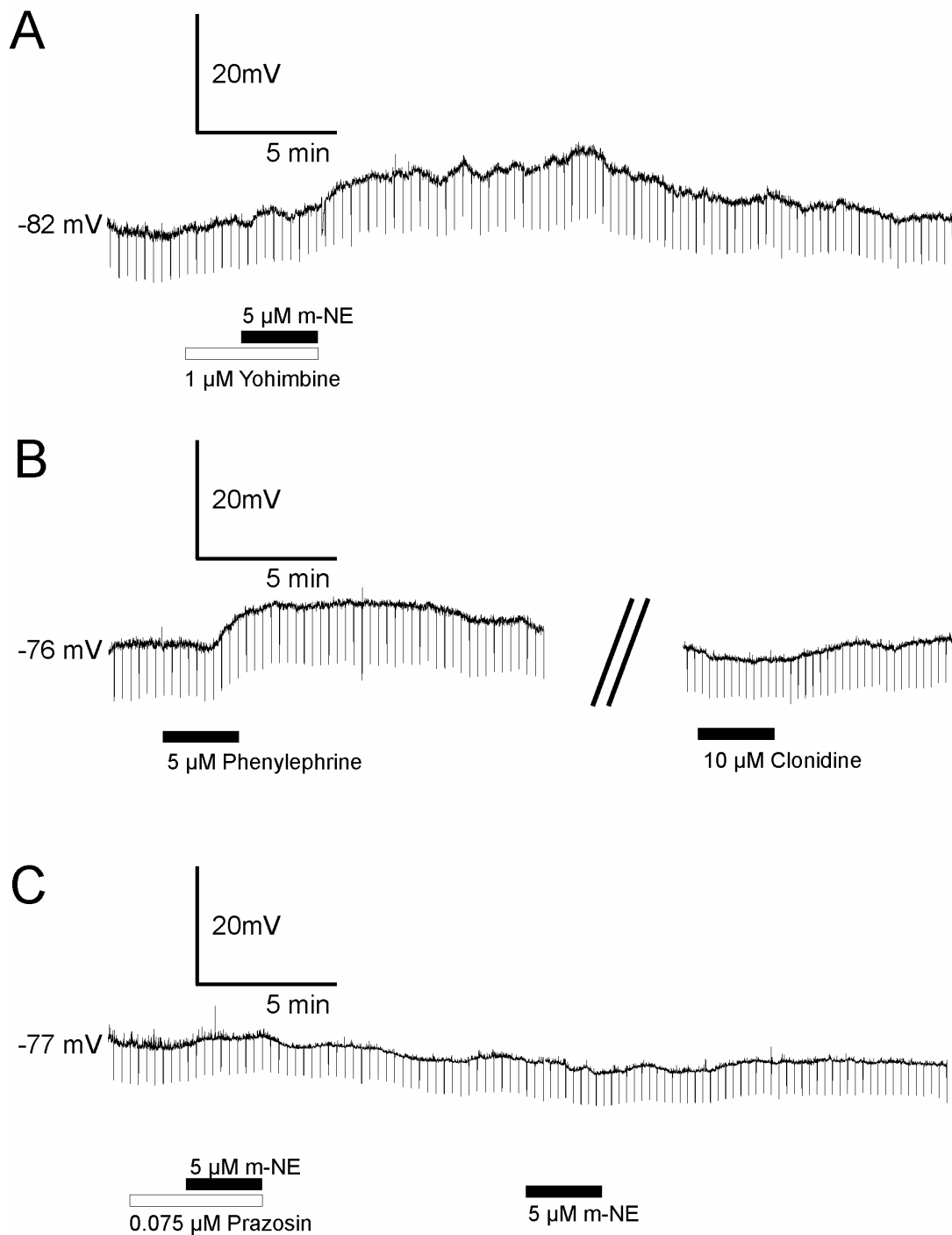
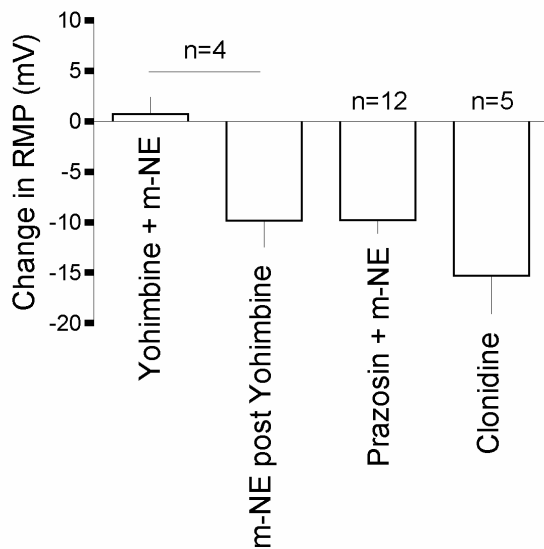


**Figure 9.** The excitatory response to m-NE appears to be mediated by alpha-1 adrenoceptors (depolarizing cells). Representative traces of long-term voltage recordings of PVT cells. Substance applications are indicated below the traces. The depolarizing response was not affected by yohimbine (**A**), was mimicked by phenylephrine (**B**) and was irreversibly blocked by prazosin (**C**). When clonidine was applied to the same cells which had been depolarized by phenylephrine, only a minor hyperpolarizing effect was observed (**B**).

## Hyperpolarizing Cells



## Depolarizing Cells

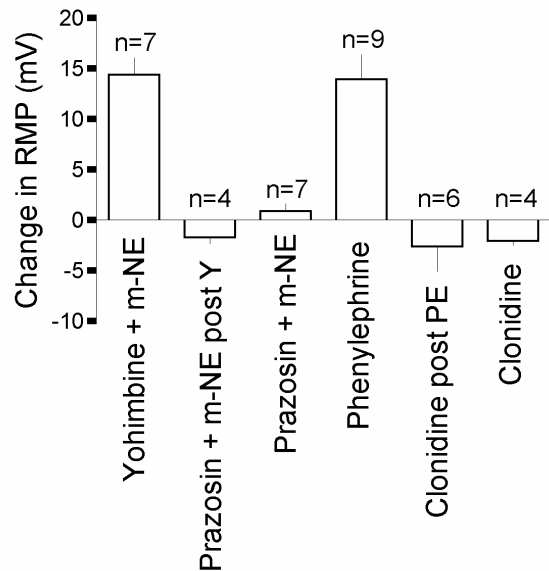


**Figure 10.** Alpha-2 adrenoceptors mediate the inhibitory effect of m-NE, and alpha-1 adrenoceptors appear to mediate the excitatory effect of m-NE in the PVT. Summary of the effects of different agonists and antagonists on the resting membrane potential (RMP) of PVT cells. The cells were grouped according to their reaction to m-NE (left: hyperpolarizing cells; right: depolarizing cells). Cells in which prazosin irreversibly blocked the putative depolarization or in which clonidine had little effect were grouped as depolarizing cells (see text). For dosage of drugs see text. The numbers of cells measured are indicated above the columns. *Abbreviations:* m-NE, alpha-methyl-norepinephrine; PE, phenylephrine; Y, yohimbine.

### Influences of alpha-methyl-norepinephrine on neuronal firing

The firing of PVT cells and its modulation by m-NE was investigated in a total of 37 PVT cells. Sixteen cells hyperpolarized,  $n = 10$  cells depolarized and  $n = 11$  cells did not show any change in the membrane potential after m-NE ( $5 \mu\text{M}$ , all cells) application. Passive properties of the cells are listed in Table 1. Figure 11 illustrates the two different firing modes observed in the PVT, burst and tonic firing. Both firing modes were observed in PVT cells, regardless of their reaction to m-NE.

The hyperpolarizing actions of m-NE on PVT cells via an alpha-2 mediated effect are depicted in figure 12. Upon application of m-NE,  $n = 4$  cells changed from tonic to burst firing mode (Fig. 12A). In  $n = 7$  cells, m-NE reduced excitability so that a purely passive response of the membrane was observed to the same current step (Fig. 12B). In these cells, the burst firing mode was observed before and after application of m-NE. It was also found that a

subset of PVT cells ( $n = 5$ ) fired spontaneously at the resting membrane potential (Fig. 13A-C). This spontaneous firing was completely abolished by application of m-NE and was reversible in 4 of 5 cells. Influences of the depolarizing actions of m-NE via a putative alpha-1 mediated effect on PVT cell firing are depicted in Fig. 14. In  $n = 5$  cells, m-NE enhanced the excitability so that spike firing was observed at a lower current step than before agonist application (Fig. 14A). Of these cells,  $n = 4$  fired in burst mode and  $n = 1$  cell fired in tonic mode before and after application of m-NE. It was also found that in  $n = 5$  cells, the depolarizing actions of m-NE brought the cells into a state of spontaneous firing (Fig. 14B). This effect was reversible in  $n = 3$  cells. Cells in which the RMP was not altered by m-NE all fired in burst mode, both before and during application of the agonist (Fig. 15).

**Table 1.** Summary of the resting properties of the investigated cells and the actions of m-NE (5  $\mu$ M) on spike firing. In the spontaneously firing cells, the input resistance was not determined. The data were analyzed by one-way ANOVA (the p value is indicated in the right column) followed by Tukey's *post hoc* test. *Symbols*:; \* - significance compared to *No effect*  $p < 0.05$ ; \*\* - significance compared to *No effect*;  $p < 0.01$ . *Abbreviations*: AP – action potential; exc. – excitability; freq. – frequency; RMP – resting membrane potential; spont. – spontaneous.

	<i>Hyperpolarizing</i>	<i>Depolarizing</i>	<i>No effect</i>	<i>p</i>
<b>Total number of cells (n)</b>	<b>16</b>	<b>10</b>	<b>11</b>	
<b>Input resistance</b>				
Baseline (M $\Omega$ )	469.3 $\pm$ 50**	326.6 $\pm$ 57	224 $\pm$ 22.6	< 0.001
n	11	10	11	
Change (to 5 $\mu$ M m-NE; %)	65.52 $\pm$ 5.85	138.2 $\pm$ 8.5	100.8 $\pm$ 7.4	
n	11	5	11	
<b>Membrane potential</b>				
Baseline (mV)	-76.8 $\pm$ 2.3*	-85.2 $\pm$ 2.2	-85.7 $\pm$ 2.1	< 0.05
n	11	10	11	
Change (to 5 $\mu$ M m-NE ; mV)	-8.7 $\pm$ 1.5	9.6 $\pm$ 3.7	1.0 $\pm$ 0.5	
n	11	5	11	
<b>Change in firing mode</b>				
Tonic to burst (n)	4	-	-	
Reduced exc. (n)	7	-	-	
Spont. firing (n)	5	-	-	
AP freq. (Hz)	2.97 $\pm$ 0.97	-	-	
Increased exc. (n)	-	5	-	
Spont. firing after m-NE	-	5	-	

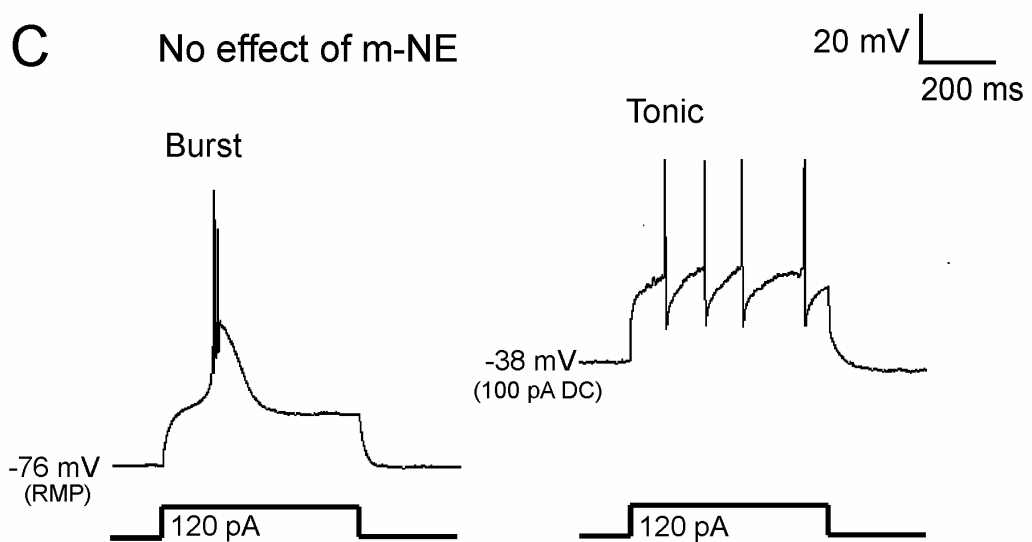
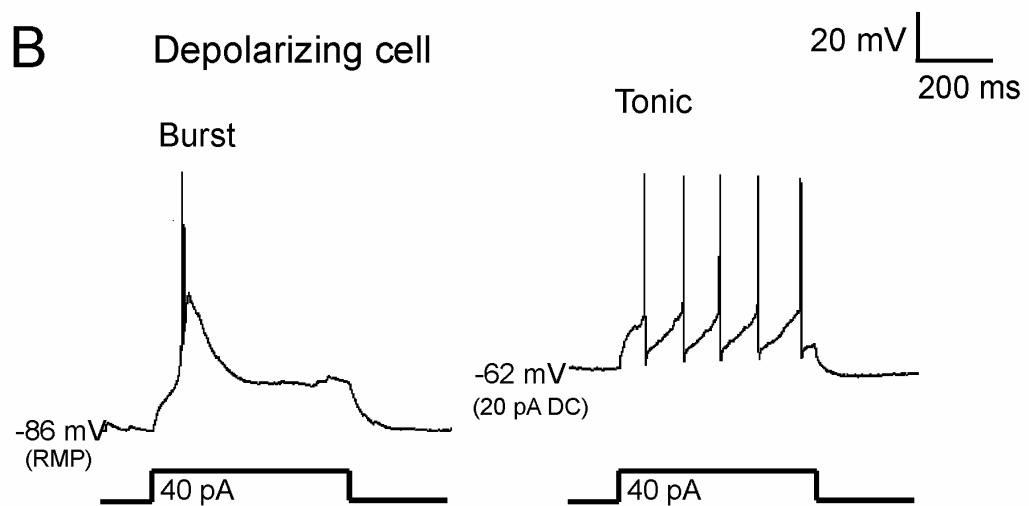
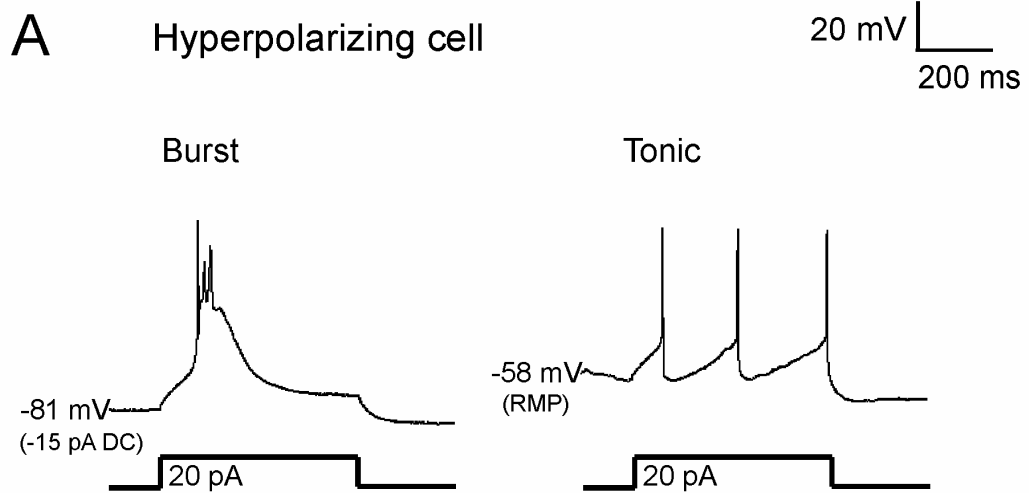


**Figure 11.** [previous page] Burst and tonic firing modes in the PVT. The cells show different firing modes depending on the resting membrane potential (RMP). Note that no agonist was applied; only the membrane potential was altered by direct current (DC) injection. For details see text. **A** PVT cell that hyperpolarized to subsequent application of m-NE (not shown here). Right: at the RMP of approximately  $-58$  mV, a current step of 20 pA elicits tonic firing. Left: when the RMP is hyperpolarized to  $-81$  mV by DC injection ( $-15$  pA), the same current step elicits burst firing. **B** PVT cell that depolarized to subsequent application of m-NE (not shown here). Left: At the RMP of  $-86$  mV, a current step of 40 pA elicits burst firing. Right: when the RMP is depolarized by DC injection (20 pA) to approximately  $-62$  mV, the same current elicits tonic firing. **C** PVT cell on which subsequent application of m-NE had no effect (not shown here). Left: At the RMP of  $-76$  mV, a current step of 120 pA elicits burst firing. Right: when the RMP is depolarized by DC injection (100 pA) to  $-38$  mV, the same current step elicits tonic firing.

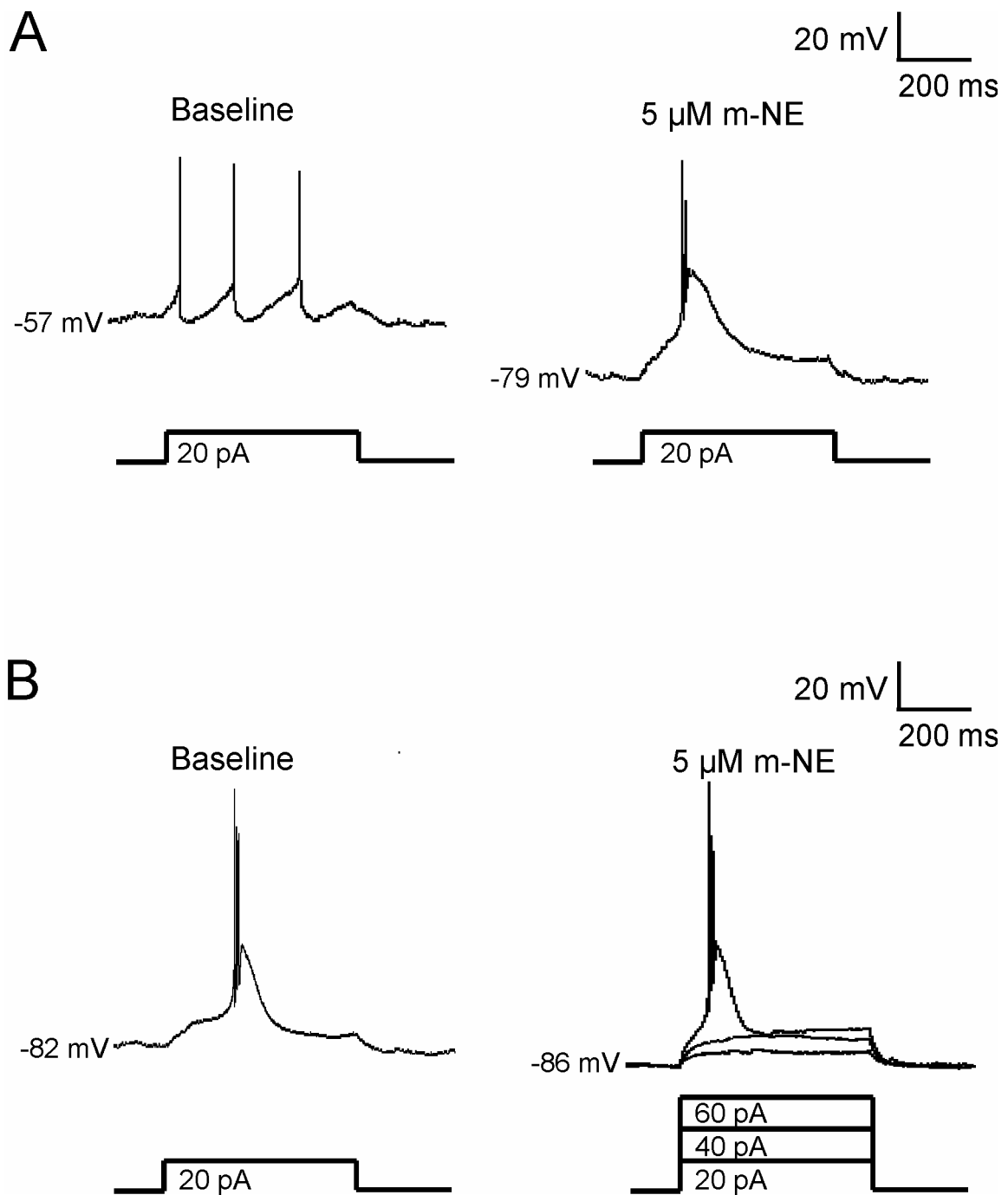


**Figure 12.** The effects of alpha-2 AR activation on the firing of PVT cells. Current clamp experiments ( $I = 0$  pA) of two cells are shown (**A,B**). **A** m-NE can switch firing modes in the PVT. Left: PVT cell in which a current step of 20 pA elicits tonic firing. Right: same cell after m-NE (5  $\mu$ M) is applied and hyperpolarized the membrane. The current step of 20 pA now elicits burst firing. **B** m-NE reduces excitability. Left: PVT cell in which a current step of 20 pA elicits burst firing. Right: After m-NE (5  $\mu$ M) application, the same cell is hyperpolarized. Current steps of 20 and 40 pA now elicit a passive response of the membrane and burst firing is observed when cells are challenged with a 60 pA current step. See text.



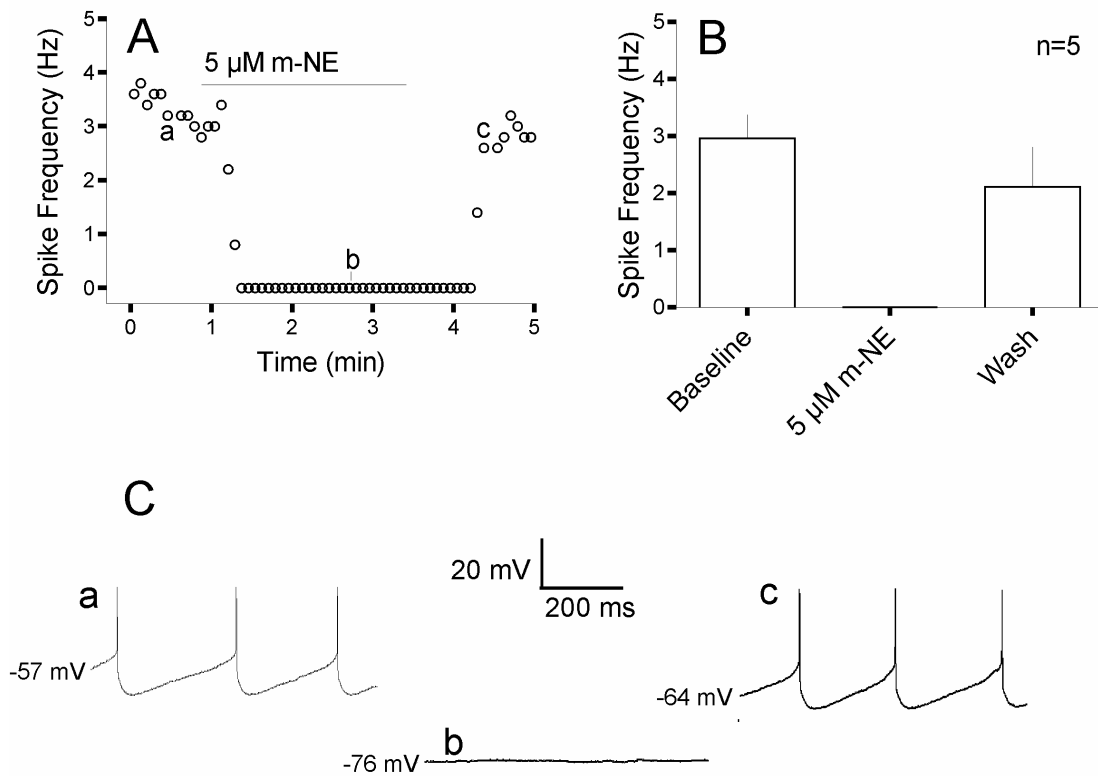


**Figure 13.** Alpha-2 adrenoceptor activation reversibly abolishes spontaneous firing in the PVT. **A** Time course of the inhibitory effect of m-NE (5  $\mu$ M) on spike frequency in one PVT cell that fired spontaneously at the resting membrane potential. Each point represents 5 seconds. **B** Mean inhibitory effect of m-NE (5  $\mu$ M) on spike frequency. The frequency was determined by counting spikes over a period of 20 seconds. The effect was reversible in 4 of 5 cells. **C** Representative membrane potential traces from the time points a, b and c in **A**.

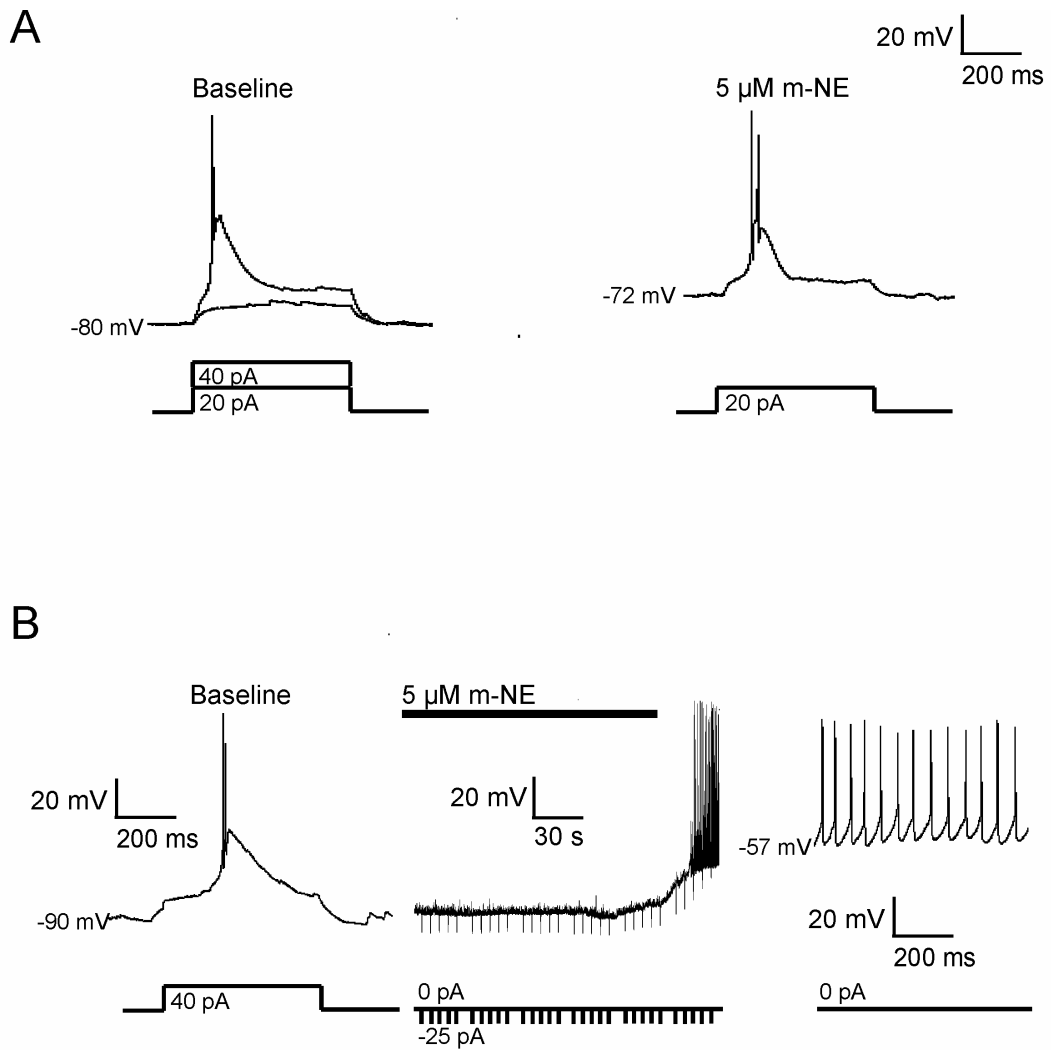


**Figure 14.** The effects of a presumptive alpha-1 AR activation on the firing of PVT cells. **A** Alpha-1 ARs increase excitability. Left: PVT cell under baseline conditions in which a current step of 20 pA elicits only a passive response of the membrane. A current step of 40 pA leads to burst firing. Right: Same cell depolarizes the membrane after m-NE (5  $\mu$ M) is applied. The current step of 20 pA now elicits burst firing. **B** Current clamp traces of one PVT cell that is brought to spontaneous firing by application of m-NE (5  $\mu$ M). Left: Under baseline conditions, challenge with a 40 pA current step leads to burst firing. Middle trace: The cell depolarizes after application of m-NE and starts to discharge spontaneously. Substance application is indicated above the trace. Right: Enlarged membrane potential trace recorded approximately 2 min after the middle trace.

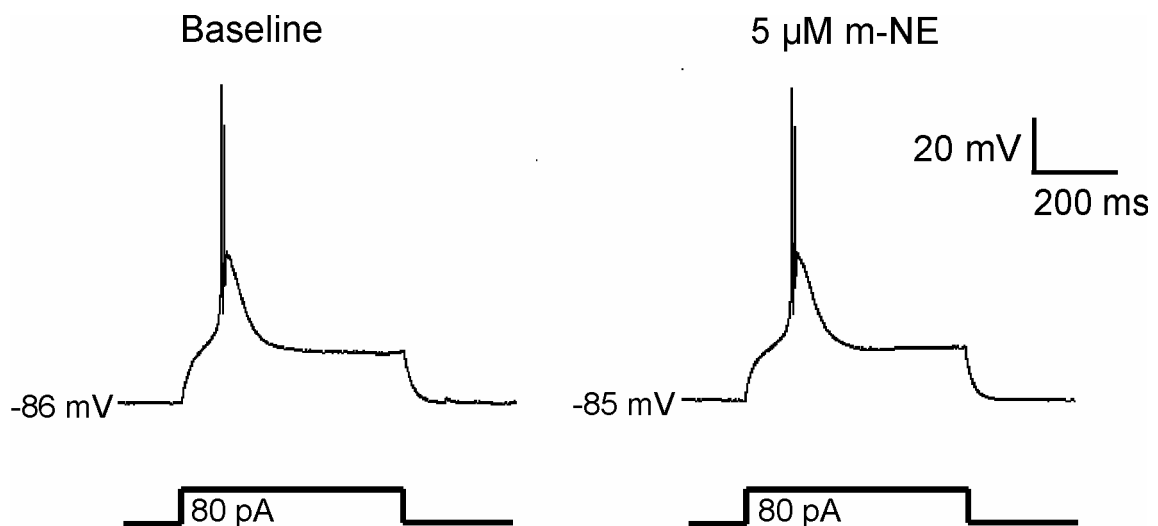
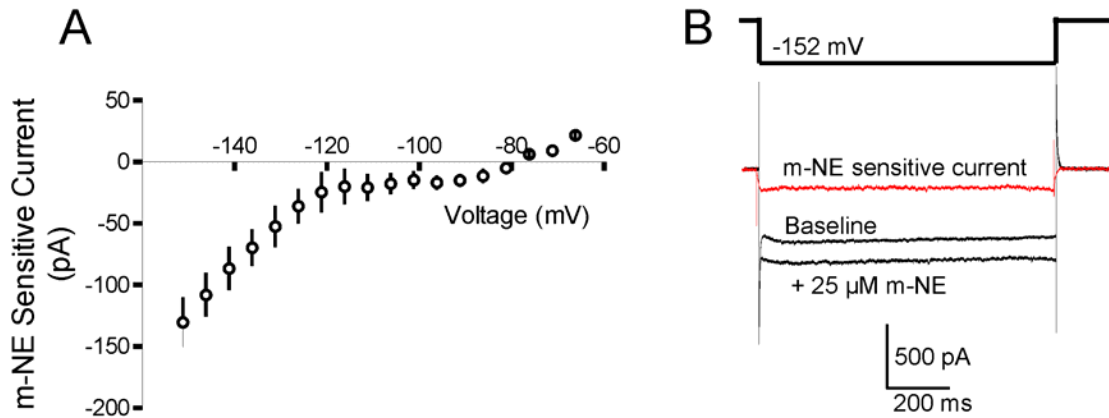


**Figure 15.** In a subset of PVT cells, application of m-NE does not influence firing. The PVT cell depicted here fires in burst mode both before (left) and after application of m-NE (5  $\mu$ M; right). The recording on the right was made approximately 3 min after m-NE was applied.

#### **Involvement of putative $K^+$ conductances in the actions of alpha-methylnorepinephrine**

The possible involvement of  $K^+$  conductances in the inhibitory and excitatory actions of m-NE was investigated as both alpha-2 and alpha-1 ARs have been shown to modulate  $K^+$  currents (e.g. Bünemann, 2001; Osborne et al., 2002). In the presence of the  $I_h$  blocker ZD7288 (20  $\mu$ M; see Methods), hyperpolarizing voltage steps from -67 to -152 mV of 1 sec duration in 5 mV increments elicited inward currents in PVT cells (Fig. 16B,D show the currents elicited by a single step to -152 mV). In these experiments, the extracellular  $K^+$  concentration was elevated to 5 mM. Application of m-NE (25  $\mu$ M) increased these currents in cells that hyperpolarized (Fig. 16A,B;  $n = 4$ ) and decreased them in cells that depolarized (Fig. 16C,D;  $n = 4$ ; the currents were measured at the end of each voltage step). In  $n = 3$  cells, no current was induced (m-NE sensitive current < 50 pA at -152 mV; data not shown). The m-NE-sensitive currents were obtained by subtracting baseline current values from those in the presence of m-NE. The reversal potentials of the m-NE sensitive currents were -79.4 mV for the hyperpolarizing cells and -81.9 mV for the depolarizing cells as calculated by a linear fit of the three points closest to the X-axis, and thus near the Nernst potential for  $K^+$  ( $E_K = -89.0$  mV at 31°C), suggesting a possible involvement of  $K^+$  currents in both the hyperpolarizing and depolarizing actions of m-NE on the membrane potential.

## Hyperpolarizing Cells



## Depolarizing Cells

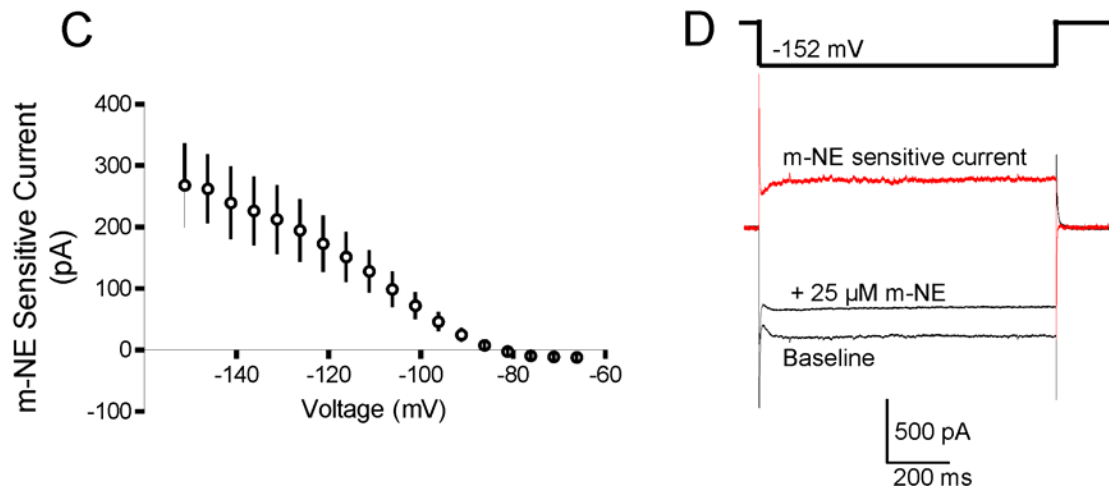


**Figure 16.** The effects of m-NE involve putative  $K^+$  conductances. In these experiments, the extracellular  $K^+$  concentration was elevated to 5 mM and both TTX (0.5  $\mu$ M) and the  $I_h$  blocker ZD7288 (20  $\mu$ M) were added to the perfusing saline (see *Solutions for electrophysiological recording*). Upper panel: **A** In hyperpolarizing cells ( $n = 4$ ) m-NE (25  $\mu$ M) induced a current that reversed near  $E_K$  (see text). **B** Example of one PVT cell in which application of m-NE increased the current in response to a -152 mV step. The trace indicated as m-NE sensitive current (in red color) was obtained by digital subtraction. Lower panel: **C** In depolarizing cells ( $n = 4$ ) also induced a current that reversed near  $E_K$  (see text). **D** Example of one PVT cell in which application of m-NE decreased the current in response to a -152 mV step. The trace indicated as m-NE sensitive current (in red color) was obtained by digital subtraction.

The outward current induced by m-NE in hyperpolarizing cells (Fig. 5C) was further investigated. Application of 50  $\mu\text{M}$  m-NE induced a prolonged outward current of  $30.4 \pm 4.0$  pA (Fig. 17A;  $n = 3$ ) in hyperpolarizing cells. This outward current was sensitive to the  $\text{K}^+$  channel blocker barium (200  $\mu\text{M}$ ), which reduced the outward current (maximal amplitude of  $30.3 \pm 8.8$  pA) to  $29.4 \pm 7.6\%$  ( $n = 5$ ; Fig. 17B; the reduction in current was calculated as ratio of the current amplitude in the presence of 200  $\mu\text{M}$  barium and the current amplitude just before application of the blocker). Application of barium (200  $\mu\text{M}$ ) alone had no effect on the membrane current ( $n = 3$ ; Fig. 17C). Furthermore, the honey bee venom tertiapin (50 nM) which blocks G-protein coupled inwardly rectifying  $\text{K}^+$  channels (Takigawa and Alzheimer, 2002) reduced the outward current induced by 50  $\mu\text{M}$  m-NE (maximal amplitude of  $27.1 \pm 3.3$  pA; same experimental protocol) to  $44.1 \pm 10.5\%$  ( $n = 4$ ; Fig. 17D). Application of tertiapin (50 nM) alone had no effect on the membrane current (Fig. 17E;  $n = 3$ ).

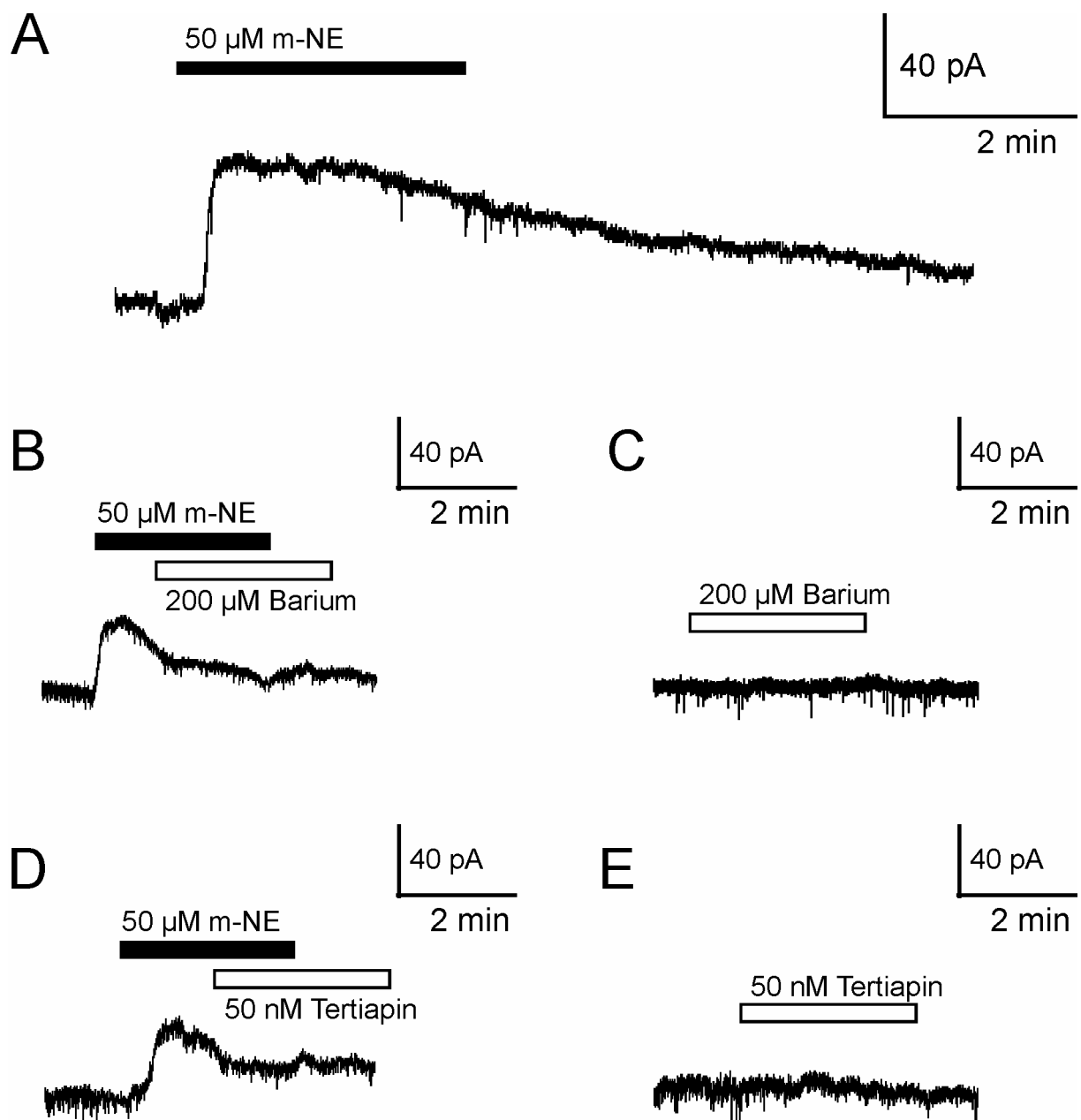


**Figure 17.** The outward current induced by m-NE involves  $K^+$  conductances. Long term current recordings of PVT cells (voltage clamp). All cells were recorded at a constant holding potential of  $-76$  mV. Substance application is indicated above the current traces. **A** Application of  $50 \mu\text{M}$  m-NE induces a prolonged outward current in a subset of PVT cells (determined in  $n = 3$  cells). **B** The current is attenuated by application of the  $K^+$  channel blocker barium ( $200 \mu\text{M}$ ; determined in  $n = 5$  cells), which had no effect when applied alone to PVT cells (**C**;  $n = 3$ ). **D** Furthermore, the current is attenuated by tertiapin ( $50$  nM; determined in  $n = 4$  cells) a blocker of G-protein coupled  $K^+$  channels. **E** Application of tertiapin ( $50$  nM; determined in  $n = 3$  cells) alone to PVT cells had no effect.

### **Morphology of neurons in the paraventricular thalamus**

The complete dendritic tree of 10 cells that hyperpolarized, 12 cells that depolarized and 6 cells that did not react upon application of m-NE could be recovered, allowing quantitative analysis of their essential morphological aspects. Figure 18 shows drawings of three representative cells. Table 2 summarizes data from the cell body and the total dendritic tree of PVT neurons (see *Morphometric analysis of neurons*). All data were compared using a one way ANOVA followed by Tukey's *post hoc* test. A correlation between the total membrane areas and the input resistances of the investigated cells yielded a significant association between these two variables (Fig. 19).

The somata of investigated cells had a round to ovoid appearance and the surface area was significantly larger (approximately 26%;  $p < 0.05$ ) in cells that depolarized to m-NE compared to those that hyperpolarized to m-NE (Table 2). The soma perimeter did not differ between these two groups of neurons, suggesting that the shape of the somata might be different. Indeed, a t-test between those groups revealed a significant difference in the dimensionless roundness factor that describes the relationship between the cell body area and its maximal diameter ( $p < 0.04$ ). A one way ANOVA comparing the three different groups showed a trend towards significance ( $p = 0.076$ ) with this variable. The total number of primary dendrites did not differ between groups. Highly significant differences in the total dendritic length, surface and volume of cells were found between groups ( $p < 0.0065$  in all cases; see Table 2). *Post hoc* analysis showed that cells which did not react to m-NE differed significantly from the groups that reacted to m-NE ( $p < 0.05$ - $0.01$ , see Table 2 for details). The aforementioned parameters did not differ significantly between cells that showed hyperpolarization or depolarization to m-NE. In order to evaluate the distribution of dendritic arborizations in detail, Sholl plots (Sholl, 1953) were created (see Methods; Fig. 3). Results of the Sholl analysis are shown in Fig. 20. The Sholl circle radius used in this analysis was 10  $\mu\text{m}$ . The number of intersections with these circles as well as the summed dendritic length between two circles can be evaluated (see *Morphometric analysis of neurons*). The cells that hyperpolarized to m-NE had a significantly shorter dendritic length at 20 ( $p < 0.001$ ), 40 ( $p < 0.05$ ), 50 ( $p < 0.05$ ), 60 ( $p < 0.01$ ) and 150  $\mu\text{m}$  ( $p < 0.05$ ) distance from the soma and a significantly smaller number of intersections with Sholl circles of 10 ( $p < 0.05$ ), 20 ( $p < 0.001$ ), 30 ( $p < 0.05$ ), 40 ( $p < 0.05$ ), 50 ( $p < 0.001$ ), 60 ( $p < 0.01$ ) and 70 ( $p < 0.01$ ) and 150 ( $p < 0.05$ )  $\mu\text{m}$  than cells depolarizing to m-NE. The aforementioned types of cells differed significantly in dendritic length from the cells in which no clear effect was induced by m-NE (Table 2, Fig. 20).

The axons identified in the present study did often go towards the slice surface, indicating that they were eventually cut, and were thus not further analyzed. Figure 21 shows the approximate location of the morphologically analyzed cell bodies in the PVT. Except for a

lower number of cells depolarizing to m-NE in the middle PVT, no obvious anatomical separation of the cells reacting differentially to m-NE is evident.

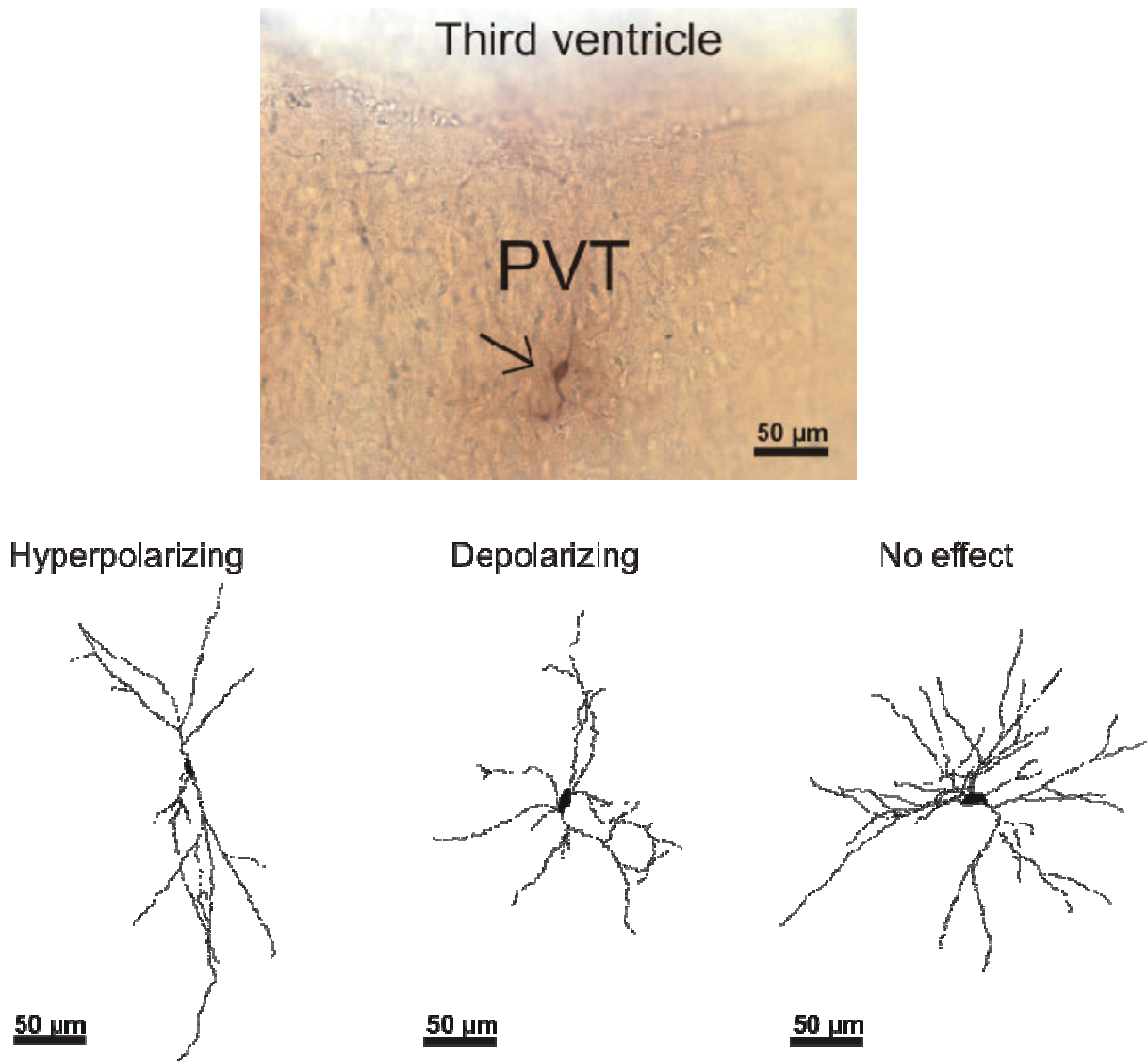


**Figure 18.** Morphology of PVT cells. *Above:* photomicrograph of one neurobiotin-filled PVT cell that depolarized upon application of m-NE (arrow). *Below:* line drawings of PVT cells reacting differently to m-NE. Left: Cell that hyperpolarized upon application of m-NE. Middle: Cell that depolarized upon application of m-NE. Right: Cell that did not show a clear effect upon application of m-NE. The middle drawing was made from the cell depicted in the photomicrograph above.



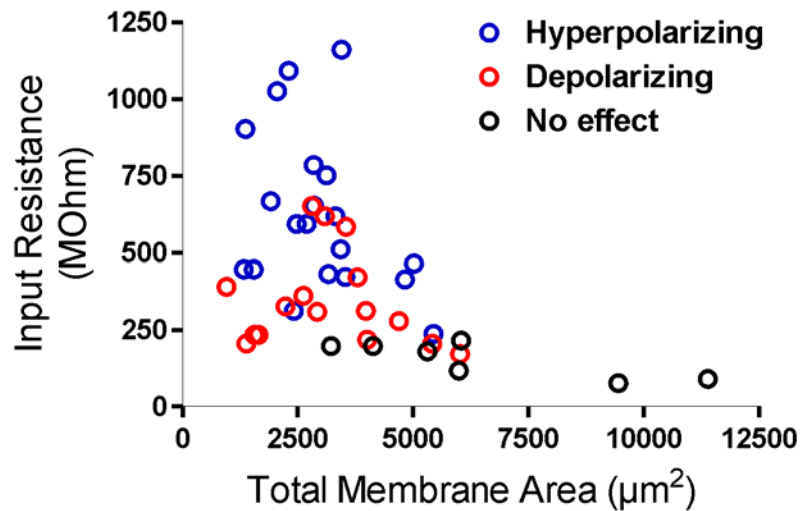


**Figure 19.** Correlation of morphological and physiological data. The graph shows the input resistances of all cells subjected to morphological analysis ( $n = 43$ ) and the corresponding total membrane area (dendritic area + axon area + cell body area). The Pearson correlation coefficient is  $-0.47$  ( $P < 0.0014$ ).

In summary, the data from the first part of this thesis show that a subset of PVT cells hyperpolarize upon application of alpha-2 AR agonists, a subset depolarizes when stimulated with m-NE, most likely due to alpha-1 ARs, while another group of cells does not react to the drug. The data strongly suggest that the hyperpolarizing effect is mediated – at least partially – by G-protein coupled  $K^+$  channels and that the current mediating the depolarizing effect in response to m-NE reverses near the  $K^+$  equilibrium potential, pointing also to an involvement of a  $K^+$  conductance. Also, the data shows that m-NE can change the firing mode of PVT cells, leading to increased burst firing and abolishing spontaneous firing observed in a subset of cells via the alpha-2 AR mediated inhibitory effect. In cells in which m-NE depolarized the membrane via a presumptive alpha-1 AR mediated effect, spontaneous firing is observed in a subset of cells. Furthermore, hyperpolarizing, depolarizing and cells in which m-NE had no clear effect show distinct morphological characteristics. The fact that the values of the resting properties of each group of cells reacting differently to m-NE appear to be normally distributed argues in favor of the hypothesis that these cells form distinct subpopulations within the PVT (Fig. 22).

**Table 2.** Morphological parameters of the analyzed PVT neurons. The cells are grouped according to their reaction of the membrane potential to m-NE. The data were analyzed by one-way ANOVA (the p value is indicated in the right column) followed by Tukey's *post hoc* test. The location of the cells was determined with the help of a rat brain atlas (Paxinos, 1986). *Symbols:* § - significance compared to *Hyperpolarizing*,  $p < 0.05$ ; \* - significance compared to *No effect*  $p < 0.05$ ; \*\* - significance compared to *No effect*;  $p < 0.01$ ; n.s. – not significant.

	<i>Hyperpolarizing</i>	<i>Depolarizing</i>	<i>No effect</i>	<i>p</i>
<b>Cell body</b>				
<b>n</b>	20	16	7	
<b>Soma perimeter (<math>\mu\text{m}</math>)</b>	$58 \pm 3.1$	$59 \pm 3.8$	$60.6 \pm 4.5$	<b>n.s.</b>
<b>Soma area (<math>\mu\text{m}^2</math>)</b>	$98.1 \pm 6.3$	$126.0 \pm 9.0^{\S}$	$112.1 \pm 10.6$	<b>&lt;0.05</b>
<b>Cell body roundness</b>	$0.36 \pm 0.03$	$0.45 \pm 0.04$	$0.36 \pm 0.03$	<b>&lt;0.07</b>
<b>Location of the cells (n)</b>				
<b>Anterior PVT</b>	6	8	2	
<b>PVT</b>	9	3	3	
<b>Posterior PVT</b>	5	5	2	
<b>Total dendritic tree</b>				
<b>n</b>	12	11	6	
<b>Primary dendrites (#)</b>	$4.17 \pm 0.41$	$4.36 \pm 0.34$	$5.67 \pm 1.15$	<b>n.s.</b>
<b>Length (<math>\mu\text{m}</math>)</b>	$1969 \pm 150^{**}$	$2420 \pm 352^*$	$4401 \pm 948$	<b>0.003</b>
<b>Surface (<math>\mu\text{m}^2</math>)</b>	$2813 \pm 204^{**}$	$3408 \pm 431^*$	$5901 \pm 1165$	<b>0.002</b>
<b>Volume (<math>\mu\text{m}^3</math>)</b>	$390 \pm 41^*$	$505 \pm 61^*$	$861 \pm 180$	<b>0.003</b>
<b>Nodes (#)</b>	$10.4 \pm 1.9^{**}$	$15.5 \pm 3.1$	$27.0 \pm 5.1$	<b>0.007</b>
<b>Endings (#)</b>	$15.2 \pm 0.19^{**}$	$19.9 \pm 3.3^*$	$33.7 \pm 3.6$	<b>0.004</b>
<b>Max. branch order</b>	$4.8 \pm 0.3^{**}$	$5.6 \pm 0.5^*$	$7.2 \pm 0.6$	<b>0.004</b>
<b>Total # of axons</b>	4	4	0	

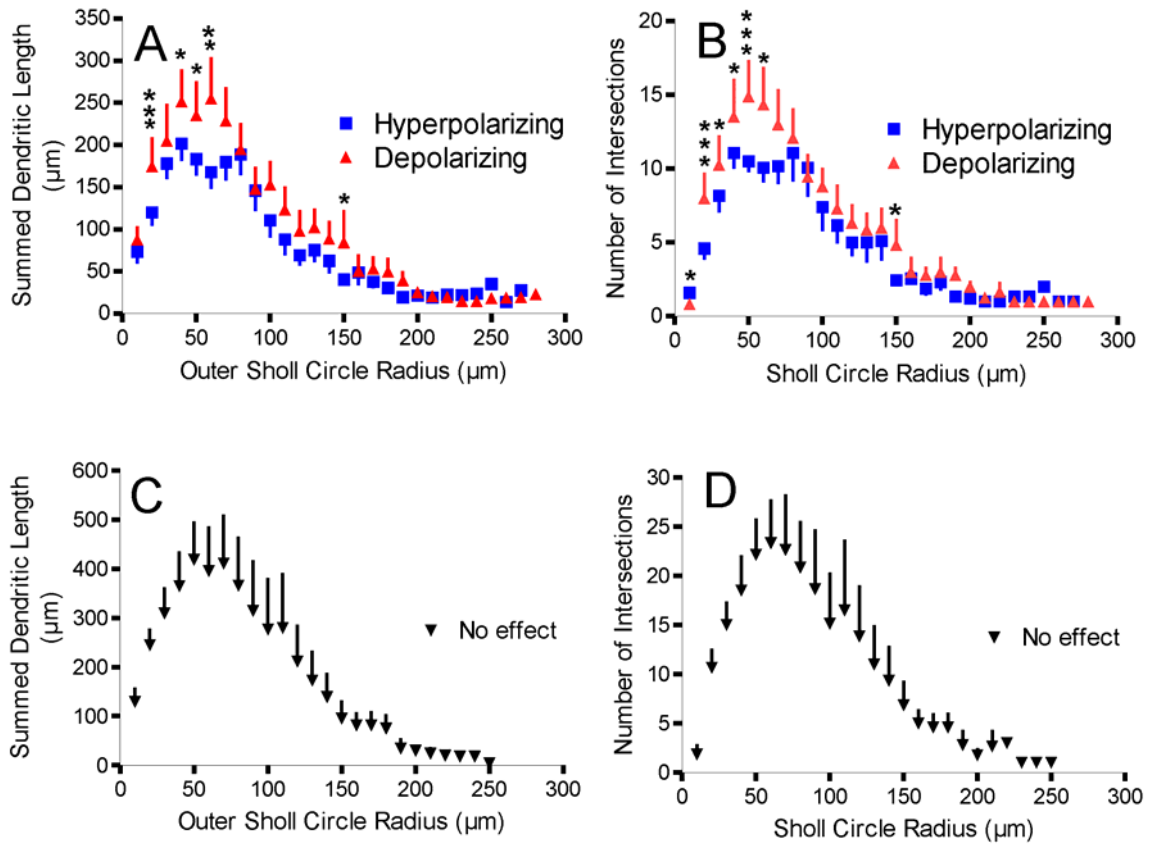


**Figure 20.** Dendritic analysis of PVT cells according to their reaction to m-NE. Sholl analysis of the summed dendritic length within two circles (**A**, **B**) and number of intersections with Sholl circles (**C**, **D**). **A**, **B** The dendritic tree of the two groups of cells (hyperpolarizing versus depolarizing) differed significantly at certain distances from the soma (\* =  $p < 0.05$ , \*\* =  $p < 0.01$ , \*\*\*  $p < 0.001$ ). For statistics see text. **C**, **D** Cells on which application of m-NE had no clear effect had a somewhat shorter but significantly more branched dendritic tree. For statistics see Table 2.

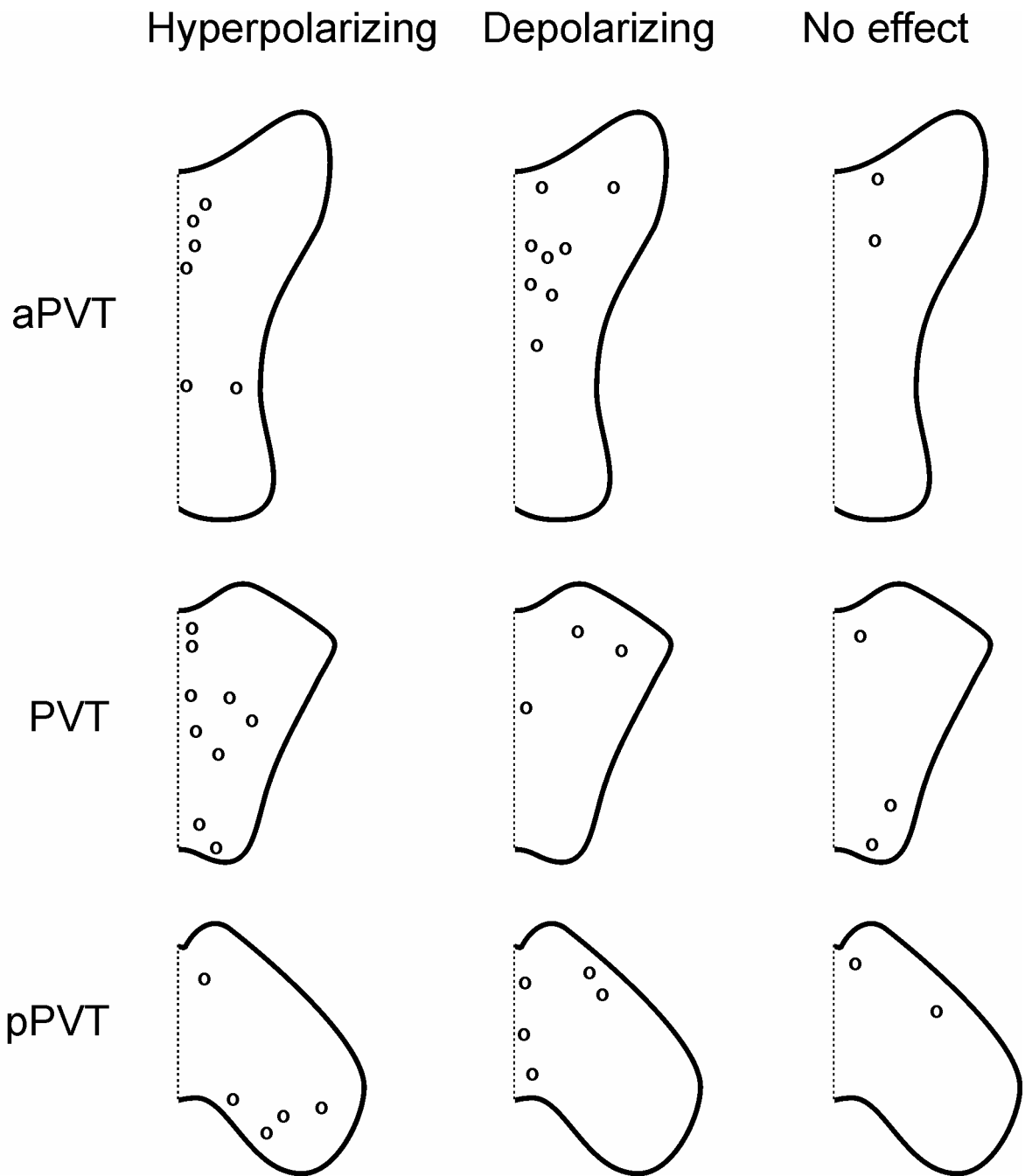


**Figure 21.** Anatomical localization of the morphologically analyzed PVT cell bodies. Shown are drawings of unilateral coronal sections of the rat PVT at different anterior-posterior levels (redrawn from Paxinos and Watson (1986)). The positions of the drawings according to bregma are (in mm): anterior PVT (aPVT): -1.4; posterior PVT (pPVT): -2.56; posterior PVT (pPVT): -3.6. The approximate dorsal-ventral and medial-lateral localization of cell bodies located in the anterior PVT (-1.3 to -2.12 bregma), PVT (-2.3 to -2.8 bregma) and posterior PVT (-3.14 to -3.8 bregma) are indicated in the drawings (circles).

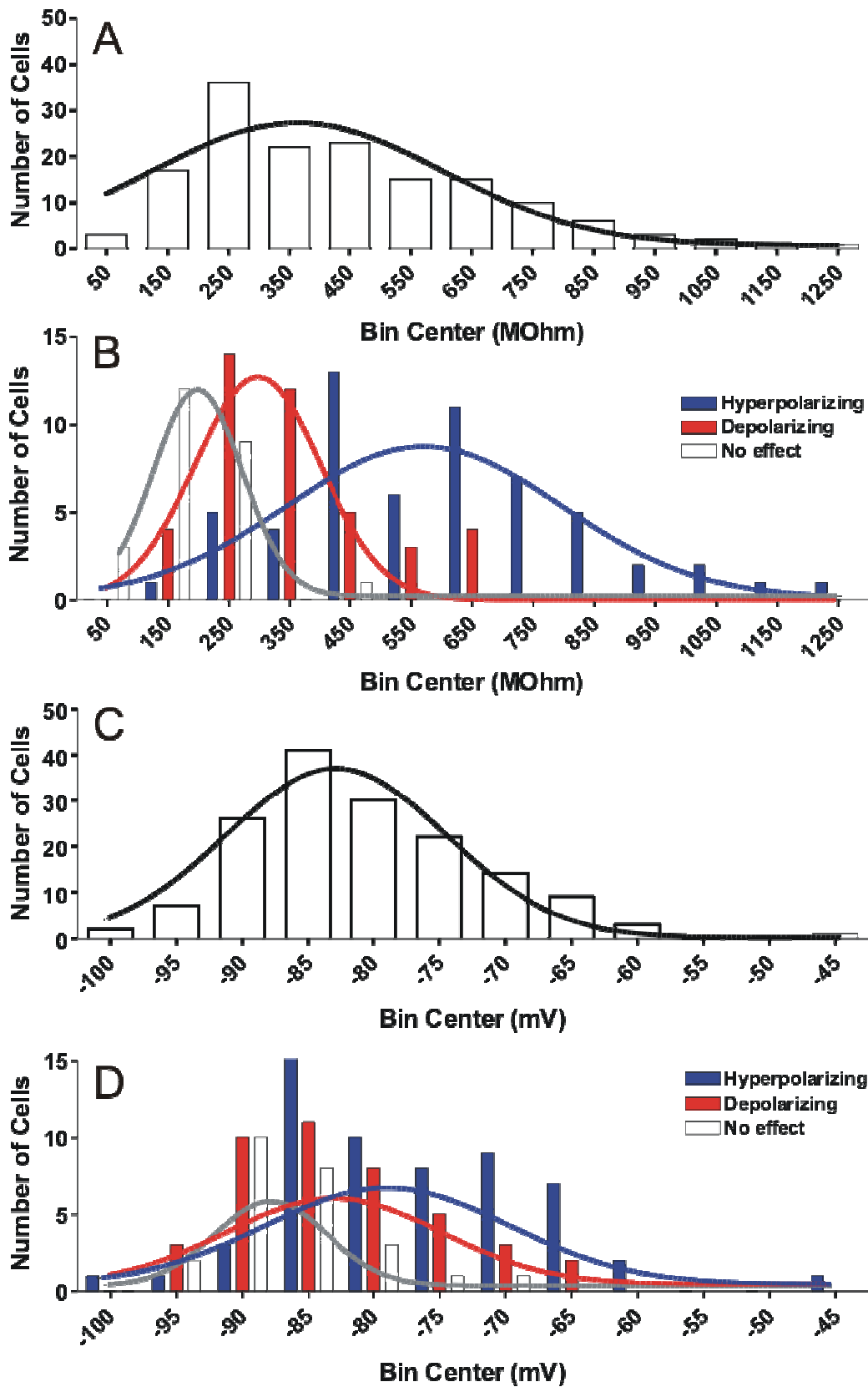


**Figure 22.** [previous page]. In the PVT, cells reacting differently to m-NE appear to form distinct populations. Histograms of the baseline input resistances and membrane potentials of all cells in which these parameters were determined and where no blockers were present in the extracellular solution. Gaussian distributions could be fitted to all the data sets. Deviation from normal distribution was tested using Runs test ( $p > 0.05$ , all cases). The bin sizes were 100 MOhm and 5 mV, respectively. **A** Input resistances of all cells ( $n = 154$ ). The mean input resistance of the cells was  $440.8 \pm 19.2$  MOhm. **B** Input resistances of all cells reacting to m-NE (hyperpolarizing, depolarizing or no effect;  $n = 125$ ). **C** Membrane potentials of all cells. The mean membrane potential of the cells was  $-80.8 \pm 0.7$  mV. **D** Membrane potentials of all cells reacting to m-NE (hyperpolarizing, depolarizing or no effect;  $n = 125$ ).

## Part II: The alpha-2B adrenoceptor is persistently upregulated by chronic psychosocial stress

### Immunocytochemistry with antibodies against dopamine-beta-hydroxylase and phenylethanolamine-N-methyl-transferase

The aim of the second part of the thesis was find out whether expression of the alpha-2 adrenoceptors in the PVT are regulated by chronic stress, a physiological situation accompanied by noradrenergic and adrenergic hyperactivity. To show that the PVT is innervated by noradrenergic fibers, an antibody against dopamine-beta-hydroxylase (DBH) was used. An antibody against phenylethanolamine-N-methyl-transferase (PNMT) was used to visualize adrenergic structures. Figure 23 shows a dense pattern of both DBH and of PNMT immunopositive fibers and nerve terminals in the PVT. These results show that the PVT is strongly innervated by noradrenergic as well as adrenergic fibers.

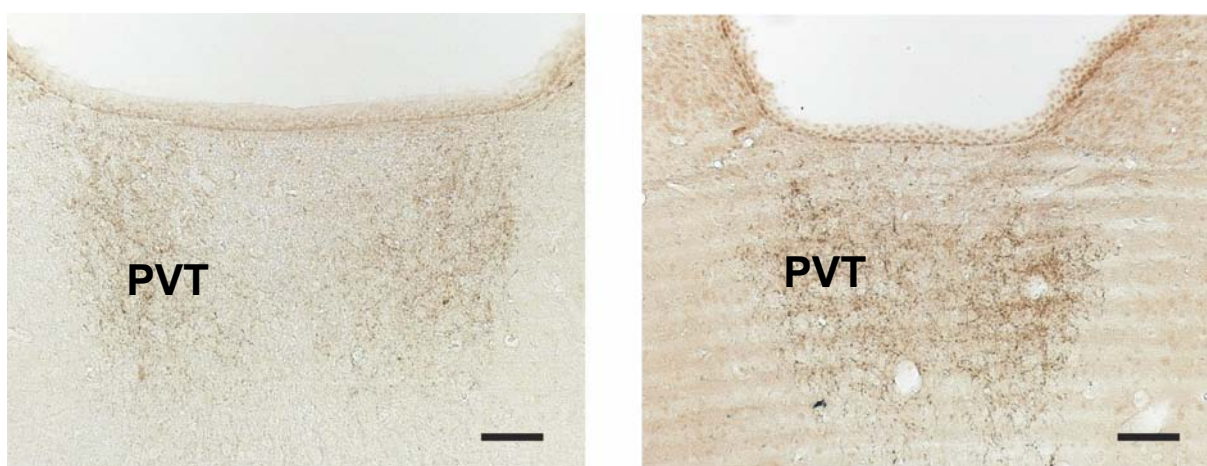


**Figure 23.** Photomicrographs of the rat PVT in coronal brain sections which were stained with an anti-DBH antibody (left) and an anti-PNMT antibody (right; peroxidase-anti peroxidase technique). Note the dense pattern of immunoreactive fibers and nerve terminals (brown color). Scale bars: 250  $\mu$ m.

### Characterization of [ $^3$ H]RX821002 binding in the rat brain: Competition experiments

To visualize alpha-2 adrenoceptor binding in the PVT, binding studies with the antagonist [ $^3$ H]RX821002 were performed on sections of rat brain using *in-vitro* receptor autoradiography. In the first step, binding of this radioligand was characterized by competition experiments. Displacement of [ $^3$ H]RX821002 binding in the PVT where primarily alpha-2B ARs are expressed was compared to that in the locus coeruleus (LC) which is rich

in alpha-2A ARs. Figure 24 shows displacement of [<sup>3</sup>H]RX821002 by UK14,304 (specific alpha-2 agonist), chlorpromazine (a ligand at D<sub>2</sub>-like dopamine receptors) and imiloxan (alpha-2B AR antagonist). In the PVT, IC<sub>50</sub> values for UK 14,304, imiloxan and chlorpromazine were 4.29 nM, 3.40 μM and 2.86 μM, respectively. In the LC, IC<sub>50</sub> values for UK 14,304, imiloxan and chlorpromazine were 3.84 nM, 1.35 μM and 2.52 μM, respectively. The low IC<sub>50</sub> for the specific alpha-2 AR agonist UK 14,304 (4.29 and 3.84 nM, respectively) shows that in both nuclei, PVT and LC, [<sup>3</sup>H]RX821002 binds specifically to alpha-2 ARs.

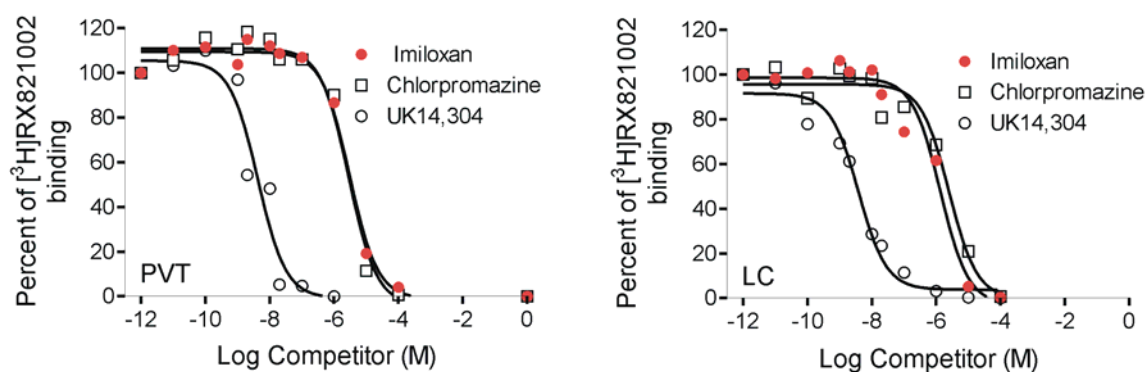


**Figure 24.** Results of the competition experiment. The radioactively labeled ligand used was [<sup>3</sup>H]RX821002. The competitors were imiloxan, chlorpromazine and UK14,304 (see text). Results of the experiment in the PVT (left) and the LC (right) of the rat brain are shown. For the IC<sub>50</sub> values see text.

### Quantification of [<sup>3</sup>H]RX821002 binding in the tree shrew thalamus

In the experiment on the influence of chronic psychosocial stress on alpha-2 ARs, receptor binding was determined by *in vitro* receptor autoradiography (for experimental design see Fig. 4). Film autoradiography revealed strong [<sup>3</sup>H]RX821002 binding in PVT and AV (Fig. 25B). Saturation curves for the PVT showed higher binding in *Stress* and *Recovery* animals than in *Controls* (Fig. 26A), and  $B_{max}$  values revealed that recovery increased radioligand binding in the PVT (Fig. 26B). Although no significant effect on  $B_{max}$  could be detected by one-way ANOVA ( $p = 0.067$ ), Student's t-test showed a significant difference between  $B_{max}$  values of *Control* and *Recovery* animals in the PVT ( $p = 0.046$ ). In the AV, no significant differences in  $B_{max}$  values were found. Receptor affinities ( $K_d$  values, nM) in the PVT of *Control* ( $2.23 \pm 0.37$ ), *Stress* ( $1.53 \pm 0.16$ ) and *Recovery* ( $1.79 \pm 0.24$ ) groups did not differ significantly. In the AV, no significant differences in  $B_{max}$  and  $K_d$  values were detected ( $K_d$  values for AV: *Control*  $1.31 \pm 0.25$ , *Stress*:  $1.08 \pm 0.12$  and *Recovery*  $0.99 \pm 0.15$  nM).



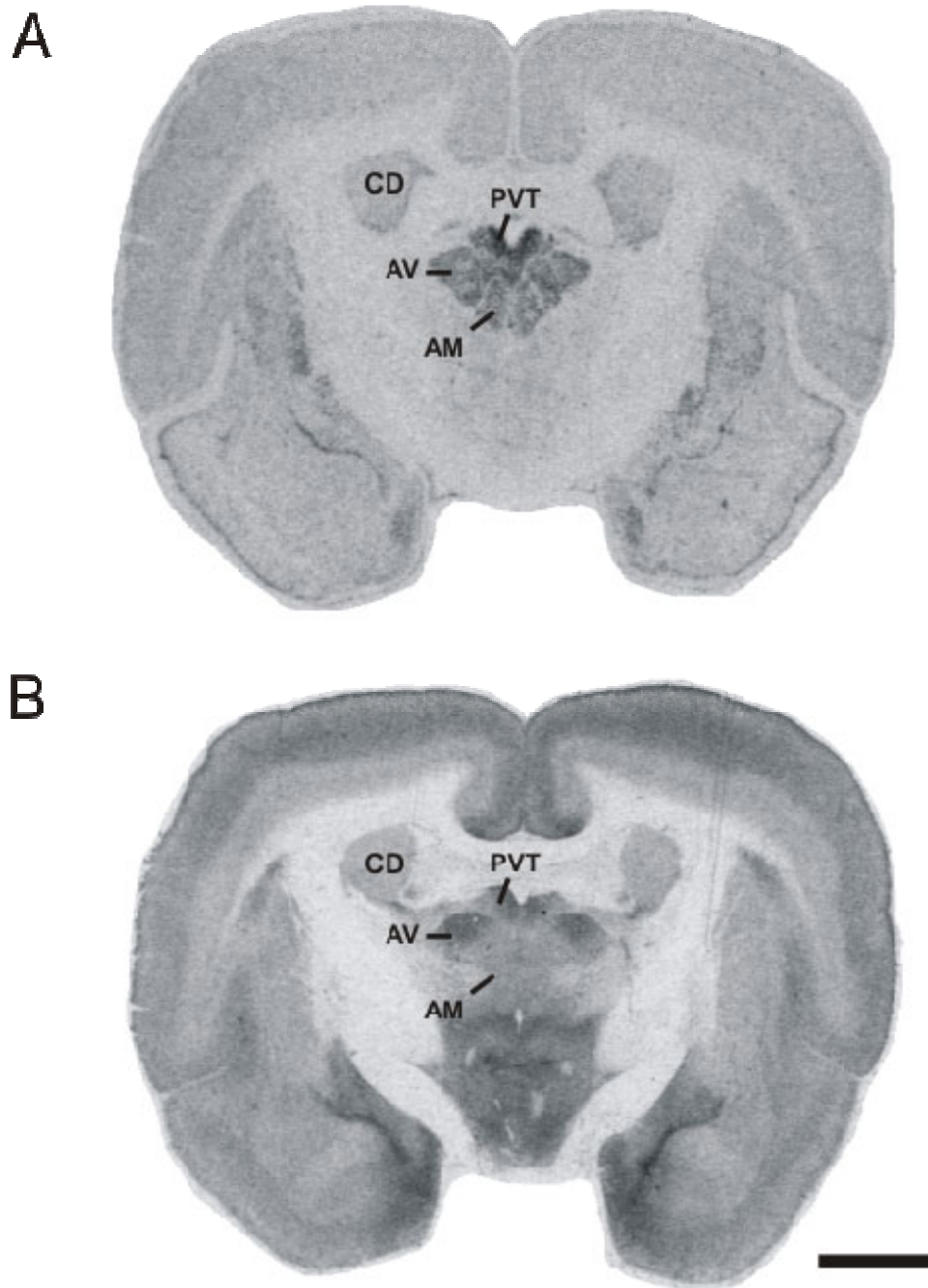


**Figure 25.** Alpha-2B AR expression and alpha-2 AR binding in the anterior thalamus of the tree shrew. (Anatomical level A 5.0 according to Tigges and Shanta, 1969). **A** *In situ* hybridization. Autoradiographic image of a coronal brain section hybridized with  $[^{33}\text{P}]$ UTP-labeled antisense alpha-2B AR cRNA probe. Note the strong hybridization signal in the PVT. No hybridization signals were detected in sections incubated with sense alpha-2B AR cRNA probe (data not shown; see Fig. 27). **B** *In vitro* receptor binding. Autoradiogram of a coronal brain section incubated with  $[^3\text{H}]$ RX821002 (8 nM). Note the strong binding in the PVT and the AV. *Abbreviations:* AM, anteromedial thalamic nucleus; AV, anteroventral thalamic nucleus; CD, caudate nucleus. Scale bar: 25 mm.

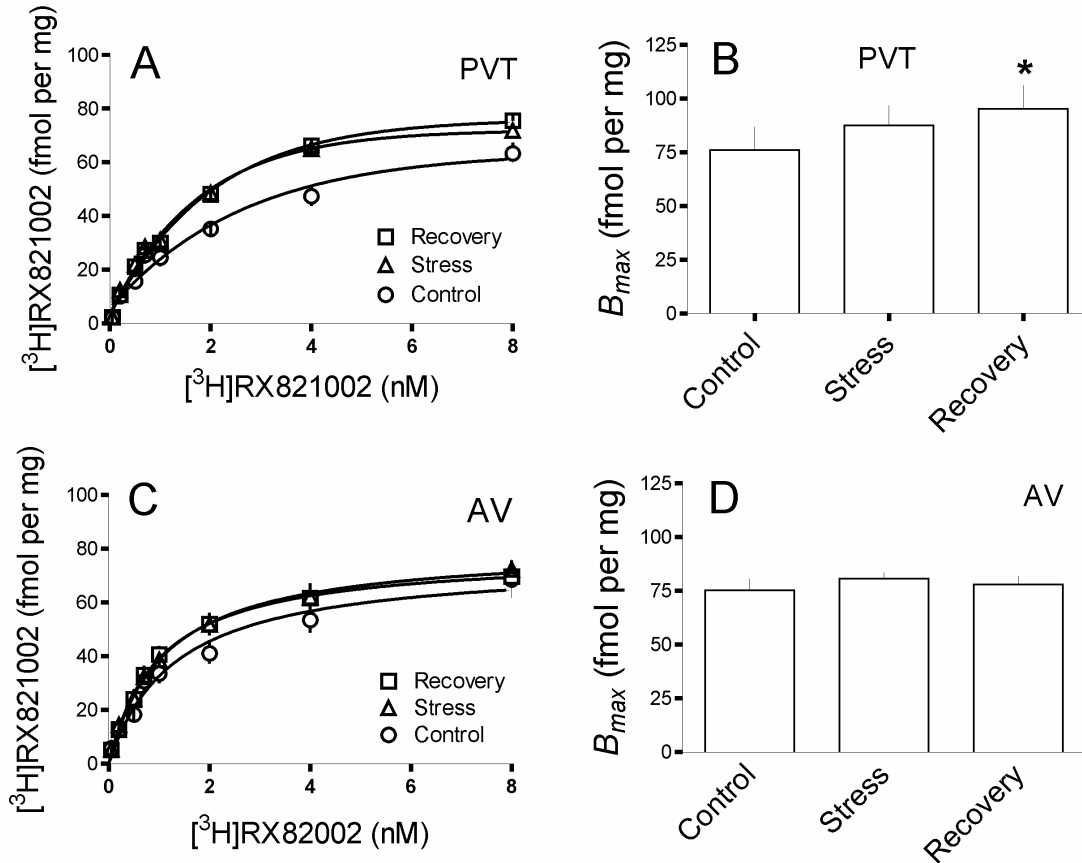


**Figure 26.** Quantification of [<sup>3</sup>H]RX821002 binding in the tree shrew thalamus as determined by *in vitro* receptor autoradiography. Saturation curves for binding of the alpha-2 AR antagonist [<sup>3</sup>H]RX821002 in the PVT (**A**) and (**C**) the anteroventral thalamic nucleus (AV) of *Control*, *Stress* and *Recovery* animals. Each data point represents data from 5 animals per group with three data points per radioligand concentration and animal.  $B_{max}$  values of [<sup>3</sup>H]RX821002 binding in the PVT (**B**) and the AV (**D**) nucleus. Asterisk denotes significant difference to control (Student's t-test;  $p < 0.05$ ).

#### Expression studies: alpha-2B AR cDNA and cRNA probe

To study expression of the alpha-2 AR subtype B in the PVT, *in situ* hybridization experiments with a subtype B specific probe were performed. The expression of the alpha-2B AR was studied in animals that had been subjected to daily psychosocial stress for 44 days, and in animals that experienced the same stress-time period followed by a subsequent 10-day recovery period (for experimental design see Fig. 4). In the presence of [<sup>33</sup>P]UTP, antisense run-off transcription of the linearized cDNA-clone generated a cRNA probe. *In situ* hybridization of brain sections using this probe resulted in a specific hybridization pattern on autoradiography films (Fig. 25A). In the thalamus, the PVT showed the strongest hybridization signal.

### Quantification of alpha-2B AR expression by *in situ* hybridization

To quantify alpha-2B AR expression in neurons of the tree shrew PVT, cryostat sections were hybridized with the [<sup>33</sup>P]UTP labeled riboprobe and then covered with photographic emulsion. After development, sections were counter stained with toluidine blue and silver grains were counted over single neurons in the PVT (Fig. 27A,B). Three sections per animal were analyzed yielding 2 843 to 3 103 neurons that were specifically labeled by the alpha-2B AR probe. The number of silver grains over these neurons was found to be significantly increased in *Stress* and *Recovery* animals (Fig. 27C;  $p < 0.01$ , ANOVA followed by Tukey's *post hoc* test).

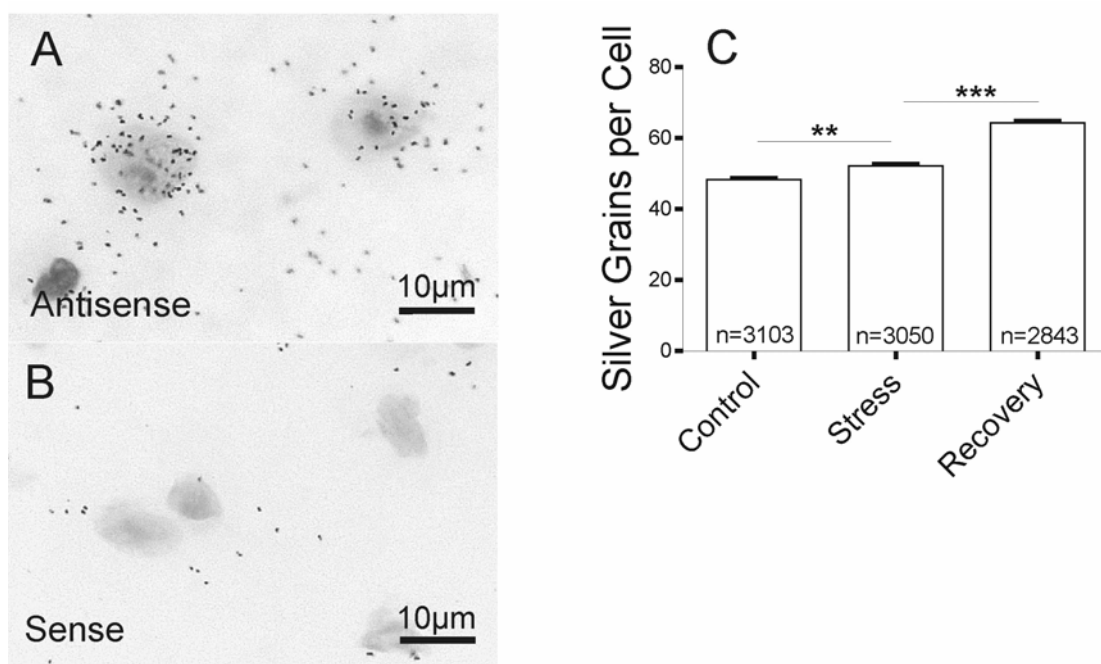


**Figure 27.** Expression of alpha-2B AR mRNA in single neurons of the tree shrew PVT. Left: photomicrographs of sections incubated with antisense (A) or sense (B) cRNA probe for the alpha-2B AR. C Numbers of silver grains over single neurons in sections hybridized with antisense cRNA probe were counted (see Methods). Cell numbers that were analyzed are indicated in the bars (n). Asterisks denote significant differences (\*\*  $p < 0.01$ ; \*\*\*  $p < 0.001$ ; ANOVA followed by Tukey's *post hoc* test).

### **Peripheral reactions of the experimental animals during chronic psychosocial stress**

Each morning during the entire experimental period (for experimental design see Fig. 4), urine was collected and the body weights of animals were determined. The data were analyzed by repeated measures ANOVA followed by Dunnet's *post hoc* test to detect differences to the *No stress* phase. The results are summarized in Table 3. Urinary cortisol levels were significantly increased in the *Stress* group during *Stress 1* ( $p < 0.05$ ; Table 3). Also in the *Recovery* group, significant differences to the *No stress* phase were present during *Stress 1* and *3* ( $p < 0.01$ ), and *Stress 4* ( $p < 0.05$ ), but not during the *Recovery* period. No significant changes were detected in the *Control* group. The body weights of animals in the *Stress* group decreased during the period of social stress. Compared to the *no stress* period, significant differences were present during *Stress 1*, *Stress 2* ( $p < 0.01$ ) and *Stress 3* ( $p < 0.05$ ). In *Recovery* animals, weights decreased during *Stress 1* and *2* ( $p < 0.01$ ) but then gradually normalized. No significant changes of body weights were observed in the *Control* group.

**Table 3.** Peripheral reactions of the experimental animals during chronic psychosocial stress. Cortisol (pg per  $\mu\text{mol}$  creatinine) was determined in morning urine and body weight (g) was recorded: *No stress*, days 1–10; *Stress 1*, days 11–21; *Stress 2*, days 22–32; *Stress 3*, days 33–43; *Stress 4*, days 44–54; *Recovery*, days 55–64. Data were evaluated using repeated measures ANOVA with Dunnet’s multiple comparison *post hoc* test. Asterisks denote significant differences compared with the *No stress* phase of the same experimental group (\*  $p < 0.05$ ; \*\*  $p < 0.01$ ).

	<b>Stress</b>	<b>Recovery</b>	<b>Control</b>
<b>Cortisol</b>			
<i>No stress</i>	105.8 $\pm$ 16.2	125.9 $\pm$ 10.8	84.8 $\pm$ 13.2
<i>Stress 1</i>	170.8 $\pm$ 28.8*	235.2 $\pm$ 22.0**	89.4 $\pm$ 11.7
<i>Stress 2</i>	167.1 $\pm$ 32.8	189.6 $\pm$ 22.2	105.9 $\pm$ 12.0
<i>Stress 3</i>	122.5 $\pm$ 27.4	249.4 $\pm$ 45.3**	110.1 $\pm$ 13.5
<i>Stress 4</i>	161.6 $\pm$ 29.4	215.0 $\pm$ 32.2*	96.0 $\pm$ 13.9
<i>Recovery</i>		155.1 $\pm$ 11.6	105.2 $\pm$ 15.7
<b>Body weight</b>			
<i>No stress</i>	197.5 $\pm$ 6.0	210.8 $\pm$ 6.6	219.1 $\pm$ 9.4
<i>Stress 1</i>	186.9 $\pm$ 6.6**	193.7 $\pm$ 4.0**	218.4 $\pm$ 9.6
<i>Stress 2</i>	186.7 $\pm$ 5.8**	196.0 $\pm$ 8.3**	214.1 $\pm$ 11.8
<i>Stress 3</i>	189.1 $\pm$ 5.2*	203.6 $\pm$ 8.5	218.0 $\pm$ 10.6
<i>Stress 4</i>	191.9 $\pm$ 4.9	209.1 $\pm$ 7.6	221.7 $\pm$ 8.6
<i>Recovery</i>		214.2 $\pm$ 7.9	221.5 $\pm$ 9.1

## **Discussion**

The present thesis shows that activation of postsynaptic alpha-2 ARs has inhibitory actions on neurons in the paraventricular thalamic nucleus (PVT). These neurons in the PVT could be classified according to their reactions to alpha-2 adrenoceptor (AR) agonists. A subpopulation of them was hyperpolarized by alpha-2 AR agonists, others were depolarized by alpha-methyl-norepinephrine (m-NE) and a third group did not react to this agonist. The data indicate that the depolarizing effect of m-NE in a subset of neurons can be attributed to alpha-1 ARs, implying that m-NE also stimulates these receptors. The differentially reacting neurons could be distinguished both in terms of morphology and in terms of their resting properties. Immunocytochemistry against dopamine-beta-hydroxylase and phenylethanolamine-N-methyl transferase showed that the PVT is strongly innervated by fibers containing norepinephrine (NE) and epinephrine (E), indicating that this nucleus is influenced by both NE and E. Chronic psychosocial stress experiments in male tree shrews, a valid animal model of depression, show that stress upregulates transcription of the alpha-2B AR gene in the PVT, thus demonstrating that chronic stress has an impact on the thalamus. Enhanced expression of the receptor gene persisted and even exacerbated throughout a *post* stress period of 10 days, indicating that alpha-2B AR upregulation contributes to the long-term consequences of chronic psychosocial stress. In accordance with this result, we observed that alpha-2 AR protein levels increased after chronic psychosocial stress.

### **Cellular effects of alpha-2 adrenoceptor activation in the paraventricular thalamic nucleus**

Activation of postsynaptic alpha-2 ARs has inhibitory influences on a subset of PVT neurons. The alpha-2 agonist m-NE hyperpolarizes the membrane via an increase of K<sup>+</sup> conductance (see below), abolishes spontaneous firing in a subset of cells and favors the transition from tonic to burst firing in cells that do not fire spontaneously. Similar effects of alpha-2 AR activation have been observed in other brain regions such as the locus coeruleus (LC; e.g. Aghajanian and Wang, 1987), the dorsolateral geniculate nucleus (Funke et al., 1993) or in hypothalamic hypocretin/orexin neurons (Li and van den Pol, 2005). Thus, it seems that the function of alpha-2 ARs in the brain is general inhibitory.

### **Activation of alpha-1 and alpha-2 adrenoceptors by alpha-methyl-norepinephrine**

In several experiments of the present thesis the alpha-2 AR agonist m-NE was used. Clinically, a precursor of m-NE, methyl-dihydroxyphenylalanine, which is thought to be metabolized to m-NE in the brain, is used as a centrally acting antihypertensive (trade name Aldomet). This drug is thought to exert its central antihypertensive action by its agonism at central alpha-2 ARs (see Hoffman and Lefkowitz, 1996). Surprisingly, m-NE had different effects on the resting properties of distinct PVT cell populations. The potency of the drug to elicit these effects was higher in hyperpolarizing cells than in depolarizing cells (the  $IC_{50}$  value for the reduction in input resistance was  $0.88 \mu\text{M}$  for hyperpolarizing cells and the  $EC_{50}$  value for the increase in input resistance was  $1.14 \mu\text{M}$  for depolarizing cells). The concentration of m-NE with which robust effects were observed was  $5 \mu\text{M}$ . This is similar to the concentration Czesnik et al. (2001) used ( $5\text{-}10 \mu\text{M}$ ; personal communication) when recording  $Ca^{2+}$  currents influenced by alpha-2 ARs in brain slices of the tadpole olfactory bulb (Czesnik et al., 2001).

It has been described that in cell culture, alpha-2 AR stimulation has dual effects on  $Ca^{2+}$  currents (Soini et al., 1998) and a number of investigations demonstrated that alpha-2 ARs can affect different biochemical cascades depending on the cell type which they are expressed in (e.g. Duzic and Lanier, 1992; see also Nestler et al., 2001). However, it is also known that not all adrenergic drugs are entirely specific. Therefore, in order to evaluate whether the actions of m-NE are due to different adrenergic receptors, electrophysiological experiments using different adrenergic agonists and antagonists were performed. The results show that alpha-2 ARs are responsible for the hyperpolarization and the reduction in input resistance observed in a subset of PVT cells, as this effect was reversibly blocked by the specific alpha-2 AR antagonist yohimbine and was mimicked by the alpha-2 agonist clonidine. In contrast, the depolarizing response seems to be induced by alpha-1 ARs, as it was mimicked by the alpha-1 agonist phenylephrine and blocked, although irreversibly, by low doses of prazosin. The input resistance of the neurons blocked by prazosin indicates that they belong to the group of depolarizing cells. Furthermore, the depolarizing response was also blocked when prazosin was applied together with m-NE after the very same cells had depolarized to m-NE applied together with yohimbine. However, it has to be remarked that the depolarizing response could not always be elicited for a second or third time, indicating that the cellular constituents for the pathway that mediates this response are mainly cytoplasmic and therefore prone to wash-out as the pipette solution gradually replaces the cytosol during recording (see below). The irreversible block of prazosin is likely also due to the fact that the compound is highly lipophilic, as shown by its high solubility in dimethyl sulfoxide (DMSO). Earlier studies by Flügge et al. (personal communication) also indicated the high lipophilicity of prazosin, and it was observed that [ $^3\text{H}$ ]prazosin tightly stuck to glass

slides. In accordance with these previous observations, it was also noted in the course of the present experiments that the bath chamber had to be thoroughly cleaned with ethanol after application of prazosin in order to observe the depolarizing response to m-NE in a subsequent experiment with another slice. The experiments mentioned above therefore show that the AR mediating the depolarizing response is of the alpha-1 type. This is in accordance with previous studies that found alpha-1 ARs to mediate a prolonged depolarization (for review see McCormick et al., 1991). The alpha-1 AR has been shown to exert its actions via  $G_q$  proteins which are thought to activate several intracellular reactions in order to affect ion channels. This chain of reactions is prone to dialysis as in whole-cell patch clamp experiments, the cytoplasm is gradually exchanged with the pipette solution. In favor of this hypothesis is also the fact that the alpha-1 mediated effects of m-NE were slower in onset than the alpha-2 mediated effects. In the brain, alpha-2 mediated effects have been shown to use  $G_{i/o}$ -proteins, molecules that remain close to the plasma membrane. Furthermore, the beta-gamma-subunit of the  $G_{i/o}$ -protein directly opens a  $K^+$  channel in a membrane delimited fashion, being less prone to the above mentioned wash-out effect observed in cells depolarizing to m-NE. A relatively low selectivity of m-NE for alpha-1 versus alpha-2 ARs was also concluded from earlier studies that examined the effects on blood pressure of various adrenergic agonists (Kobinger, 1984). Also Castillo et al. (1997) found that m-NE induced contractions of the rat aorta are mediated via alpha-1 ARs. The present study shows that low doses (75 -100 nM) of the alpha-1 AR antagonist prazosin blocked the depolarizing effect of m-NE. It is also known, though, that at higher doses, prazosin is also an alpha-2B AR antagonist (Latifpour et al., 1982). However, in electrophysiological brain slice experiments, the dose of prazosin found to inhibit alpha-2B ARs was 10  $\mu$ M (Chong et al., 2004), two orders of magnitude higher than the maximal dose used here. Furthermore, low doses of prazosin (100 nM) did not block the alpha-2B mediated effect in the experiments described by Chong et al. (2004). It is therefore assumed that the doses used in this study (75-100 nM) did not affect alpha-2B ARs.

The discovery that in the PVT, there are two populations of cells reacting to m-NE either in one way, via alpha-1 ARs, or in another way, via alpha-2 ARs and that these cell types differ both in their resting properties and morphology appears interesting. If the two types of receptors were located in equal amounts on the same cells, one would expect to see a relatively fast hyperpolarization followed by the slow depolarization and similar effects on membrane currents in voltage clamp mode. This was not the case in the present experiments. The small hyperpolarization in response to the alpha-2 AR agonist clonidine in cells that previously depolarized to phenylephrine indicates that alpha-2 ARs might be located also on these cells, but most probably in lower amounts and/or at different sites of



the neurites distant from the cell body. Furthermore, the two types of cells (hyperpolarizing versus depolarizing) have both different resting properties and morphology (see below).

### **Influences of alpha-methyl-norepinephrine on neuronal firing**

Similar to other thalamic nuclei, e.g. the centrolateral nucleus (Brunton and Charpak, 1998), the investigated PVT cells show two different firing modes, burst and tonic. These two firing modes are ubiquitous in the thalamus (see Sherman and Guillery, 2001). It has been shown that the molecular underpinning of the burst firing mode is a T-type  $\text{Ca}^{2+}$  conductance which is inactivated at depolarized potentials so that the tonic firing mode can be observed at these potentials. Evidence that T-type channels do also mediate the burst firing mode in the PVT comes from the observations that the low-threshold  $\text{Ca}^{2+}$  shoulder persisted in TTX (but not the spikes on top of it) and that this low-threshold  $\text{Ca}^{2+}$  shoulder was not observed when the T-type calcium channel blocker NiCl (200  $\mu\text{M}$ ) was added to the extracellular solution (data not shown).

In a subset of hyperpolarizing cells, the firing mode of PVT cells was temporarily changed during the actions of m-NE from tonic to burst firing mode, thus showing that activation of alpha-2 ARs can switch the firing mode in PVT cells. In another subset of PVT cells, spontaneous firing at the resting membrane potential was observed, and this firing was reversibly abolished by the hyperpolarizing actions of m-NE. The mechanism underlying this spontaneous activity is not clear. However, it can be speculated that the hyperpolarization-activated current  $I_h$ , which is prominent in the thalamus, is activated by the afterhyperpolarization following each action potential and involved in bringing these cells back to the firing threshold. The hyperpolarization-activated current has been shown to be modulated by the alpha-2 agonist clonidine (Yagi and Sumino, 1998). Therefore, an interesting question would be if this current is also modulated by alpha-2 agonists in the PVT, or if the abolishment of firing is merely a consequence of the hyperpolarizing actions of alpha-2 agonists.

The depolarizing actions of m-NE via alpha-1 ARs lead to excitatory actions in a subset of PVT cells via the increase in input resistance. The firing was however not qualitatively changed in some of these neurons. It was also observed that in some cells reacting to m-NE with an alpha-1 AR mediated depolarization, the mode of action potential generation was changed as a subset of cells started to discharge spontaneously. Also here, the molecular mechanisms underlying the generation of spontaneous activity are not clear, but an investigation of the modulation of the hyperpolarization-activated current  $I_h$  by alpha-1 ARs would be worthwhile to investigate.

### **Alpha-methyl-norepinephrine affects putative K<sup>+</sup> currents**

The involvement of K<sup>+</sup> conductances in the inhibitory and excitatory actions of m-NE is indicated by the reversal potential of the m-NE sensitive current near the Nernst potential for K<sup>+</sup> ( $E_K = -87$  mV). Furthermore, the involvement of K<sup>+</sup> conductances in the inhibitory actions of alpha-2 ARs was demonstrated by attenuation of the outward current induced by alpha-2 ARs by the K<sup>+</sup> channels blockers barium and tertiapin. Extracellular barium blocks several K<sup>+</sup> channels, e.g. twin pore acid-sensitive K<sup>+</sup> (TASK) channels (see Meuth et al., 2003), the classical delayed rectifier K<sup>+</sup> channels which are voltage-dependent and are responsible for the fast repolarization of the membrane following an action potential, adenosine-triphosphate (ATP)-gated K<sup>+</sup> channels and inwardly rectifying K<sup>+</sup> channels which are often influenced by G-proteins (see Hille, 1992). The family of inwardly rectifying K<sup>+</sup> channels has so far been shown to consist of seven subfamilies, based on gene homology, with G-protein coupled inwardly rectifying (GIRK) K<sup>+</sup> channels being members of the Kir3.0 subfamily (Doupnik et al., 1995; Reimann and Ashcroft, 1999). The honey bee venom tertiapin used here has been shown to block Kir1.1, Kir3.1, Kir3.2 and Kir3.5 K<sup>+</sup> channels (Jin and Lu, 1998; Alomone Labs). Neuronal GIRK channels are predominantly heteromultimers of GIRK1 (Kir3.1) and GIRK2 (Kir3.2) subunits (Kobayashi et al., 2003). As the Kir1.1 channel is only weakly expressed in the thalamus (reviewed by Doupnik et al., 1995), it is concluded that activation of alpha-2 ARs in the hyperpolarizing PVT neurons affects GIRK channels. The fact that tertiapin alone did not induce any current argues against a tonic activation of GIRK channels in the PVT. Tonic activation of GIRK channels was observed in the rat hippocampus and shown to be mediated by ambient adenosine (Takigawa and Alzheimer, 2002).

### **Resting properties of neurons in the paraventricular thalamus**

The differences in resting properties (input resistance and membrane potential) between cells that depolarized or hyperpolarized in the presence of m-NE was consistently found in the experiments evaluating the effects of adrenergic agonist and antagonists. Furthermore, normal distributions could be fitted to the data sets of all cells that showed a clear reaction to m-NE (Fig. 22), indicating that these different cell types form subpopulations within the PVT. In the hippocampus, the input resistance has been found to vary with the membrane potential so that at more negative potentials, a lower input resistance is observed (Spruston and Johnston, 1992). The authors of the latter study attributed this to the influence of voltage-dependent conductances that are activated at more hyperpolarized potentials. This hypothesis is in line with the fact that both the membrane potential and the input resistance is lower in cells that depolarized upon application of m-NE compared with those that hyperpolarized to m-NE and that only minor differences in the size of the dendritic tree could

be observed in these two cell types. The differences in passive properties indicate a larger resting conductance, possibly for  $K^+$ , in cells being depolarized through alpha-1 ARs.

In the present study, the mean input resistance of all cells was  $440.8 \pm 19.2$  MOhm and ranged (approximately) from 75 to 1250 MOhm (Fig. 22A). This range is higher than that in a previous investigation which focused primarily on another midline thalamic structure, the centrolateral thalamic nucleus (Brunton and Charpak, 1998). The authors of the latter study report input resistances that range from 100 to 300 MOhm. It thus seems that, compared to the centrolateral thalamic nucleus, the PVT is more heterogeneous concerning this variable, and that the mean input resistance is higher in the PVT. For comparison, the mean input resistance in CA3 cells of the hippocampus is about 160 MOhm (Kole, 2003).

The low resting membrane potential (around -80 mV) found in a subset of PVT neurons is unusual, as the potential of CNS neurons is typically around -75 mV. According to literature data, a resting membrane potential around -80 mV is known for glial cells, due to their larger resting conductance for  $K^+$  (see Nicolls et al., 2002). Therefore, one might argue that the cells with low membrane potentials in the present study could be glial cells, also because both alpha- and beta-ARs have been shown to have binding sites on glial cells (e.g. Hösli and Hösli, 1993). However, several points strongly argue against this assumption. Firstly, the morphology of these cells is not congruent with those of glial cells. The only glial cell type that might remotely resemble the cells in the present study is astrocytes, and one would expect to see end feet-like structures, if it were astrocytes. Secondly, axon-like processes were identified in cells of the present study (see below), which are not described for glia. Thirdly, all cells investigated in the absence of TTX fired several action potentials upon DC current injection, which glial cells do not (see Nicolls et al., 2002). Finally, a membrane potential around -80 mV is by no means unusual and can, e.g., also be observed in layer V cortical pyramidal neurons (Kole, personal communication). Therefore, the recorded PVT cells described here appear to be neurons.

### **Morphology of neurons in the paraventricular thalamus**

This is the first study describing the dendritic morphology of PVT cells in detail. In accordance with other reports using histochemistry and/or immunostaining on PVT cells from humans (van Buren and Borke, 1972; Uroz et al, 2004) it was found that the rat PVT neurons had a relatively small soma that was either round or polygonal. In agreement with other reports on the morphology of midline thalamic neurons (Brunton and Charpak, 1998; Uroz et al., 2004), the dendritic tree of PVT cells was also relatively small and less ramified compared to those of, e.g. rat hippocampal pyramidal neurons (Kole, 2003) or cells of the rat medial geniculate body (Bartlett and Smith, 1991).

The cells that responded to m-NE with an alpha-2 AR mediated hyperpolarization had a smaller soma area than the cells displaying alpha-1 AR mediated depolarization. Theoretically, cells with a smaller cell body have a higher input resistance (see Koester and Siegelbaum, 2000). Supposing that the smaller soma area reflects a smaller cell body volume, the hyperpolarizing neurons should have a higher input resistance compared to the depolarizing, which was indeed the case (see Fig. 10).

Although there was no difference between length of the dendrites in hyperpolarizing versus depolarizing neurons, Sholl analysis shows the number of intersections and the summed dendritic length at certain distances proximal to the soma to be significantly higher in depolarizing compared to hyperpolarizing neurons (Fig. 20). Based on these findings, it could be speculated that PVT cells depolarizing to m-NE via alpha-1 ARs are likely to receive more synaptic input from proximal dendrites at a distance of 20-60 and 150  $\mu\text{m}$  from the soma than the cells showing alpha-2 AR mediated hyperpolarization. Axons could not always be identified in the neurons investigated in the present study. One possibility is that these processes coursed towards the glass slide and/or were cut very close to the cell body, so that they could not be identified.

The most striking difference between cells which did not react to m-NE and the cells in which m-NE had hyper/depolarizing effects is the difference in the total dendritic tree, which is significantly larger and more complex in the cells which did not show any reaction to m-NE (Table 2). These complex dendrites probably contribute to the lower input resistance of the cells. The branching pattern of the dendrites indicates that the cells on which m-NE had no effects might represent a distinct population, possibly thalamic interneurons, which use GABA as their principal neurotransmitter and have a larger dendritic arbor compared to glutamatergic relay cells of the thalamus (see e.g. Jones, 1998). Also, it is interesting to note that in the cell on which m-NE had no effect, no clear axon could be identified. The hypothesis that certain thalamic interneurons lack axons has been proposed before (Liebermann, 1973; Wilson, 1986; see also Jones, 1998), and Sherman and Guillery (2001) discussed this issue in detail. However, the population of GABA-immunoreactive cells in the rodent thalamus is very small (approximately 5%; Arcelli et al., 1997), and in the tree shrew PVT, no GABA-like immunoreactivity was observed in perikarya (Heilbronner et al., 2002). Therefore, there are no indications that the neurons that do not react to m-NE represent thalamic interneurons.

## **Functional implications of alpha-methyl-norepinephrine in the paraventricular thalamus**

*In vivo*, the endogenous agonists NE and E act on all three classes of adrenergic receptors, alpha-1, alpha-2 and beta ARs. This study examined the role of alpha-2 ARs on PVT cells, the actions of beta-ARs in this brain region remain to be elucidated. Based on the present *in vitro* studies, an interesting detail to note about the actions of the agonist m-NE is that it influences two populations of PVT neurons which differ both in resting membrane potential and input resistance in opposite ways. When m-NE is applied, both types of neurons appear to functionally switch their states. Via alpha-2 ARs, m-NE hyperpolarizes cells that initially have a more positive membrane potential and higher input resistance (compared to the other populations) to a lower membrane potential and a reduced input resistance. In contrast, alpha-1 ARs appear to depolarize neurons and increase input resistance (in response to m-NE) in another population of cells that originally have a more negative resting potential and a lower input resistance (compared to the population of depolarizing cells). The two types of neurons thus functionally switch states. This influence on the resting properties leads to different firing behaviors, switching the firing mode from tonic to burst in alpha-2 AR sensitive cells (hyperpolarizing cells) and favoring the transition from burst to tonic firing in depolarizing cells. Furthermore, m-NE can abolish the spontaneous firing observed in a subset of alpha-2 AR sensitive neurons, whereas the depolarizing actions m-NE elicit spontaneous firing in a subset of cells. By its inhibitory actions on the cell population sensitive to alpha-2 AR activation and the excitatory actions that elicit firing via a (presumptive alpha-1 AR mediated) depolarizing effect, m-NE may significantly change the output of the paraventricular thalamic nucleus. One might therefore speculate that via these actions *in vivo*, information transfer from the PVT to different brain regions is potentially altered. An imbalance of the NE system of the brain that occurs in situations such as chronic stress, as is evident from the experiments in the tree shrews (see below), might therefore lead to qualitatively different processing of information in the PVT. It is worth to note that the different projection areas of the PVT include targets such as the prefrontal cortex and the shell of the nucleus accumbens, regions that are important for emotional information processing (see Iversen et al., 2000).

### **The alpha-2B adrenoceptor in the thalamus**

The CNS alpha-2 AR subtypes A and C have been studied in detail, but little is known about the functional role of the alpha-2B AR in the CNS (Flordellis et al., 1991; Kable et al., 2000; MacDonald et al., 1997). This might be due to its restricted expression which occurs almost exclusively in the diencephalon, but also due to the lack of truly subtype-specific agonists (Scheinin et al., 1994). The latter point is evident when considering the results of the

competition binding experiment. The allegedly highly subtype-specific alpha-2B AR antagonist imiloxan had  $K_i$  values in the micromolar range both in the LC, where the alpha-2B AR is not present, and in the PVT where alpha-2B ARs are strongly expressed. The interpretation of these results is not easy. On the one hand, the  $K_i$  values of imiloxan which are about three orders of magnitude higher than those of the specific alpha-2 agonist UK14,304 and thus in the range of those of the dopamine receptor ligand chlorpromazine, clearly show that imiloxan is less specific for alpha-2B ARs than suggested previously (Michel et al., 1990). Similar  $K_i$  values of imiloxan have been found by Michel et al. (1990) in rat kidney (interpreted as affinity to alpha-2B ARs), as in the present experiments in PVT ( $K_i = 3.40 \mu\text{M}$ ) and in the LC ( $K_i = 1.34 \mu\text{M}$ ) although alpha-2B ARs (on noradrenergic fibers) do not exist. A possible interpretation of these experiments could be that alpha-2B receptor protein is not present on the cell bodies of the PVT. However, this interpretation is highly unlikely because of several reasons. Firstly, *in situ* hybridization shows that alpha-2B AR mRNA is expressed in the PVT (Scheinin et al., 1994; this study). Secondly, experiments with PC12 cells expressing the three alpha-2 AR subtypes tagged with green-fluorescent protein (GFP) shows the alpha-2B receptor to be evenly located in the plasma membrane (Olli-Lähdesmäki et al., 1999). Also, experiments in which embryonic spinal cord neurons were transfected with GFP-tagged alpha-2 AR subtypes showed distribution of the alpha-2B AR on the somata of neurons (Wozniak and Limbird, 1998). These results were interpreted as showing that one role of the alpha-2B AR is that of a somatic receptor. Thirdly, in Western blots of whole-cell lysates of the rat thalamus, a commercial antibody directed against the alpha-2B AR recognized a band at approximately 50 kDa (data not shown). A band of this molecular weight was also reported by Huang et al. (1996) which investigated the alpha-2B AR in the rat kidney using immunocytochemistry. In the present experiments, however, the Western blot showed multiple bands and was thus concluded not to be useful for further investigations. Fourthly, if the alpha-2B AR protein were not present in the thalamus, but if instead all the receptor protein would be transported away from sites of protein synthesis in the neuronal soma to more distal sites on dendrites or the axon of the neuron, the only subtype that could mediate the inhibitory effects of alpha-2 agonists in the PVT (this study) would be the alpha-2A subtype, which is also weakly expressed in the PVT (Scheinin et al., 1994). However, receptor autoradiography with alpha-2 antagonist [ $^3\text{H}$ ]RS-79948-197 in animals with a deletion of the gene for the alpha-2A AR show that in the brains of these animals, there is still radioligand binding in the region of the PVT (Lähdesmäki et al., 2002), presumably because of alpha-2B ARs.

### **Innervation of the paraventricular thalamic nucleus by noradrenergic and adrenergic fibers**

The thalamus in general and the PVT in particular, receive a major innervation from the NE containing fibers of the LC (Otake and Ruggiero, 1995; see Jones, 1998). Immunocytochemistry with an antibody against tyrosine hydroxylase showed a strong catecholaminergic innervation of the PVT (Hökfelt et al., 1984). In accordance with previous investigations, the present study demonstrates that the PVT contains dense networks of NE- and E-containing fibers as revealed by immunocytochemistry with antibodies against the enzymes dopamine-beta-hydroxylase (DBH) and phenylethanolamine-N-methyl transferase (PNMT; for review see van der Werf et al., 2002). Compared to the PVT, the anteroventral nucleus (AV) receives fewer catecholaminergic fibers (data not shown). The AV receives its major input from the hippocampal formation via the mammillary bodies of the hypothalamus and projects to the cingulate cortex, which is thought to be important for the conscious perception of emotion (Armstrong, 1990; Price, 1995; Iversen et al., 2000). As no significant effect of stress on the alpha-2 ARs was observed in the AV, it appears that stress affects thalamic nuclei in a regional manner, possibly related to the density of the NE input.

### **Chronic psychosocial stress affects alpha-2 adrenoceptors: *in situ* hybridization and *in vitro* receptor autoradiography**

We used *in situ* hybridization to detect alpha-2B AR expression on the level of transcription. Analysis of silver grains over single neurons in sections covered with photographic emulsion showed that long-term chronic stress upregulates expression of the receptor in neurons of the PVT. The combination of *in situ* hybridization and immunocytochemistry revealed that high amounts of alpha-2B AR mRNA are present in PVT neurons that are immunoreactive for glutamate (Heilbronner, 2002). One can therefore assume that the cells displaying increased alpha-2B AR mRNA expression in the PVT after stress are glutamatergic neurons. This assumption coincides with the view that stress-induced activation of the NE system affects the primary excitatory system in the brain (Swanson and Schoepp, 2003).

We also used receptor binding studies to quantify alpha-2 ARs in the thalamic nuclei. As no truly subtype-selective ligands are available to date, this method does not allow quantification of distinct receptor subtypes. A significant increase in [<sup>3</sup>H]RX821002 binding was observed in the PVT of *Recovery* animals. This enhancement of binding site numbers probably reflects the upregulation of the alpha-2B ARs, at least partially because alpha-2A ARs are only expressed at very low levels in the thalamus and alpha-2C ARs are not expressed at all in the thalamus (Scheinin et al., 1994). The assumption that the increased binding reflects an increased amount of terminal autoreceptors on LC neurons projecting to the PVT is very

unlikely as alpha-2A expression in the LC after the same experimental protocol did not change (Flügge et al., 2003).

### **Stress and alpha-2 adrenoceptors**

Stress is known to activate the NE system, leading to increased synthesis and release of NE in brain regions to which neurons containing NE project (Saavedra, 1982; Abercrombie and Jacobs, 1987a,b; reviewed by Stanford, 1993). High NE concentrations have been shown to promote alpha-2 AR downregulation *in vitro* (e.g., Eason and Liggett, 1992), and up to four weeks of daily social stress induced downregulation of alpha-2 ARs in regions involved in the regulation of autonomic functions in the tree shrew brain (Flügge et al., 1992). Analysis of alpha-2 AR subtype expression revealed that it was the alpha-2A autoreceptor that was downregulated in the NE neurons of the LC (Meyer et al., 2000). However, after six weeks of stress, expression of alpha-2A heteroreceptors was increased in glutamatergic neurons of the lateral reticular nucleus, and this effect was interpreted as receptor upregulation due to a gradually acquired NE deficit during the late stages of chronic stress (Flügge et al., 2003). In a rat model of depression, chronic stress induced degenerative changes of axon terminals immunoreactive for DBH (Kitayama et al., 1994). As demonstrated in the present study, the alpha-2B AR in the thalamus is also upregulated after six weeks of stress. We explain the effects on alpha-2B expression and ligand binding to alpha-2 ARs by assuming autoregulation of alpha-2 ARs by NE, suggesting that also in this part of the brain, NE and/or E levels are low after long-term chronic stress. The present data thus reveal that by changing catecholamine levels in the brain, stress does not only have an impact on the limbic system but also on the thalamus (McEwen and Sapolsky, 1995). Flügge et al. (1997) already showed before that chronic psychosocial stress in tree shrews transiently upregulated beta-ARs in the pulvinar nucleus. In accordance with the inhibitory effects of alpha-2 ARs on the passive properties and on the firing of PVT cells, it can be assumed that stress effects on ARs in the PVT somehow alters information transfer to cortical and limbic regions. This is especially important as one target of the PVT is the shell of the nucleus accumbens, a major component of the reward circuitry of the mammalian brain (see van der Werf et al., 2002). The view that brain NE levels are low after chronic stress, a situation that in humans may lead to depressive diseases, coincides with the “monoamine deficit” theory that postulates a general deficit of brain monoamines as neurophysiological basis of depressive disorders. Antidepressants such as tricyclics and monoamine reuptake inhibitors counteract this deficit by inhibiting NE and/or serotonin reuptake into neurons, thus increasing their extracellular concentrations. Although we know today that depression is a highly complex disorder in which various aspects of normal brain functioning are altered (e.g. Nestler et al., 2002), low NE concentrations might play an important role both in the genesis as well as the treatment



of this disorder. The present data on alpha-2B AR upregulation due to chronic social stress in an animal model displaying depressive-like symptoms is in line with the view that an imbalance in the NE system may contribute to depression.

### **Peripheral reactions of subordinate tree shrews during chronic psychosocial stress and recovery**

In the experiments investigating the effects of chronic subordination stress on alpha-2 ARs, the stress level during the experimental periods was evaluated by determining cortisol levels in morning urine and monitoring body weights of the experimental animals. As described previously (Fuchs et al., 1993), urinary cortisol increases during periods of subordination stress, reflecting hyperactivity of the hypothalamic-pituitary-adrenal axis. Statistical significance compared with the *No stress* phase was, however, not reached for all time blocks of the stress period. This can be attributed to individual differences in the responsiveness to stress. During the *post* stress period, cortisol levels decreased reflecting recovery from the psychosocial load. As demonstrated previously, body weight of subordinate male tree shrews decreases during social stress (Fuchs and Flügge, 2002). In the present experiment, statistically significant differences compared to the *No stress* period were detected during the initial stress phases. In later phases, weights returned back to baseline indicating partial adaptation. Normal body weights were completely restored post stress pointing to a resetting of the stress axis at the end of the experimental period.

### **Conclusions**

The present thesis describes prominent inhibitory actions of postsynaptic alpha-2 AR activation in the rat PVT. It also provides data on the morphological and passive properties of the neurons in this nucleus, unveiling different populations of cells that showed opposite reactions to the agonist m-NE. An interesting question that arises from these experiments would be whether the population of alpha-2 AR sensitive neurons projects to different areas of the brain than the alpha-1 AR sensitive neurons. Furthermore, another question would be whether the cells that did not react to m-NE are thalamic cells projecting to higher brain regions or if this cell population represents thalamic interneurons.

Chronic psychosocial stress, a condition nowadays recognized to be detrimental to one's health, enhanced binding to alpha-2 ARs in the tree shrew animal model for depression. This effect is presumably due to an enhanced expression of the alpha-2B gene and a subsequently increased amount of postsynaptic alpha-2B adrenoceptors. The PVT is a thalamic nucleus that is strongly connected to the limbic system and is hypothesized to be involved in state setting properties. Also, this brain area is strongly affected by the catecholamines norepinephrine and epinephrine, strengthening the assumption that an

autoregulation of alpha-2B ARs takes place during conditions such as chronic psychosocial stress. A question that remains open is whether chronic psychosocial stress significantly influences the output of the PVT via an increased amount of alpha-2B ARs. Based on the results of the present experiments, one can speculate that if there is an increase in functional postsynaptic alpha-2 ARs, this might lead to an enhanced inhibition of this nucleus. The firing modes of the cells might be changed toward a state of increased burst firing. These actions could lead to a higher synchronization of the PVT–striatal-cortical system, as studies in awake rabbits showed that a burst in a thalamic projection neuron is almost twice as likely to elicit an action potential in a target cortical cell than a conventional action potential from a thalamic cell firing in tonic mode is (Swadlow and Gusev, 2001). Alternatively, a permanently diminished amount of norepinephrine and/or epinephrine, which is presumed to be responsible for the alpha-2 upregulation during chronic stress, could lead to the opposite scenario of an increased disinhibition of the PVT and connected striatal or cortical cells. Regardless of what the net effects of stress on the output of the paraventricular thalamic nucleus are, the findings of the present study contribute both to our understanding of the cellular constituents of the thalamus and to the neurobiology of the stress response.

## References

- Aantaa, R., and Scheinin, M. (1993). Alpha 2-adrenergic agents in anaesthesia. *Acta Anaesthesiol. Scand.* **37**:433-448.
- Abercrombie, E. D., and Jacobs, B. L. (1987a). Single-unit response of noradrenergic neurons in the locus coeruleus of freely moving cats. I. Acutely presented stressful and nonstressful stimuli. *J. Neurosci.* **7**:2837–2843.
- Abercrombie, E. D., and Jacobs, B. L. (1987b). Single-unit response of noradrenergic neurons in the locus coeruleus of freely moving cats. II. Adaptation to chronically presented stressful stimuli. *J. Neurosci.* **7**:2844–2848.
- Aghajanian, G. K., and Wang, Y. Y. (1987). Common alpha 2- and opiate effector mechanisms in the locus coeruleus: intracellular studies in brain slices. *Neuropharmacology* **26**:793-799.
- Ahlquist, R. P. (1948). A study of the adrenotropic receptors. *Am. J. Physiol.* **153**:586-600.
- Anisman, H., and Zacharko, R. M. (1992). Depression as a consequence of inadequate neurochemical adaptation in response to stressors. *Br. J. Psychiatry Suppl.* 36–43.
- Arcelli, P., Frassoni, C., Regondi, M. C., De Biasi, S., and Spreafico, R. (1997). GABAergic neurons in mammalian thalamus: a marker of thalamic complexity? *Brain Res. Bull.* **42**:27-37.
- Arima, J., Kubo, C., Ishibashi, H., and Akaike, N. (1998).  $\alpha_2$ -Adrenoceptor-mediated potassium currents in acutely dissociated rat locus coeruleus neurones. *J. Physiol.* **508**:57-66.
- Armstrong, E. (1990). Limbic thalamus: Anterior and mediodorsal nuclei. In: Paxinos G. (ed.). *The Human Nervous System*, Academic Press, London, pp. 469–479.
- Barry, P. H. (1994). JPCalc, a software package for calculating liquid junction potential corrections in patch-clamp, intracellular, epithelial and bilayer measurements and for correcting junction potential measurements. *J. Neurosci. Methods* **51**:107-116.
- Bartlett, E. L., and Smith, P. H. (1991). Anatomic, intrinsic, and synaptic properties of dorsal and ventral division neurons in rat medial geniculate body. *J. Physiol.* **81**:1999–2016.
- Beck, C. H., and Fibiger, H. C. (1995). Chronic desipramine alters stress-induced behaviors and regional expression of the immediate early gene, c-fos. *Pharmacol. Biochem. Behav.* **51**:331–338.
- Bentley, S. M., Drew, G. M., and Whiting, S. B. (1977). Evidence for two distinct types of postsynaptic  $\alpha$ -adrenoceptor. *Br. J. Pharmac.* **61**:116P-117P.
- Berthelsen, S., and Pettinger, W. A. (1977). A functional basis for the classification of  $\alpha$ -adrenergic receptors. *Life Sci.* **21**:595-606.
- Birch, P. J., Anderson, S. M. P., and Fillenz, M. (1986). Mild chronic stress leads to desensitisation of presynaptic autoreceptors and a long-lasting increase in noradrenaline synthesis in rat cortical synaptosomes. *Neurochem. Int.* **9**:329–336.
- Birnbaumer, L., Abramowitz, J., and Brown, A.M. (1990). Receptor-effector coupling by G proteins. *Biochim. Biophys. Acta* **1031**:163-224.

- Brown, E. E., Robertson, G. S. and Fibiger, H. C. (1992). Evidence for conditional neuronal activation following exposure to a cocaine-paired environment: role of forebrain limbic structures. *J. Neurosci.* **12**:4112-4121.
- Brunton, J., and Charpak, S. (1998).  $\mu$ -Opioid peptides inhibit thalamic neurons. *J. Neurosci.* **18**:1671-1678.
- Bubser, M., and Deutch, A. Y. (1999). Stress induces Fos expression in neurons of the thalamic paraventricular nucleus that innervate limbic forebrain sites. *Synapse* **32**:13–22.
- Bünemann, M., Bücheler, M. M., Phillip, M., Lohse, M. J., and Hein, L. (2001). Activation and deactivation kinetics of  $\alpha_{2A}$ - and  $\alpha_{2C}$ -adrenergic receptor-activated G protein-activated inwardly rectifying  $K^+$  channel currents. *J. Biol. Chem.* **276**:47512-47517.
- Buzsaki, G., Kennedy, B., Solt, V. B., and Ziegler, M. (1991). Noradrenergic control of thalamic oscillation: The role of alpha-2 receptors. *Eur. J. Neurosci.* **3**:222–229.
- Castillo, E. F., Valencia, I., Bobadilla, R. M., Villalon, C. M., and Castillo, C. (1997). alpha-Methylnoradrenaline-induced contractions in rat aorta are mediated via alpha 1D-adrenoceptors. *Fundam. Clin. Pharmacol.* **11**:339-345.
- Chastrette, N., Pfaff, D. W., and Gibbs, R. B. (1991). Effects of daytime and nighttime stress on fos-like immunoreactivity in the paraventricular nucleus of the hypothalamus, the habenula, and the posterior paraventricular nucleus of the thalamus. *Brain Res.* **563**:339-344.
- Chong, W., Li, L. H., Lee, K., Lee, M. H., Park, J. B., and Ryu P. D. (2004). Subtypes of  $\alpha_2$  and  $\alpha_1$  adrenoceptors mediating noradrenergic modulation of spontaneous inhibitory postsynaptic currents in the hypothalamic paraventricular nucleus. *J. Endocrinol.* **16**:450-457.
- Cooper, J. R., Bloom, F. E., and Roth R. H. (2003). *The Biochemical Basis of Neuropharmacology*. New York: Oxford University Press. Eighth edition.
- Czesnik, D., Netzlin, L., Rabba, J., Müller, B., and Schild, D. (2001). Noradrenergic modulation of calcium currents and synaptic transmission in the olfactory bulb of *Xenopus laevis* tadpoles. *Eur. J. Neurosci.* **13**:1093-1100.
- Deutch, A. Y., Bubser, M., and Young, C. D. (1998). Psychostimulant-induced fos protein expression in the thalamic paraventricular nucleus. *J. Neurosci.* **18**:10680-10687.
- Doupnik, C. A., Davidson, N., and Lester, H. A. (1995). The inward rectifier potassium channel family. *Curr. Opin. Neurobiol.* **5**:268-277.
- Duman, R. S., Heninger, G. R., and Nestler, E. J. (1997). A molecular and cellular theory of depression. *Arch. Gen. Psychiatry* **54**:597–606.
- Duzic, E., and Lanier, S. M. (1992). Factors determining the specificity of signal transduction by guanine nucleotide-binding protein-coupled receptors. III. Coupling of alpha 2-adrenergic receptor subtypes in a cell type-specific manner. *J Biol. Chem.* **267**:24045-24052.
- Eason, M. G., and Liggett, S. B. (1992). Subtype-selective desensitization of alpha 2-adrenergic receptors. Different mechanisms control short and long term agonist-promoted desensitization of alpha 2C10, alpha 2C4, and alpha 2C2. *J. Biol. Chem.* **267**:25473–25479.
- Fanselow, E. E., Koichi, S., Baccala L. A., and Nicoletis, M. A. L. (2001). Thalamic bursting in rats during different awake behavioral states. *Proc. Natl. Acad. Sci. USA* **89**:15330-15335.

- Flordellis, C. S., Handy, D. E., Bresnahan, M. R., Zannis, V. I., and Gavras, H. (1991). Cloning and expression of a rat brain alpha 2B-adrenergic receptor. *Proc. Natl. Acad. Sci. USA* **88**:1019–1023.
- Flügge, G. (1996). Alterations in the central nervous alpha 2-adrenoceptor system under chronic psychosocial stress. *Neuroscience* **75**:187–196.
- Flügge, G. (2000). Regulation of monoamine receptors in the brain: dynamic changes during stress. *Int. Rev. Cytol.* **195**:145–213.
- Flügge, G., Ahrens, O., and Fuchs, E. (1997). Beta-adrenoceptors in the tree shrew brain. II. Time-dependent effects of chronic psychosocial stress on [125I]iodocyanopindolol binding sites. *Cell Mol. Neurobiol.* **17**:417–432.
- Flügge, G., Jöhren, O., and Fuchs, E. (1992). [<sup>3</sup>H]Rauwolscine binding sites in the brains of male tree shrews are related to social status. *Brain Res.* **597**:131–137.
- Flügge, G., van Kampen, M., Meyer, H., and Fuchs, E. (2003). Alpha-2A and alpha-2C-adrenoceptor regulation in the brain: Alpha-2A changes persist after chronic stress. *Eur. J. Neurosci.* **17**:917–928.
- Fuchs, E., and Flügge, G. (2002). Social stress in tree shrews: Effects on physiology, brain function, and behavior of subordinate individuals. *Pharmacol. Biochem. Behav.* **73**:247–258.
- Fuchs, E., Jöhren, O., and Flügge, G. (1993). Psychosocial conflict in the tree shrew: Effects on sympathoadrenal activity and blood pressure. *Psychoneuroendocrinology* **18**:557–565.
- Fuchs, E., Kramer, M., Hermes, B., Netter, P., and Hiemke, C. (1996). Psychosocial stress in tree shrews: Clomipramine counteracts behavioral and endocrine changes. *Pharmacol. Biochem. Behav.* **54**:219–228.
- Funke, K., and Eysel, U. T. (1993). Modulatory effects of acetylcholine, serotonin and noradrenaline on the activity of cat perigeniculate neurons. *Exp. Brain Res.* **95**:409–420.
- Funke, K., Pape, H.-C., and Eysel, U. T. (1993). Noradrenergic modulation of retinogeniculate transmission in the cat. *J. Physiol.* **463**:169–191.
- Groenewegen, H. J., and Berendse, H. W. (1994). The specificity of the ‘nonspecific’ midline and intralaminar thalamic nuclei. *Trends Neurosci.* **17**:52–57.
- Groenewegen, H. J., Wright, C. I., Beijer, A. V., and Voom, P. (1999). Convergence and segregation of ventral striatal inputs and outputs. *Ann. N. Y. Acad. Sci.* **877**:49–63.
- Hamam B. N., and Kennedy T. E. (2003). Visualization of the dendritic arbor of neurons in intact 500 µm thick brain slices. *J. Neurosci. Methods* **123**:61-67.
- Hamill, O. P., Marty, A., Neher, E., Sakmann, B., and Sigworth F. J. (1981). Improved patch-clamp techniques for high-resolution current recording from cells and cell-free membrane patches. *Pflügers Arch.* **391**:85-100.
- Heilbronner, U. (2002). *α<sub>2B</sub>-Adrenoceptor Expression in Cells of the Tree Shrew (Tupaia belangeri) Thalamus: Co-Localization with GABA- and Glutamate-like Immunoreactivity.* Master’s thesis. University of Göttingen.
- Heilbronner, U., van Kampen, M, and Flügge, G. (2004). The alpha-2B adrenoceptor is persistently upregulated by chronic psychosocial stress. *Cell. Mol. Neurobiol.* **24**:815-831.
- Henze, D. A., Cameron, W. E., and Barrionuevo, G. (1996). Dendritic morphology and its effects on the amplitude and rise-time of synaptic signals in hippocampal CA3 pyramidal cells. *J. Comp. Neurol.* **369**:331-344.

- Hieble, J. P., and Ruffolo, R. R. (1995). Subclassification of the  $\beta$ -adrenoceptors. In: Ruffolo, R. R. (ed.). *Adrenoceptors. Structure, function and pharmacology*. Luxembourg: Harwood Academic Publishers, pp. 183-193.
- Hieble, J. P., Ruffolo, R. R. Jr., and Starke, K. (1997). Identification and subclassification of  $\alpha$ 2-adrenoceptors: an overview. In: Lanier, S.M., and Limbird, L.E. (eds.).  *$\alpha$ 2-Adrenergic Receptors: Structure, Function and Therapeutic Implications*. Luxembourg: Harwood Academic Publishers, pp. 1-19.
- Hille, B. (1992). *Ionic Channels of Excitable Membranes*. Massachusetts: Sinauer Associates Inc.. Second Edition.
- Hoffman, B. B., and Lefkowitz, R. L. (1996). Catecholamines, sympatomimetic drugs and adrenergic receptor antagonists. In: Hardman, J. G., Limbird, L. E., Molinoff, P. B., Ruddon, R. W., Gilman, A. G. (eds.). *The Pharmacological Basis of Therapeutics*, Ninth Edition. New York: McGraw-Hill, pp 199-248.
- Hökfelt, T., Martensson, R., Björklund, A., Kleinau, S., and Goldstein, M. (1984). Distribution maps of tyrosine-hydroxylase-immunoreactive neurons in the rat brain. In: Björklund, A., and Hökfelt, T. (eds.). *Classical Transmitters in the CNS*. Handbook of Chemical Neuroanatomy 2, Part I. Amsterdam: Elsevier Science Publishers, pp. 277–379.
- Holmberg, M., Scheinin, M., Kurose, H., and Miettinen, R. (1999). Adrenergic  $\alpha_{2C}$  receptors reside in rat striatal GABAergic projection neurons: comparison of radioligand binding and immunohistochemistry. *Neuroscience* **93**:1323-1333.
- Hosli, E. and Hosli, L. (1993). Receptors for neurotransmitters on astrocytes in the mammalian central nervous system. *Prog. Neurobiol.* **40**:477-506.
- Hsu, D. T., Lombardo, K. A., Herringa, R. J., Bakshi, V. P., Roseboom, P. H., and Kalin, N. H. (2001). Corticotropin-releasing hormone messenger RNA distribution and stress-induced activation in the thalamus. *Neuroscience* **105**:911–921.
- Huang, L., Wie, Y. Y., Momose-Hotokezaka, A., Dickey, J., and Okusa, M. D. (1996). Alpha 2B-adrenergic receptors: immunolocalization and regulation by potassium depletion in rat kidney. *Am. J. Physiol.* **270**:1015-1026.
- Ishizuka, N., Cowan W. M., and Amaral D. G. (1995). A quantitative analysis of the dendritic organization of pyramidal cells in the rat hippocampus. *J. Comp. Neurol.* **362**:17-45
- Jin, W., and Lu, Z. (1998). Synthesis of a stable form of tertiapin: a high-affinity inhibitor for inward-rectifier  $K^+$  channels. *Biochemistry* **38**:14286-14293.
- Jones, E. G. (1998). The thalamus of primates. In: Bloom, F. E., Björklund, A., and Hökfelt, T. (eds.). *Handbook of Chemical Neuroanatomy*, Vol. 14. Amsterdam: Elsevier Science Publishers, pp. 1–246.
- Kable, J. W., Murrin, L. C., and Bylund, D. B. (2000). In vivo gene modification elucidates subtype-specific functions of alpha-2 adrenergic receptors. *J. Pharmacol. Exp. Ther.* **293**:1–7.
- Kessler, R. C. (1997). The effects of stressful life events on depression. *Annu. Rev. Psychol.* **48**:1991-214.
- Kitayama, I., Nakamura, S., Yaga, T., Murase, S., Nomura, J., Kayahara, T., and Nakano, K. (1994). Degeneration of locus coeruleus axons in stress-induced depression model. *Brain Res. Bull.* **35**:573–580.

- Kobayashi, T., Washiyama, K, and Ikeda, K. (2003). Inhibition of G protein activated inwardly rectifying K<sup>+</sup> channels by fluoxetine (Prozac). *Br. J. Pharmacol.* **138**:1119-1128.
- Kobilka, B. K., Matsui, H., Kobilka, T. S., Yang-Feng, T. L., Francke, U., Caron, M. G., Lefkowitz, R. J., and Reagan, J. W. (1987). Cloning, sequencing, and expression of the gene coding for the human platelet  $\alpha_2$ -adrenergic receptor. *Science* **238**:650-656.
- Kobinger, W. (1984). New concepts on  $\alpha$ -Adrenoceptors in Pharmacology. *J. Pharmacol. (Paris)* supplement I, 5-22.
- Koester, J., and Siegelbaum, S. (2000). Local signaling: Passive electrical properties of the neuron. In: Kandel, E. R., Schwartz, J. H., and Jessel, T. M. (eds.). *Principles of Neural Science*, Fourth edition. New York: McGraw-Hill, pp. 140–149.
- Kole, M. (2003). *CA3 Pyramidal Neuron Correlates of the Stress Response: Analyses of Form and Function*. Doctoral thesis, University of Groningen.
- Kröner, S., Rosenkranz, J. A., Grace, A. A., and Barrionuevo, G. (2005). Dopamine modulates excitability of basolateral amygdala neurons in vitro. *J. Neurophysiol.* **93**:1598-1610.
- Lähdesmäki, J., Sallinen, J., MacDonald, E., Kobilka, B. K., Fagerholm, V., Scheinin, M. (2002). Behavioral and neurochemical characterization of alpha(2A)-adrenergic receptor knockout mice. *Neuroscience*. **113**:289-299.
- Langer, S. Z. (1974). Presynaptic regulation of catecholamine release. *Biochem. Pharmacol.* **23**:1793-1800.
- Latifpour, J., Jones, S. B., and Bylund, D. B. (1982) Characterization of [<sup>3</sup>H]yohimbine binding to putative alpha-2 adrenergic receptors in neonatal rat lung. *J. Pharmacol. Exp. Therap.* **223**:606-611.
- Leonard, B. E. (2001). Stress, norepinephrine and depression. *J. Psychiatry Neurosci.* **26**(Suppl): S11–S16.
- Li, Y., and van den Pol, A. N. (2005). Direct and indirect inhibition by catecholamines of hypocretin/orexin neurons. *J. Neurosci.* **25**:173-183.
- Liebermann, A. R. (1973). Neurons with presynaptic perikarya and presynaptic dendrites in the rat lateral geniculate nucleus. *Brain Res.* **59**:35-59.
- Link, R., Daunt, D., Barsh, G., Chruscinski, A. and Kobilka, B. K. (1992). Cloning of two mouse genes encoding  $\alpha_2$ -adrenergic receptor subtypes and identification of a single amino acid in the mouse  $\alpha_2$ -C10 homolog responsible for an interspecies variation in antagonist binding. *Mol. Pharmacol.* **42**:16-27.
- Lomasney, J. W., Lorenz, W., Allen, L. F., King, K., Regan, J. W., Yang-Feng, T. L., Caron, M. G., and Lefkowitz, R. J. (1990). Expansion of the alpha-2 adrenergic receptor family: Cloning and characterization of a human alpha-2 adrenergic receptor subtype, the gene for which is located on chromosome 2. *Proc. Natl. Acad. Sci. USA* **87**:5094–5098.
- Iversen, S., Kupferman, I., and Kandel, E. R. (2000). Emotional states and feelings. In: Kandel, E. R., Schwartz, J. H., and Jessel, T. M. (eds.). *Principles of Neural Science*. Fourth edition. New York: McGraw-Hill, pp. 982–995.
- Ma, D., Rajakumaraswamy, N., and Maze, M. (2005).  $\alpha_2$ -Adrenoceptor agonists: shedding light on neuroprotection. *Br. Med. Bull.* **71**:77-92.
- MacDonald, E., Kobilka, B. K., and Scheinin, M. (1997). Gene targeting - homing in on alpha-2 adrenoceptor-subtype function. *Trends Pharmacol. Sci.* **18**:211–219.

- McCormick, D. A., and Bal, T. (1997). Sleep and arousal: thalamocortical mechanisms. *Annu. Rev. Neurosci.* **20**:185–215.
- McCormick, D. A., and Pape, H.-C. (1990). Noradrenergic and serotonergic modulation of a hyperpolarization-activated cation current in thalamic relay neurones. *J. Physiol.* **431**:319-342.
- McCormick, D. A., Pape, H.-C., Williamson, A. (1991). Actions of norepinephrine in the cerebral cortex and thalamus: implications for function of the central noradrenergic system. *Prog. Brain Res.* **88**:293-305.
- McEwen, B. S., and Sapolsky, R. M. (1995). Stress and cognitive function. *Curr. Opin. Neurobiol.* **5**:205–216.
- Meister, B., Dagerlind, A., Nicholas, A. P., Hökfelt, T. (1994). Patterns of messenger RNA expression for adrenergic receptor subtypes in the rat kidney. *J. Pharmacol. Exp. Ther.* **268**:1605-1611.
- Meuth, S. G., Budde, T., Kanyshkova, T., Broicher, T., Munsch, T., and Pape, H.-C. (2003). Contribution of TWIK-related acid-sensitive K<sup>+</sup> channel 1 (TASK1) and TASK3 channels to the control of activity modes in thalamocortical neurons. *J. Neurosci.* **23**:6460-6469.
- Meyer, H. (2000). *Klonierung und Untersuchung der zentralnervösen Genexpression  $\alpha_2$ -adrenerger Rezeptoren und ihre Regulation durch chronischen psychosozialen Stress bei *Tupaia belangeri**. Doctoral thesis, University of Göttingen.
- Meyer, H., Palchadhuri, M., Scheinin, M., and Flügge, G. (2000). Regulation of alpha-2A adrenoceptor expression by chronic stress in neurons of the brain stem. *Brain Res.* **880**:147–158.
- Michel, A. D., Loury, D. N., and Whiting, R. L. (1989). Differences between the alpha 2-adrenoceptor in rat submaxillary gland and the alpha 2A-and alpha 2B-adrenoceptor subtypes. *Br. J. Pharmacol.* **98**:890-897.
- Michel, A. D., Loury, D. N., and Whiting, R. L. (1990). Assessment of imiloxan as a selective  $\alpha_{2B}$ -adrenoceptor antagonist. *Br. J. Pharmacol.* **99**:560-564.
- Moga, M. M., Weis, R. P., Moore, R. Y. (1995). Efferent projections of the paraventricular thalamic nucleus in the rat. *J. Comp. Neurol.* **359**:221-238.
- Neher, E. (1992). Correction for liquid junction potentials in patch clamp experiments. *Methods Enzymol.* **207**:123-31.
- Nestler, E. J., Barrot, M., DiLeone, R. J., Eisch, A. J., Gold, S. J., and Monteggia, L. M. (2002). Neurobiology of depression. *Neuron* **34**:13-25.
- Nestler, E. J., Hyman, S. E., and Malenka, R. C. (2001). *Molecular Neuropharmacology*. New York: McGraw-Hill.
- Nicolls, J. G., Martin, A. R., and Wallace, B. G. (2002). *Vom Neuron zum Gehirn*. Berlin: Spektrum Akademischer Verlag.
- North, R. A., Williams, J. T., Surprenant, A., and Christie, M. J. (1987). Mu and delta receptors belong to a family of receptors that are coupled to potassium channels. *Proc. Natl. Acad. Sci. USA* **84**:5487-5491.
- Olli-Lähdesmäki, T., Kallio, J., and Scheinin, M. (1999). Receptor subtype-induced targeting and subtype-specific internalization of human alpha(2)-adrenoceptors in PC12 cells. *J. Neurosci.* **19**:9281-9288.



- Osborne, P. B., Vidovic, M., Chieng, B., Hill, C. E., and Christie, M. J. (2002). Expression of mRNA and functional alpha(1)-adrenoceptors that suppress the GIRK conductance in adult rat locus coeruleus neurons. *Br. J. Pharmacol.* **135**:226-32.
- Otake, K., and Nakamura, Y. (1995). Sites of origin of corticotropin-releasing factor-like immunoreactive projection fibers to the paraventricular thalamic nucleus in the rat. *Neurosci. Lett.* **201**:84-86.
- Otake, K., and Ruggiero, D. A. (1995). Monoamines and nitric oxide are employed by afferents engaged in midline thalamic regulation. *J. Neurosci.* **15**:1891-1911.
- Otake, K., Kin, K., and Nakamura, Y. (2002). Fos expression in afferents to the rat midline thalamus following immobilization stress. *Neurosci. Res.* **43**:269-282.
- Paxinos, G. and Watson, C. (1986). *The Rat Brain in Stereotaxic Coordinates*. Second edition. San Diego: Academic Press.
- Price, J. L. (1995). *Thalamus*. In: Paxinos, G. (ed.) *The Rat Nervous System*. Second edition. San Diego: Academic Press, pp. 629-648.
- Reagan, J. W., Kobilka, T. S., Yang-Feng, T. L., Caron, M. G., Lefkowitz, R. J., and Kobilka, B. K. (1988). Cloning and expression of a human kidney cDNA for an  $\alpha$ 2-adrenergic receptor subtype. *Proc. Natl. Acad. Sci. USA* **85**:6301-6305.
- Reimann, F., and Ashcroft, F. M. (1999). Inwardly rectifying potassium channels. *Curr. Opin. Cell. Biol.* **11**:503-508.
- Rogawski, M. A., and Aghajanian, G. K. (1980). Activation of lateral geniculate neurons by norepinephrine: Mediation by an  $\alpha$ -adrenergic receptor. *Brain Res.* **182**:345-359.
- Rosin, D. L., Talley, E. M., Lee, A., Stornetta, R. L., Gaylinn, B. D., Guyenet, P. G., and Lynch, K. R. (1996). Distribution of  $\alpha_{2C}$ -adrenergic receptor-like immunoreactivity in the rat central nervous system. *J. Comp. Neurol.* **372**:135-165.
- Saavedra, J. M. (1982). Changes in dopamine, noradrenaline and adrenaline in specific septal and preoptic nuclei after acute immobilization stress. *Neuroendocrinology* **35**:396-401.
- Sakmann, B. and Stuart, G. (1995). Patch-pipette recordings from the soma, dendrites, and axon of neurons in brain slices. In: Sakmann, B. and Neher, E. (eds.). *Single-channel recording*. New York: Plenum Press, pp.199-211.
- Sallinen, J., Haapalinna, A., MacDonald, E., Viitamaa, T., Lahdesmaki, J., Rybnikova, E., Pelto-Huikko, M., Kobilka, B. K., and Scheinin, M. (1999). Genetic alteration of the alpha-2 adrenoceptor subtype C in mice affects the development of behavioral despair and stress-induced increases in plasma corticosterone levels. *Mol. Psychiatry* **4**:443-452.
- Saunders, C., and Limbird, L. E. (1999). Localization and trafficking of alpha-2 adrenergic receptor subtypes in cells and tissues. *Pharmacol. Ther.* **84**:193-205.
- Sawamura, S., Kingery, W. S., Davies, M. F., Agashe, G. S., Clark, J. D., Kobilka, B. K., Hashimoto, T., and Maze, M. (2000). Antinociceptive action of nitrous oxide is mediated by stimulation of noradrenergic neurons in the brainstem and activation of alpha-2B adrenoceptors. *J. Neurosci.* **20**:9242-9251.
- Scheinin, M., Lomasney, J. W., Hayden-Hixson, D. M., Schambra, U. B., Caron, M. G., Lefkowitz, R. J., and Fremeau, R. T., Jr. (1994). Distribution of alpha-2 adrenergic receptor subtype gene expression in rat brain. *Brain Res. Mol. Brain Res.* **21**:133-149.

- Sherman, S. M., and Guillery, R. W. (2001). *Exploring the Thalamus*. San Diego: Academic Press.
- Sholl, D. A. (1953). Dendritic organization in the neurons of the visual and motor cortices of the cat. *J. Anat.* **87**:387-406.
- Siegelbaum, S. A., Schwartz, J. H., and Kandel, E. (2000). Modulation of synaptic transmission: second messengers. In: Kandel, E. R., Schwartz, J. H., and Jessel, T. M. (eds.). *Principles of Neural Science*, Fourth edition. New York: McGraw-Hill, pp. 229-251.
- Soini, S. L., Duzic, E., Lanier, S. M., and Akerman, K. E. (1998). Dual modulation of calcium channel current via recombinant alpha2-adrenoceptors in pheochromocytoma (PC-12) cells. *Pflügers Arch.* **435**:280-285.
- Spruston, N., and Johnston, D. (1992). Perforated patch-clamp analysis of the passive membrane properties of three classes of hippocampal neurons. *J. Neurophysiol.* **67**:508-529.
- Stanford, S. C. (1993). Monoamines in response and adaptation to stress. In: Stanford, S.C., Salmon, P. (eds.). *Stress: From Synapse to Syndrome*. London: Academic Press, pp. 281-331.
- Steriade, M., McCormick, D. A., and Sejnowski, T. J. (1993). Thalamocortical oscillations in the sleeping and aroused brain. *Science* **262**:679-685.
- Swadlow, H. A. and Gusev, A. G. (2001). The impact of 'bursting' thalamic impulses at a neocortical synapse. *Nat. Neurosci.* **4**:402-408.
- Swanson, C. J., and Schoepp, D. D. (2003). A role for noradrenergic transmission in the actions of phencyclidine and the antipsychotic and antistress effects of mGlu2/3 receptor agonists. *Ann. N. Y. Acad. Sci.* **1003**:309-317.
- Takigawa, T., and Alzheimer, C. (2002). Phasic and tonic attenuation of EPSPs by inward rectifier K<sup>+</sup> channels in rat hippocampal pyramidal neurons. *J. Physiology* **539**:67-75.
- Talley, E. M., Rosin, D. L., Lee, A., Guyenet, P. G., and Lynch, K. R. (1996). Distribution of  $\alpha_{2A}$ -adrenergic receptor-like immunoreactivity in the rat central nervous system. *J. Comp. Neurol.* **372**:111-134.
- Taraviras, S., Olli-Lahdesmaki, T., Lymperopoulos, A., Charitonidou, D., Mavroidis, M., Kallio, J., Scheinin, M., and Flordellis, C. (2002). Subtype-specific neuronal differentiation of PC12 cells transfected with alpha2-adrenergic receptors. *Eur. J. Cell. Biol.* **81**:363-374.
- Tigges, J., and Shanta, T. R. (1969). *A Stereotaxic Brain Atlas of the Tree Shrew (Tupaia Glis)*. Baltimore: Williams and Wilkins.
- Trendelenburg, A. U., Klebroff, W., Hein, L., and Starke, K. (2001). A study of presynaptic alpha2-autoreceptors in alpha2A/D-, alpha2B- and alpha2C-adrenoceptor-deficient mice. *Naunyn Schmiedebergs Arch. Pharmacol.* **364**:117-130.
- Turner, B. H., and Herkenham, M. (1991). Thalamoamygdaloid projections in the rat: a test of the amygdala's role in sensory processing. *J. Comp. Neurol.* **313**:295-325.
- Uroz, V., Prensa, L., and Giménez-Amaya, J. M. (2004). Chemical anatomy of the human paraventricular thalamic nucleus. *Synapse* **51**:173-185.
- van Buren, J. M. and Borke, R. C. (1972). *Variations and connections of the human thalamus*. Berlin: Springer-Verlag.

- van der Werf, Y. D., Witter, M. P., and Groenewegen, H. J. (2002). The intralaminar and midline nuclei of the thalamus. Anatomical and functional evidence for participation in processes of arousal and awareness. *Brain Res. Rev.* **39**:107–140.
- van Kampen, M., Kramer, M., Hiemke, C., Flügge, G., and Fuchs, E. (2002). The chronic psychosocial stress paradigm in male tree shrews: evaluation of a novel animal model for depressive disorders. *Stress* **5**:37-46.
- Vertes, R. P. (2004). Differential projections of the infralimbic and prelimbic cortex of the rat. *Synapse*. **51**:32-58.
- Weiss, J. M., and Simson, P. G. (1986). Depression in an animal model: focus on the locus ceruleus. *Ciba Found. Symp.* **123**:191–215.
- Williams, J. T., and Marshall, K. C. (1987). Membrane properties and adrenergic responses in locus coeruleus neurons of young rats. *J. Neurosci.* **7**:3687-3694.
- Willner, P. (1991). Animal models as simulations of depression. *Trends Pharmacol. Sci.* **12**:131-136.
- Wilson, J. R. (1986). Synaptic connections of relay and local circuit neurons in the monkey's dorsal lateral geniculate nucleus. *Neurosci. Lett.* **66**:79-84.
- Wozniak, M. and Limbird, L. E. (1998). Trafficking itineraries of G protein-coupled receptors in epithelial cells do not predict receptor localization in neurons. *Brain Res.* **780**:311-322.
- Yagi, J., and Sumino, R. (1998). Inhibition of a hyperpolarization-activated current by clonidine in rat dorsal root ganglion neurons. *J. Neurophysiol.* **80**:1094-1104.
- Zeng, D. W., Harrison, J. K., D'Angelo, D. D., Barber, C. M., Tucker, A. L., Lu, Z. H., and Lynch, K. R. (1990). Molecular characterization of a rat alpha-2B adrenergic receptor. *Proc. Natl. Acad. Sci. USA* **87**:3102–3106.

## List of Figures

<i>Figure 1.</i> Important connections of the PVT.....	13
<i>Figure 2.</i> Schematic description of the recording sites.....	19
<i>Figure 3.</i> Schematic description of the Sholl analysis.....	23
<i>Figure 4.</i> Time course of the stress experiment.....	28
<i>Figure 5.</i> Inhibitory actions of m-NE in the PVT (hyperpolarizing cells).....	30
<i>Figure 6.</i> Excitatory actions of m-NE in the PVT (depolarizing cells).....	31
<i>Figure 7.</i> The three types of recorded cells differ in their resting properties.....	32
<i>Figure 8.</i> The inhibitory response to m-NE is mediated by alpha-2 adrenoceptors.....	33
<i>Figure 9.</i> The excitatory response to m-NE appears to be mediated by alpha-1 adrenoceptors.....	34
<i>Figure 10.</i> Alpha-2 adrenoceptors mediate the inhibitory effect of m-NE and alpha-1 adrenoceptors appear to mediate the excitatory effect of m-NE in the PVT.....	35
<i>Figure 11.</i> Burst and tonic firing modes in the PVT.....	38
<i>Figure 12.</i> The effects of alpha-2 AR activation on the firing of PVT cells.....	40
<i>Figure 13.</i> Alpha-2 AR activation reversibly abolishes spontaneous firing in PVT cells.....	41
<i>Figure 14.</i> The effects of a presumptive alpha-1 AR activation on firing of PVT cells.....	42
<i>Figure 15.</i> In a subset of PVT cells, application of m-NE does not influence firing.....	43
<i>Figure 16.</i> The effects of m-NE involve putative K <sup>+</sup> conductances.....	44
<i>Figure 17.</i> The outward current induced by m-NE involves K <sup>+</sup> conductances.....	46
<i>Figure 18.</i> Morphology of PVT cells.....	48
<i>Figure 19.</i> Correlation of morphological and physiological data.....	49
<i>Figure 20.</i> Dendritic analysis of PVT cells according to their reaction to m-NE.....	51
<i>Figure 21.</i> Anatomical localization of the morphologically analyzed PVT cell bodies.....	52
<i>Figure 22.</i> In the PVT, cells reacting differently to m-NE appear to form distinct populations.....	53
<i>Figure 23.</i> Photomicrographs of the rat PVT in coronal brain sections which were stained with an anti-DBH antibody and an anti-PNMT antibody.....	55
<i>Figure 24.</i> Results of the competition experiment.....	56
<i>Figure 25.</i> Alpha-2B AR expression and alpha-2 AR binding in the anterior thalamus of the tree shrew.....	57
<i>Figure 26.</i> Quantification of [ <sup>3</sup> H]RX821002 binding in the tree shrew thalamus as determined by <i>in vitro</i> receptor autoradiography.....	58
<i>Figure 27.</i> Expression of alpha-2B AR mRNA in single neurons of the PVT.....	59

## List of Tables

<i>Table 1.</i> Summary of the resting properties of the investigated cells and the actions of m-NE (5 $\mu$ M) on spike firing.....	37
<i>Table 2.</i> Morphological parameters of the analyzed PVT neurons.....	50
<i>Table 3.</i> Peripheral reactions of the experimental animals during chronic psychosocial stress.....	61

## Publications

### *Articles in peer-reviewed journals:*

**Heilbronner, U.**, van Kampen, M, and Flügge, G. (2004) The alpha-2B adrenoceptor is persistently upregulated by chronic psychosocial stress. *Cell. Mol. Neurobiol.* **24**:815-831.

Czéh, B, Pudovkina, O., van der Hart, M. G. C., Simon, M., **Heilbronner, U.**, Michaelis, T., Watanabe, T., Frahm J., and Fuchs, E. (2005). Examining SLV-323, a novel NK1 receptor antagonist, in a chronic psychosocial stress model for depression. *Psychopharmacology.* **180**:548–557.

Perez-Cruz, C., Müller-Keuker, J.R.H., **Heilbronner, U.**, Fuchs, E. (2005). Asymmetric morphology of pyramidal cells of the rat prefrontal cortex and sub-area specific dendritic remodeling after chronic restraint stress. *Submitted.*

### *Poster presentations:*

**Heilbronner, U.**, and Flügge, G. (2002). Alpha-2B Adrenoceptors in the Thalamus of *Tupaia belangeri*. Congress “Neurobiology of Stress in Health and Disease”. Elba, Italy.

**Heilbronner, U.**, and Flügge, G. (2002). Alpha-2B Adrenoceptors in the Thalamus of *Tupaia belangeri*. Proc. Soc. Neurosci. 543.9, 2002.

**Heilbronner, U.**, van Kampen, M., and Flügge G. (2003). Persistent upregulation of thalamic alpha-2B adrenoceptors after chronic psychosocial stress. In: Elsner, N., Zimmermann, H. (eds.): Proceedings of the 29th Göttingen Neurobiology Conference and the 5th Meeting of the German Neuroscience Society 2003. Thieme Verlag, Stuttgart. 809.

**Heilbronner, U.**, Kole, M.H.P., van Kampen, M. and Flügge, G. (2003). Persistent upregulation of thalamic alpha-2B adrenoceptors after chronic psychosocial stress. Proc. Soc. Neurosci. 573.2, 2003.

**Heilbronner, U.**, Kole, M., and Flügge, G. (2005). Alpha-methyl-noradrenaline stimulates alpha-1 and alpha-2 adrenoceptors in the paraventricular thalamic nucleus of the rat. In: Zimmermann H., Kriegstein, K. (eds.) Proceedings of the 6th Meeting of the German Neuroscience Society / 30th Göttingen Neurobiology Conference 2005. Neuroforum, 1 Suppl.: 294A.

## Courses taken during the M.Sc./Ph.D. Program

„Scientific Communication“. Instructor: H. Sylin-Roberts, Ph.D. January 2002.

“Intercultural Communication”. Instructors: Dr. S. Petersen und A. Petersen, M.Sc. May 2004.

“The Drug Discovery Process”. Instructor: Dr. B. Seilheimer, Schering AG. May 2004.

Seminar „Molecular Physiology of Synaptic Transmission“. Instructor: PD Dr. R. Schneggenburger. Summer semester 2002.

## **Acknowledgements**

First of all, I would like to thank my supervisor PD Dr. Gabriele Flügge for helpful criticism and her constant support of my work. I am also indebted to Prof. Friedrich-Wilhelm Schürmann and Prof. Willhart Knepel who provided constructive comments and support as members of my thesis committee.

I would also like to thank Prof. Eberhard Fuchs for giving me the opportunity to work in his laboratory.

Dr. Simone Cardoso d'Oliveira, Dr. Steffen Burkhardt, and Dr. Dorothee Wegener did an excellent job in managing all the administrative matters of the M.Sc./Ph.D. Program Neuroscience.

My gratitude goes also to the Study Committee of the M.Sc./Ph.D. Program Neuroscience for funding me during the final part of this thesis.

Furthermore, my thanks go out to all members of the Clinical Neurobiology Laboratory at the German Primate Center, especially to the alumnus Dr. Maarten Kole, who taught me the whole-cell patch-clamp technique. I am also grateful to the alumni Dr. Marja van Kampen, who performed the tree shrew animal experiments, and Dr. Heiko Meyer, who cloned the tree shrew alpha-2B adrenoceptor.

I also would like to thank the Deutsche Forschungsgemeinschaft (DFG), who financed the initial part of my studies (SFB 406, project C4 to PD Dr. G. Flügge).

Last, but certainly not least, I would like to thank my girlfriend Katja Schmidt, M.A. and my whole family and friends for encouraging me and being there for me when I needed them.

## Curriculum Vitae

### Personal Details

Name: Urs Heilbronner

Date and Place of Birth: 16.06.1977 in Tübingen, Germany

Nationality: German

Contact: Levinstrasse 10, 37079 Göttingen.  
Mobile phone: 0179-1129020  
Email: urs\_heilbronner@hotmail.com

### Scientific Education

04/2002 - 10/2005 Ph.D. thesis in the Graduate Program Neuroscience, University of Göttingen, performed at the German Primate Center in the Laboratory of Clinical Neurobiology. Scientific Head: Prof. E. Fuchs. Supervisor: PD Dr. G. Flügge.

10/2000 - 04/2002 M.Sc. in the Graduate Program in Neuroscience, University of Göttingen. Grade: excellent (A). Title of the Master's thesis: Alpha-2B adrenoceptor expression in the tree shrew brain: co-localization with GABA- and glutamate-like immunoreactivity.

08/1999 – 07/2000 Academic exchange year to the University of California in Santa Cruz, California, USA.

10/1997 – 07/1999 Studying psychology at the Georg-August-University Göttingen. Grade of the undergraduate examinations (Vordiplom): 1.4 (A-).



### Alternative Military Service

08/1996 – 09/1997 Intensive care of severely handicapped people (Intensive Schwerstbehinderten Betreuung) at the Körperbehindertenförderung Neckar-Alb, Mössingen, Germany.

### High School

10/1988 – 06/1996 Carlo-Schmid-Gymnasium, Tübingen, Germany. Grade in final exams (Abitur): B+ (1.7).

### Stipends

Heräus-Platzhoff Stipend 2000 – 2001.

Stipend of the M.Sc./Ph.D. Program Neurosciences 01/2005 – 06/2005.

### Employment

1991 – 1996 Vacation jobs as laboratory assistant in the Department of Clinical Genetics, Frauenklinik Stuttgart, Germany.

*“...Unfortunately, nature seems unaware of our intellectual need for convenience and unity, and very often takes delight in complication and diversity...”*

S. Ramón y Cajal, 1906.